Theses and Dissertations   Graduate School

2009

Optimization of Functional MRI methods for olfactory interventional studies at 3T

Vishwadeep Ahluwalia
Virginia Commonwealth University

SIGNATURE PAGE (TO BE REPLACED BY APPROVAL FORM)

FOR MY GRANDMA

"OPTIMIZATION OF FUNCTIONAL MRI METHODS FOR OLFACTORY

INTERVENTIONAL STUDIES AT 3T"

A Dissertation submitted in partial fulfillment of the requirements for the degree of Doctor of

Philosophy at Virginia Commonwealth University.

by

Vishwadeep Ahluwalia

Master of Science, Virginia Commonwealth University, 2003

Thesis Advisor: Birgit Kettenmann, Ph.D.

Assistant Research Professor, Division of Radiation Physics and Biology,

Department of Radiology, Virginia Commonwealth University

Virginia Commonwealth University

Richmond, Virginia

December 2009

Table of Contents

List of Tables

List of Figures

List of Abbreviations

AMY   Amygdala

AUC   Area Under the Curve

BET   Brain Extraction Tool

BOLD   Blood Oxygenation-Level Dependent

CBF   Cerebral Blood Flow

CMR   Cerebral Metabolic Rate

CNR   Contrast to Noise Ratio

CV   Coefficient of variation

dHb   Deoxyhaemoglobin

FEAT   FMRI Expert Analysis Tool

FILM   FMRIB's Improved Linear Model

FLAME   FMRIB's Local Analysis of Mixed Effects

FLIRT   FMRIB's Linear Image Registration Tool

FMRI   Functional Magnetic Resonance Imaging

FMRIB   Oxford Centre for Functional MRI of the Brain

FSL   FMRIB Software Library

FT   Fall Time

GLM   General Linear Model

Hb   Oxyhaemoglobin

HRF   Hemodynamic Response Function

INS   Insular cortex

ISI   Inter-Stimulus Interval

McFLIRT	FLIRT for Motion Correction
MNI	Montreal Neurological Institute
NIH	National Institutes of Health
OFC	Orbitofrontal cortex
PET	Positron Emission Tomography
PIR	Piriform cortex
PSC	Peak Signal Change
ROI	Region of Interest
SD	Standard Deviation
SNR	Signal to Noise Ratio
T_2*	Transverse magnetization decay time (includes phase differences + inhomogeneities)
TDI	(odor) Threshold, Discrimination and Identification score
TE	Echo Time
TR	Repetition Time
TTP	Time To Peak
VPC	Velo-Pharyngeal Closure

Abstract

OPTIMIZATION OF FUNCTIONAL MRI METHODS FOR OLFACTORY INTERVENTIONAL STUDIES AT 3T

By Vishwadeep Ahluwalia, Ph.D.

A Dissertation submitted in partial fulfillment of the requirements for the degree of Doctor of Philosophy at Virginia Commonwealth University.

Virginia Commonwealth University

Thesis Advisor: Birgit Kettenmann, Ph.D.
Assistant Research Professor, Division of Radiation Physics and Biology,
Department of Radiology, Virginia Commonwealth University

Functional MRI technique is vital in investigating the effect of an intervention on cortical activation in normal and patient population. In many such investigations, block stimulation paradigms are still the preferred method of inducing brain activation during functional imaging sessions because of the high BOLD response, ease in implementation and subject compliance especially in patient population. However, effect of an intervention can be validly interpreted only after reproducibility of a detectable BOLD response evoked by the stimulation paradigm is first verified in the absence of the intervention. Detecting a large BOLD response that is also reproducible is a difficult task particularly in olfactory Functional MRI studies due to the factors such as (a) susceptibility-induced signal loss in olfactory related brain areas and (b) desensitization to odors due to prolonged odor stimulation, which is typical when block paradigms are used. Therefore, when block paradigms are used in olfactory interventional Functional MRI studies, the effect of the intervention may not be easily interpretable due to the

factors mentioned above. The first task of this thesis was to select a block stimulation paradigm that would produce a large and reproducible BOLD response. It was hypothesized that a BOLD response of this nature could be produced if within-block and across-session desensitization could be minimized and further, that desensitization could be minimized by reducing the amount of odor by pulsing the odor stimulus within a block instead of providing a continuous odor throughout the block duration. Once the best paradigm was selected, the second task of the thesis was to select the best model for use in general linear model (GLM) analysis of the functional data, so that robust activation is detected in olfactory related brain areas. Finally, the third task was to apply the paradigm and model that were selected as the best among the ones tested in this thesis, to an olfactory interventional Functional MRI study investigating the effect of food (bananas) eaten to satiety on the brain activation to the odor related to that food. The methods used in this thesis to ensure valid interpretation of an interventional effect, can serve as a template for the experimental design of future interventional Functional MRI studies.

PREFACE

This preface gives an outline of this thesis.

Chapter 1 is an introduction to this thesis and provides a background and various concepts related to Functional MRI of the human olfactory system as well as topics contributing to the overall rationale for conducting research as part of this thesis. For the final goal of the thesis i.e. to ensure that the effect of intervention is validly interpreted, two tasks are undertaken.

Chapter 2 is dedicated to the first task i.e. to select a paradigm that gives a large and reproducible BOLD response. BOLD response from continuous and pulsed-odor paradigms are compared for this purpose.

Chapter 3 is dedicated to the second task i.e. to select a model that best represents the functional timeseries data of the best paradigm selected in the first task, to be used in GLM analysis so that robust activation is detected in olfactory related brain areas.

Chapter 4 includes the results of an interventional olfactory Functional MRI study investigating sensory specific satiety to a food related odor, for which the best paradigm and model selected from previous tasks in this thesis are used.

Finally, Chapter 5 provides a summary of the results and describes future work related to the topics in this thesis.

CHAPTER 1   INTRODUCTION

The background and various concepts related to Functional MRI of the human olfactory system as well as topics contributing to the overall rationale for conducting research as part of this thesis have been discussed briefly in this chapter.

1.1 History of the study of Brain function

For many centuries, scientists and philosophers have been on a quest to relate brain structure and function to sensory perception, behavior and emotion. Inspite of the incessant pondering, the brain still remains a relatively mysterious organ. It is only in the past two decades that we have gained vital insights into the functioning of the brain especially with the advent of novel neuroimaging techniques.

In the 19th century, Franz Joseph Gall developed and popularized the field of phrenology.[1] Phrenologists determined character, personality traits and criminality of a person based on the bumps and fissures in the skull. Although a fallacious form of science, phrenology put forth an important concept that mental processes are localized in the brain. After phrenology collapsed in the late 1830's, the study of brain function progressed through work involving the stimulation of the cortex of animal brains using electrical currents. This lead to the mapping of motor function in animals and, later, in humans. These results however contained many inconsistencies. More reliable work was carried out in the mid 20th century by Penfield[2], who managed to map the motor and somatosensory cortex using cortical stimulation of patients undergoing neurosurgery. In the latter half of the 20th century, most progress in the study of brain function came from

patients with neurological disorders or from invasive electrode measurements on animals. It has only really been in the last two decades that non-invasive brain mapping techniques such as magnetoencephalography (MEG), positron emission tomography (PET), optical imaging and blood oxygenation-level dependent (BOLD) Functional MRI have allowed the study of brain function in healthy human subjects. As part of this thesis we use the BOLD Functional MRI technique to study the human olfactory function at the cortical level. Next few sections are dedicated to acclimatizing the reader with the principals and important concepts regarding BOLD Functional MRI.

1.2 Principles of Functional Magnetic Resonance Imaging

Brain function requires a large amount of energy. This energy is obtained via glucose metabolism, which needs oxygen. Therefore the brain needs a steady supply of oxygen via the blood vessels. The blood contains a protein called haemoglobin that oxygen molecule binds with. Oxyhaemoglobin (Hb) and deoxyhaemoglobin (dHb) are the two states of haemoglobin with and without the oxygen molecule bound to it respectively. The important fact for MR imaging is that Hb with no unpaired electrons and zero magnetic moment is diamagnetic and dHb with unpaired electrons and a significant magnetic moment is paramagnetic.[3] dHb in the blood vessels affects the magnetic susceptibility within and around the vessels. This creates microscopic inhomogeneities, which in turn causes dephasing of the MR proton signal leading to a decrease[4] in the T_2^*. Areas of signal loss in rat brain were observed in a T_2^* weighted image when the rats breathed-in normal air as compared to pure oxygen indicating signal loss due to deoxygenated blood.[5] The same group further verified this by spin-echo (T_2-weighted) and gradient-echo (T_2^*-weighted) imaging of test tubes with oxygenated or deoxygenated blood in a saline-filled

container. It was found that only the gradient-echo image of the test tube with deoxygenated blood led to substantial signal loss in the adjacent space.[6] This contrast between oxygenated and deoxygenated blood in gradient-echo images came to be known as the blood-oxygen level dependent (BOLD) contrast.

Based on the above findings, Ogawa and colleagues speculated that in response to a neural activity the oxygen consumption increases which results in an increase in dHb and thus decrease in the T_2^* and consequently the MR signal. However, instead of a decrease, they observed that the MR signal increases upon neural activity. PET and optical imaging methods have been used to explain this paradox. A PET study showed that following neural activity, the increase in cerebral blood flow (CBF) and cerebral metabolic rate for glucose (CMR-glu), are not accompanied by any significant increase in cerebral metabolic rate for oxygen[7] (CMR-O_2).

Another study using high-resolution near-infrared spectroscopy showed that the evoked changes in Hb and dHb were quite distinct.[8] The dHb time curve increased rapidly to peak at 2s following neural activity and then declined to a minimum value at 6s after onset. The Hb time curve peaked at about 5-6s and slowly declined to about 10s. The Hb peak was also found to be much higher than dHb. These studies show that neural activity briefly results in a slight increase in oxygen extraction from the Hb but is then followed by a superfluous increase in cerebral blood flow, which brings in much more Hb. This causes a localized decrease in the dHb and hence an increase in the MR signal.
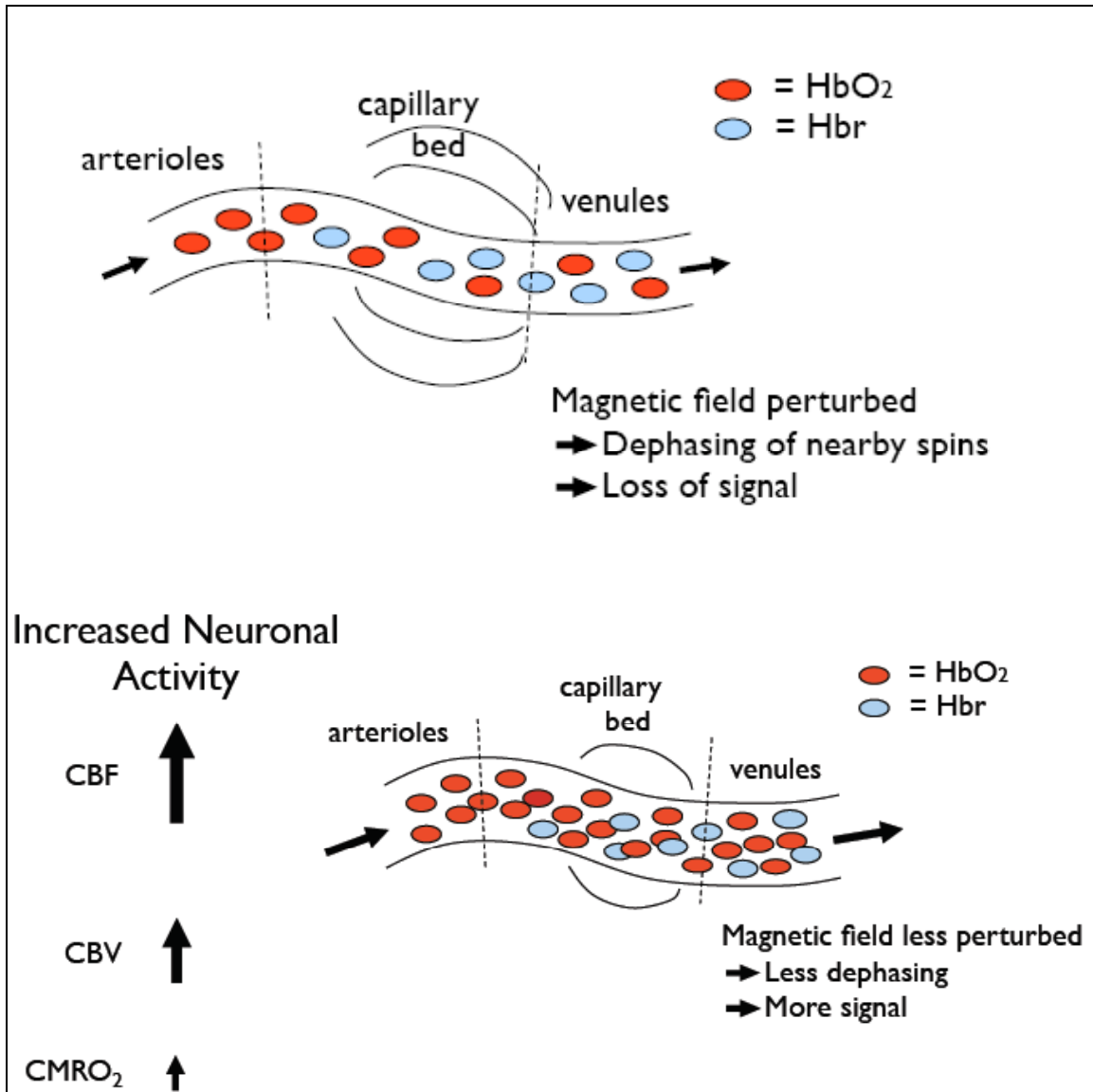
Figure 1-1: Neural activity is followed by oxygen extraction resulting in a slight increase in dHb followed by an increase in regional cerebral blood flow, which leads to a net increase in Hb.
(Adapted from http://www.fmrib.ox.ac.uk/fslcourse)

Thus dHb acts as an endogenous contrast agent providing an indirect measure of neural activity. This localized change in dHb content post-neuronal activity gets integrated into what we see as the BOLD signal and serves as the basis of Functional MRI.

1.3 BOLD signal

The first experiment in this thesis compares the BOLD responses in primary and secondary olfactory areas between different stimulation paradigms. Therefore, first it is important to understand the basic characteristics of a typical BOLD signal.

BOLD signal in a voxel reflects the total amount of dHb as well as noise (thermal, hardware, motion-related or physiological). In the first few seconds following the onset of increased neural activity, tissue metabolism increases rapidly leading to increases in oxygen consumption and CBF. With activation, CBF increases much more than $CMRO_2$ resulting in a large influx of fully oxygenated blood and a decrease in dHb.[7] As mentioned previously, the presence of dHb increases local spin dephasing and decreases the MR signal. Decreases in dHb following large CBF increases lead to a positive BOLD signal as depicted in Fig. 1-2. If in the first few seconds of the BOLD response, the $CMRO_2$ increases more quickly than CBF, it can lead to an initial transient increase in dHb and an associated "initial dip" in the BOLD signal.[8-12] The CBF and BOLD responses are typically delayed 1-2 seconds following neural activity and have a broad temporal width on the order of the duration of the stimulus.[13] A post-stimulus undershoot is often observed and is thought to reflect the slow resolution of CBV with respect to CBF following cessation of stimulus.[14]
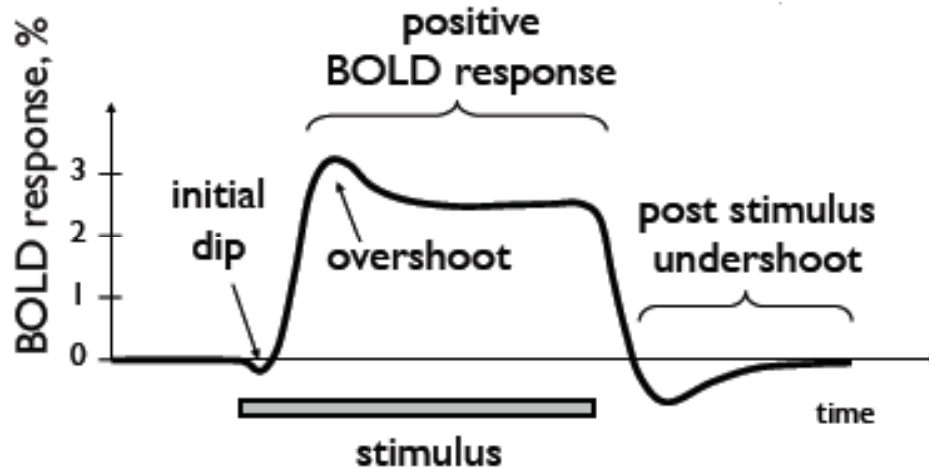
Figure 1-2: A simple illustration of a BOLD response. Following stimulus onset, the initial increase in CMRO2 leads to increased dHb and to an "initial dip" in the BOLD response. CBF then increases more than CMRO2 driving dHb down and leading to the positive BOLD response. The post-stimulus undershoot recovers slowly back to baseline and is thought to arise from the slow resolution of CBV relative to CBF. (Adapted from http://www.fmrib.ox.ac.uk/fslcourse)

Since the discovery of BOLD effect, Functional MRI has been extensively used for brain mapping. The first few studies verified the efficacy of the technique by stimulating well-known cortical areas such as visual[15] and motor cortex.[13] In order to study brain function based on the BOLD signal, T_2^* weighted brain images are acquired at a relatively fast rate ~1-3s while the subject is performing a task or is being presented with some stimulus. Echo planar imaging (EPI) sequence is typically used to acquire T_2^* weighted images. T_2^* weighting and therefore BOLD contrast is dependent on the echo time (TE). If TE is too short or too long there will be no signal between the activated and resting state. Therefore, to obtain maximum signal change for a region with a particular T_2^*, the optimal value of echo time can be shown to be equal to the T_2^* value of that tissue. Also important is the relationship between the BOLD signal change and static field strength. Raw MR signal increases with the square of the field strength[16], while thermal noise increases linearly with field strength. The ratio of the two, the raw SNR, thus increases linearly with field strength. However, the contribution of physiological noise (cardiac pulsations and respiration) also increases with the square of the field strength. Therefore, although it would

appear that higher field strengths are desirable, the functional SNR may reach an asymptote at higher field strengths. There are various post-processing strategies available to correct for cardiac and respiration induced noise.[17,18] Subject motion can reduce functional SNR in Functional MRI images, and introduce artefacts in the activation maps if the motion is stimulus correlated. This problem can never be completely eliminated but can be minimized by restraining the head of the subject during the scan and by using postprocessing motion correction algorithm. The BOLD contrast also depends on the voxel size. If there is localized cortical activity and if a larger voxel is chosen over that area then the contrast to noise ratio in that voxel decreases due to partial volume effects.

The choice of the optimum parameters for Functional MRI is always a compromise and rather depends on what is available than what is desirable.

1.4 Paradigm Design

As important as choosing the optimum imaging parameters for a good experiment, are designing an appropriate stimulus paradigm. Optimizing the paradigm design is one aspect of this thesis. Therefore, we discuss briefly the general considerations involved in the design of a stimulation paradigm. Specific discussion regarding olfactory stimulation paradigms will be done in a later section.

A lot of experience regarding paradigm design has come from electroencephalography (EEG) and PET, but since Functional MRI has a temporal resolution somewhere between these two techniques, new approaches can be taken. The earliest Functional MRI experiments were much in the form of PET studies, where a set of resting images were acquired along with a set of

activation images, and one set was subtracted from the other. However since the BOLD contrast is relatively rapid in its onset and decay (on the order of a few seconds) it is possible to follow time courses for much shorter events occurring more frequently.

The most common stimulus presentation pattern is that of regular epochs of stimulus and rest, usually labeled 'on' and 'off'. These are typically called block design paradigms. The duration of these epochs needs to be long enough to accommodate the hemodynamic response, and so a value of at least 8 seconds, or more commonly 16 to 40 seconds is chosen. These epochs are repeated for as long as is necessary to gain enough functional SNR to detect the activation response. The total experimental duration however must be a balance between how long the subject can comfortably lie still without moving, and the number of data points required to obtain enough functional SNR. There are often some technical limitations to the experimental duration, and there is the possibility of the subject habituating to the stimulus causing the BOLD contrast to reduce with time.

Instead of epochs of stimuli, it is possible to use single events as a stimulus, much in the same way that EEG or MEG does. These paradigms are called event related paradigms. Again due to the hemodynamic response, these must be separated by a much longer period of time than would be required for EEG, but this type of stimulus presentation has the major advantage of being able to separate out the relative timings of activations in different areas of the brain. One of the major disadvantages of event related paradigms is that the experiments need to be much longer than block related paradigms, in order to gain the necessary functional SNR.

1.5 Analysis of Functional MRI Data

   Data analysis strategies are another important tool to optimize Functional MRI data output. One of the aims of this thesis is to optimize data analysis for a specific purpose, which will be discussed in the proceeding parts of this thesis. Therefore this topic is introduced briefly in this section. The analysis of Functional MRI data falls into two parts. (a) The raw data must be analyzed to produce a brain image showing the regions of activation and (b) Some level of significance must be assigned so that the probability of producing such a result purely by chance is suitably low. The most straightforward way to analyze the data is to subtract the mean 'off' image from the mean 'on' image.[19] This has the disadvantage that any small movement of the head can drastically change the voxel intensity at the boundaries of the image. This can give rise to a ring of apparent activation near the brain boundaries. To reduce this effect, and to give a statistic of known distribution, a better statistical method to apply is a student's t-test.[20,21] This biases the result against voxels in either 'on' or 'off' set with very large variability, and so can reduce movement artefact. An image where each voxel is assigned a value based on the output of a statistical test is commonly called a statistical parametric map. Another commonly used technique is that of correlation coefficient mapping. Here the time response of the activation to the stimulus is predicted, usually with some knowledge of the hemodynamic response, and the correlation coefficient between each voxel time course and this reference function is calculated. Other methods that have been used include Fourier transformation, which identifies voxels with a high Fourier component an the frequency of stimulus presentation, principal component analysis, which locates regions in the brain which show synchronous activity using eigen-functions, clustering techniques, which again look for synchrony using iterative methods, and various non-parametric tests which do not require the assumption of normality in the signal

distribution.[22-25] Currently, the most commonly used method of statistical analysis is using the General Linear Model[20] (GLM). Equation 1 is the form of a simple linear model:

$$y(t) = a*x(t) + b + e(t) \qquad\qquad Eq.(1)$$

where y(t) is the 1D vector of intensity values of one voxel for each time point.

      x(t) is the 1D vector of model

      a is the parameter estimate for x(t)

      b is a constant (baseline intensity value in the data)

      e is the minimum error term after model fitting

There may well be more than one model factor in the GLM that may be of interest (e.g. an experiment with two or more type of stimuli) or may be confounds (e.g. subject's respiration pattern or head motion). GLM used in Functional MRI is formulated as a design matrix consisting of all the model factors, each being a 1D vector of all the time points. To test the significance of a model factor for a given voxel, the parameter estimate at that voxel is divided by the residual error. Furthermore, linear contrasts can be tested e.g. between a model factor and baseline or between two model factors. Thus, GLM provides a powerful and flexible way of Functional MRI data analysis, although it is model dependent.

The main criteria for any technique however are simplicity, speed, statistical validity, and sensitivity. Having obtained a statistical map it is necessary to display the regions of activation, together with some estimate as to the reliability of the result. If the distribution of the statistic, under the null hypothesis of no activation present, is known, then statistical tables can be used to threshold the image, showing only those voxels that show strong stimulus correlation. When displaying the results as an image usually of several thousand voxels, it is necessary to account

for multiple comparisons, since the probability of any one voxel in the image being falsely labeled as active is much greater than the probability of a lone voxel being falsely labeled. There are several ways to account for this, for example the Bonferoni correction or the theory of Gaussian random fields.

The preceding sections conclude a brief overview on the basics of Functional MRI. The following sections discuss topics relevant to the research conducted in this thesis. We first introduce briefly the anatomical and functional subunits of the human olfactory system followed by various problems associated with functional imaging of this system.

1.6 Human Olfactory System

Cortical regions defined as primary olfactory cortex are those regions that get direct inputs from the olfactory bulb.[26] Primary olfactory areas include anterior olfactory nucleus, the tenia tecta, the olfactory tubercle, the piriform cortex, the anterior cortical amygdaloid nucleus, the periamygdaloid cortex and the entorhinal cortex. These cortical sub-regions project information into different areas of the brain. Piriform cortex, the largest recipient of bulbar input, projects to the dorsomedial nucleus of the thalamus. It has direct connections with a wide expanse of orbitofrontal cortex, and also has reciprocal connections projecting back to the olfactory bulb (Fig. 1-3). There are two aspects of olfactory cortical organization that are significantly different from the cortical organization of the other sensory systems.[26]
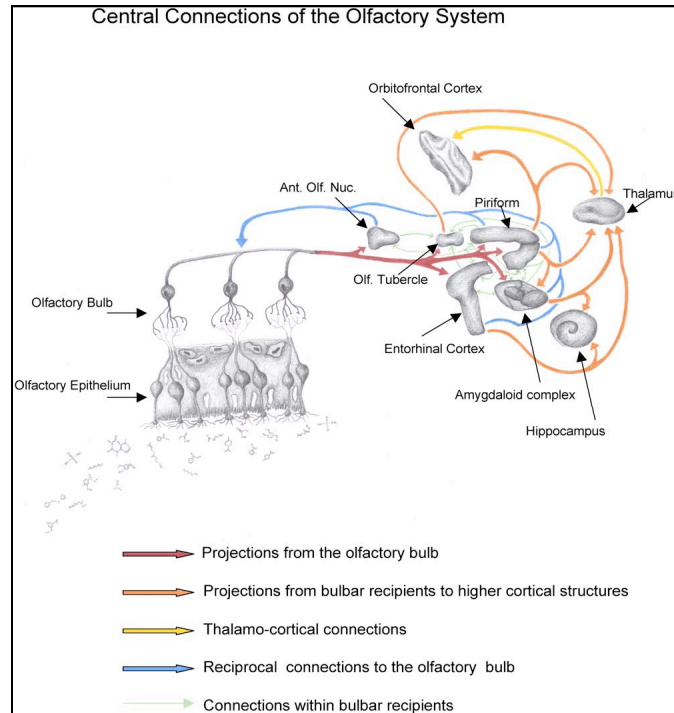
Figure 1-3: Primary and Secondary Olfactory Areas and their connections. (Adapted from Zelano et al.[27])

First there is a direct projection from second-order sensory neurons to cortex, without a thalamic relay. In broad terms, the thalamus serves to gate sensory information based on states of attention and arousal.[28] In olfaction, this process may be achieved intrinsically at the level of piriform cortex. A second aspect of olfactory cortical organization that differentiates it from the cortical organization of other distal senses is the extent of centrifugal connections. This complex network of connections provides the basis for odor-guided regulation of behavior, feeding, emotion, autonomic states and memory. Although the anatomy and structural organization of the olfactory cortex is well characterized, much less is known about the information processing within these cortical structures.[29] Development of neuroimaging techniques such as PET and Functional MRI in recent years has been useful to gain insight into the processing of olfactory information in the brain. However, technical challenges in imaging the olfactory system remain and are discussed below.

1.7 Problems in Functional MRI Studies of Olfaction

One rationale for this thesis is derived from two primary limitations involved in Functional MRI of olfaction (a) susceptibility induced signal loss and (b) odor desensitization.

a) Susceptibility induced signal loss: The very factor that gives Functional MRI its signal of interest also contributes to its disadvantages, especially while imaging the olfactory system. This is because, while the susceptibility differences between various levels of blood oxygenation contribute to BOLD contrast, the susceptibility differences at tissue and air/bone boundaries contribute to a MR signal loss. This is particularly significant in studies involving the olfactory system because of the proximity of its primary and secondary sensory cortical regions to sinuses. Therefore studies involving this sensory modality cannot be performed reliably by simply using a standard gradient-echo echo planar imaging (GE-EPI) pulse sequences devoid of any correctional measures. Even though various strategies developed to mitigate this signal loss have been fairly successful[30-33], their implementation is not always possible at all Functional MRI facilities.

One approach to reduce susceptibility based signal losses is to use other T_2* weighted sequences instead of the traditional GE-EPI sequence. With this in mind, Glover and Law[34] developed the spiral in/out sequence. They showed that the weighted combination of spiral in/out significantly improves SNR and activation in inferior frontal and temporal areas. Preston and colleagues[35] further showed that spiral in/out methods recover more raw signal as well as BOLD contrast in regions affected by susceptibility field gradients relative to conventional spiral-out acquisitions, and these advantages were greater at a 3 T magnet than at a 1.5 T magnet. They also showed that spiral in/out provide significant benefits in magnetically uniform brain areas.

This research study will utilize the combined benefits of a spiral in/out pulse sequence to reduce the susceptibility induced signal losses and a high field strength GE-3T magnet to increase the BOLD contrast in olfactory related brain areas.
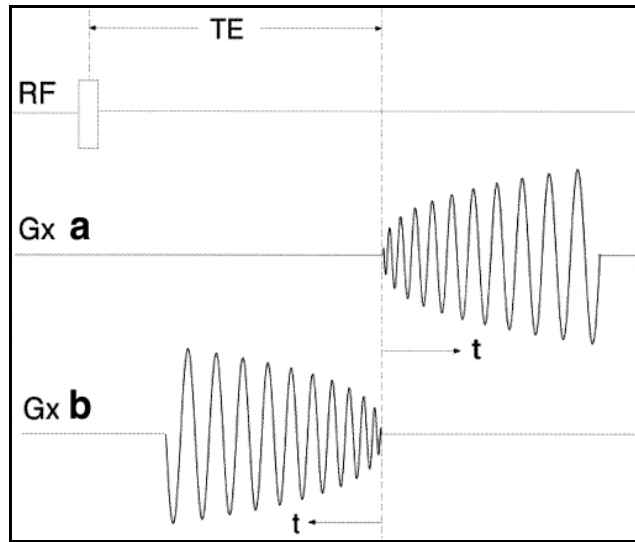
Figure 1-4: (**a**) Spiral-out and (**b**) Spiral-in pulse sequences; the two images are then combined using a weighted combination method. In regions in which the spiral-out average image has lower intensity, the resultant image is weighted toward the spiral-in image, whereas in uniform regions the combination is a simple average.

b) Odor desensitization: Desensitization in olfaction refers to a decrease in the physiological response of the neurons at either the receptor level or cortical level due to prolonged or repeated odor stimulation. In a Functional MRI setting, stimulation paradigms used for sensory stimulation are either block paradigms or event related paradigms. Block paradigms consist of extended alternating epochs of control and experimental conditions, e.g., an odor condition versus a no-odor condition (see Section 1.5). A typical Functional MRI Block paradigm study may consist of blocks ranging between 16 to 40 seconds in duration that are repeated four to six times within a single experimental run.

However, in olfactory Functional MRI studies, block paradigms can have the disadvantage of causing odor desensitization due to prolonged blocks of odor stimulation. Desensitization not

only causes a drop in BOLD signal within the 'Odor-On' block but may also cause signal drops over consecutive trials and sessions. This prolonged desensitization may also affect the reproducibility of activation in olfactory related areas when the same stimulation paradigm is repeated within a short time. This is especially consequential in interventional olfactory Functional MRI studies when pre- and a post-intervention scans are planned. In contrast, event-related paradigms (short duration pulses of stimuli separated by fixed/variable interstimulus intervals) can be used to reduce desensitization effects and have been used in many olfactory Functional MRI studies.[36-38] Even so, the event related paradigms yield a much lower BOLD response as compared to block paradigms. Block paradigms have excellent detection power (knowing which voxels are active). Since block paradigms yield a high BOLD response, less number of stimuli are needed to achieve good statistics and hence the overall experimental time is greatly reduced as compared to the event related paradigms. Block paradigms are particularly useful in yielding activation in response to passive or sensory stimulation. Additionally, they are easy for the researcher to create and analyze and the repetitive nature of the tasks are easy for the subjects to understand and perform. Many of the above features are a necessity in clinical settings involving patients and therefore block paradigms are the preferred stimulation method used in such situations. (*see Huettel, Song*[39] *for more on Functional MRI paradigms*). Due to these advantages, Block paradigms continue to be widely used in many olfactory Functional MRI studies.[40-44] However, the choice of paradigm design (Block or event-related) depends foremost on the experimental goals of the study.[45-48] In an olfactory interventional Functional MRI study where block paradigms are to be used, minimizing desensitization is critical in order to validly interpret the effect of the intervention. As an example of an interventional study, and to apply an optimized experimental design we chose to investigate the sensory specific satiety

related decrease in BOLD response in the orbitofrontal cortex (OFC) in normal volunteers in the post-satiety session.[49-51] Details regarding sensory specific satiety are mentioned in the next section.

1.8 Investigating sensory specific satiety in normal volunteers: An example of interventional Functional MRI study in olfaction

One of the ways in which food intake may be controlled is by a process called sensory specific satiety. When a food is eaten to satiety, its reward value decreases. This decrease is usually greater for the food eaten to satiety than for other foods. In a Functional MRI investigation, O'Doherty and colleagues[49] showed that in a region of the OFC (which also encodes pleasantness of odors[52]) activation produced by the odor of food just eaten to satiety decreased, whereas there was no similar decrease for the odor of a food not eaten in that meal. These findings were supported by a PET study demonstrating a larger increase of neuronal activity in the OFC and antero-medial lobe in obese patients compared to lean individuals who had just eaten a satiating amount of liquid meal.[53] Such sensory-specific satiety related activation in the OFC is not only specific for olfactory stimuli but also for taste and visual stimuli.

With the prevalence of obesity in current times and its associated health issues (NIH Obesity Research Task Force[54])., it is necessary to understand the brain mechanisms that control food intake. Hence, more interventional olfactory Functional MRI studies need to be done to further investigate the role of sensory specific satiety in controlling food intake. However, prior to an interventional study, reproducibility of the activation produced by the olfactory stimulation paradigm has to be verified.

The overall goal of this thesis was to set the stage for proper design, conduct and interpretation of treatment effects in olfactory interventional Functional MRI studies. The specific goal was to optimize the olfactory block stimulation paradigm and statistical model and then apply the two to an actual interventional study. The criteria for successful optimization in this thesis was (a) a block stimulation paradigm that would produce minimal or no desensitization in the response in the olfactory related brain areas and at the same time also evoke a response that is reproducible when repeated within a time frame of an hour and (b) to select a model to be used in a voxel-wise GLM analysis that best represented the underlying functional timeseries in olfactory related brain areas. This paradigm and model would then be used for stimulation and analysis respectively in a sensory specific satiety experiment involving normal volunteers (similar to O'Doherty[49]) to guarantee that the effect seen can most likely be considered as an interventional effect and not an effect created by confounds like desensitization.

CHAPTER 2   COMPARISON OF SUSTAINABILITY AND REPRODUCIBILITY BETWEEN BOLD SIGNAL CHANGES EVOKED BY CONTINUOUS VERSUS PULSED ODOR BLOCK PARADIGMS

During the first part of this thesis, the aim was to characterize different olfactory stimulation paradigms with the goal of selecting a paradigm that would provide a high, sustainable and reproducible BOLD response in olfactory related brain areas. Two different types of block paradigms, continuous and pulsed odor blocks were compared. No event-related paradigms were investigated in this work due to the ultimate goal of applying this experimental design to a clinical study (see Section 1.5).

2.1. Introduction

Block paradigms continue to be widely used in Functional MRI studies due to several advantages mentioned in the previous chapter especially their applicability in clinical settings. When applied to olfactory Functional MRI and electrophysiological studies, block paradigms have been found to cause desensitization in the primary olfactory areas, e.g., amygdala, piriform and entorhinal cortices.[55-58] When applied to an interventional study, this desensitization (within block and/or between sessions) can make it difficult to interpret the effect of the intervention. Some studies have tried to optimize their statistical models used in GLM analysis to account for the desensitization, thus showing marked improvement in the detection of activation in the primary olfactory areas.[56-58] Then there are other studies as well that have used non-statistical

approaches to reduce desensitization. Rather than presenting a continuous stream of an odorant, these studies pulsed an odorant within the on-block duration several times and interleaved the odorant pulses with periods of clean air.[42,44,59-64] This method takes advantage of the insensitivity of block designs to the shape of the BOLD response while reducing the total amount of odor presented. In this part of the thesis, the latter approach was used in an attempt to reduce desensitization by comparing BOLD responses from five olfactory block stimulation paradigms that systematically vary the manner in which odors are presented. This was done under the assumption that it may be better to reduce desensitization by first improving the manner in which the odors were presented and then finding an optimum way of modeling the functional data. The hypothesis was that as seen in olfactory evoked potential[65-69] and electro-olfactogram[70,71] experiments in humans, splitting the continuous odor block into pulses would reduce the effect of desensitization and would thus result in a sustained BOLD response albeit at the cost of peak BOLD response. Three different response parameters were selected to compare the BOLD responses of the five paradigms. These parameters i.e. (a) percent signal change (PSC) (b) time-to-peak (TTP) and (c) area under the curve (AUC), have been used successfully in many Functional MRI studies[72-75] to characterize BOLD response. In this study, PSC was used to compare the magnitude of the BOLD response across paradigms. TTP along with averaged peristimulus plots was used to determine whether the paradigms differ in their temporal dynamics. Lastly, the sustainability of the BOLD response of a paradigm was evaluated by the AUC parameter.

In lieu of the final aim of this dissertation, reproducibility of the response parameters was evaluated for each paradigm repeated across two sessions. This was done using an index of reproducibility of a measure called the coefficient of variation[76, 77] (CV). CV is expressed as the

ratio between the standard deviation and the mean. This method has been successfully applied in various studies to evaluate the reproducibility of neuroimaging data.[75, 78]

The specific hypothesis of this study was that the pulsed odor paradigms would have larger mean AUC (better sustainability) and lower CV (better reproducibility) than the continuous odor paradigm. However, for subsequent experiments in this thesis, the only paradigm with the best tradeoff between peak response, sustainability and reproducibility was implemented.

2.2. Materials and Methods

2.2.1 Subjects

Twelve healthy volunteers (8/12 males, average age= 30years [SD 6.43], 7 Asians and 5 Caucasians) participated in the Functional MRI study described here. Volunteers were nonsmokers and reported an absence of nasal or sinus complaints, allergies, and nasal deformities or obstruction. All volunteers had normal olfactory function (mean bilateral TDI score=36.82 [SD=3.38]) as assessed by Sniffin' Sticks odor threshold, discrimination and identification tests.[79-81] The Virginia Commonwealth University's Institutional Review Board approved the study and informed consent was obtained from all volunteers prior to the experiments.

2.2.2 Stimulus presentation

Two odor qualities, Banana and Cinnamon were used in this study. Isoamyl acetate (98%, Sigma-Aldrich, product no. 112674) and trans-Cinnamaldehyde (99+%, Sigma-Aldrich, product

no. 239968) were each dissolved in 1,2-Propanediol (99%, Acros, product no. 158720025) in a 1:10 ratio to produce samples for banana and cinnamon odors respectively. Choice of odorants was based on the aim of the final interventional study investigating sensory specific satiety. Banana and Cinnamon can both be considered as easily identifiable; both are rated as pleasant odors by most human subjects and can be used as pure chemicals without possible confounding influence of mixtures. Both odorants used were matched in intensity and pleasantness in a pre-test. Odorants were applied by a vapor-dilution olfactometer (Burghart OM4b, Hamburg, Wedel) at a constant flow rate of 140 ml/s, relative humidity of 80% and physiologic temperature of 37°C. This olfactometer allowed the presentation of chemical compounds without simultaneous activation of mechano- or thermoreceptors in the nasal mucosa. The olfactory stimuli were delivered while the subjects performed velo-pharyngeal closure.[71] Velo-pharyngeal closure was first practiced by subjects outside the scanner, using a mirror placed under their nostrils. The goal was to avoid producing mist on the mirror during breathing. After successful training, the subject was placed in the scanner. To ensure that the stimulation system was functioning correctly, a couple of 800ms duration stimuli of each odorant were presented to the subject before the start of each session and proper perception was tested.

2.2.3 Olfactory Stimulation Paradigms

Five different olfactory stimulation block paradigms (A1, A2, A3, A4, A5) were tested on five separate days. A simple Latin square design was used to counterbalance the use of a paradigm across subjects. On each day there were two functional scans acquired using the same paradigm separated by a gap of approximately 30 minutes. Each paradigm started with 20s of clean air and

had four 16s blocks of banana odor and four 16s blocks of cinnamon odor alternating with 32s blocks of clean air (see Fig.1.1).
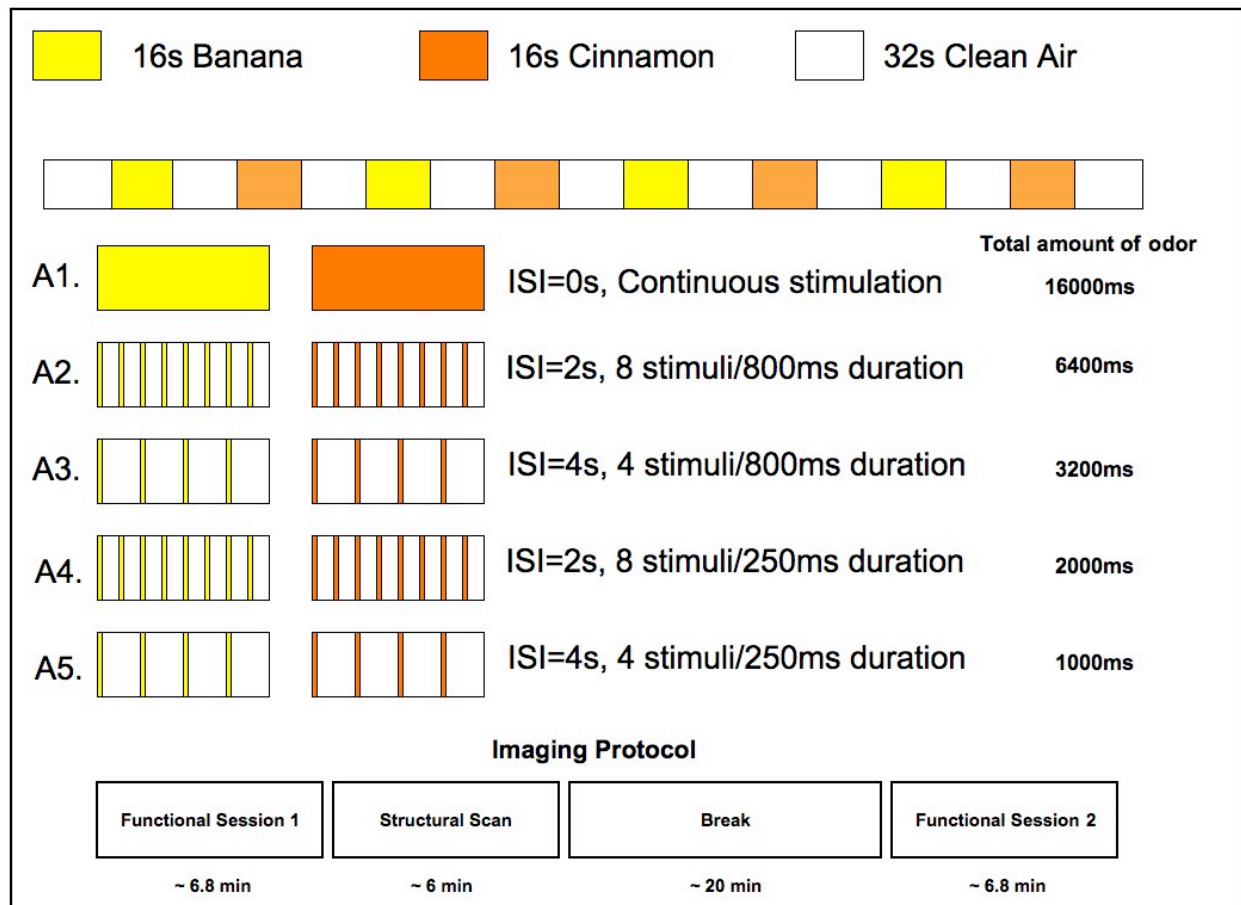
Figure 2-1: Illustration of the five olfactory stimulus block paradigms tested and the imaging protocol.

In paradigm A1, a continuous odor stimulus was provided to the left nostril of the subject for the entire 16s. As opposed to paradigm A1, the odor delivery within the on-blocks in the remaining four paradigms was pulsed. Paradigm A2 had eight pulses of 800ms duration separated by a 2s inter-stimulus interval (ISI) during the on-blocks, whereas paradigm A3 had four pulses of 800ms duration separated by an ISI of 4s. Paradigms A4 and A5 were the same as paradigms A2 and A3 except the pulse duration was 250ms.

The duration of the odor block used in previous olfactory Functional MRI studies has typically been in the 12s - 32s range.[57, 58, 82, 83] Similar to these studies, the choice of 16s block duration in this experiment was based on a tradeoff between high BOLD response and desensitization due to longer duration blocks. The 16s block duration was split in a systematic fashion by using either 4 stimuli or 8 stimuli and also by using either 800ms stimuli or 250ms stimuli; thus forming 4 different paradigms in addition to the continuous odor paradigm (see Fig. 2-1). The choice of the number of within-block stimuli and within-block stimulus duration comes from previous electrophysiological[67, 71] and neuroimaging [82-84] olfactory studies.

2.2.4 Data Acquisition

The volunteers were scanned using a GE-3T Signa magnet. A vacuum pillow was molded around the subject's head to minimize motion. Functional images were obtained with a T2*-sensitive spiral in/out sequence. This sequence was specifically designed to increase both signal to noise (SNR) and BOLD contrast to noise ratio (CNR) in Functional MRI.[34] The spiral sequence functional acquisition used an echo time (TE) of 30 ms, TR 2000 ms, flip angle 90°, field of view 240 cm, and an image matrix of 64 x 64. The in-plane resolution was 3.75 mm x 3.75 mm. Approximately, twenty-eight 4-mm-thick slices with no gap covering the whole brain were acquired with a slice orientation of 30° clockwise to the anterior commissure to posterior commissure (AC–PC) plane. This slice orientation was chosen to minimize signal dropout in the orbital frontal and medial temporal areas due to in-plane susceptibility gradients.[85] Each Functional MRI scan consisted of a total of 202 temporal volumes. The onset of the stimulus presentation automatically triggered the image acquisition. The first five frames were automatically discarded from the Functional MRI dataset. This eliminated transients arising

before the achievement of a dynamic equilibrium. The first Functional MRI scan was followed by the acquisition of an anatomical image using a T1-weighted 3D spoiled gradient recalled (3DSPGR) pulse sequence with an echo time of 2 ms, TR of 15 ms, flip angle of 20°, field of view of 240 mm, imaging matrix of 256 x 256, and 124 contiguous slices with 1.2 mm slice thickness used to co-register the Functional MRI data.

Each subject participated in two sessions on the same day. After the first session, the subject was taken out of the scanner and was given a 20-minute break. During an interventional study, the intervention would be delivered during this time. However, in this study, no intervention took place and the data from the 2nd session was used to test the reproducibility of the response in each paradigm without intervention. Respiratory and cardiac signals were recorded from the subject (LabView 7.1, National Instruments Corp.) for every functional scan and were later used for offline image correction. All subjects were asked to keep their eyes closed[83] and maintain velo-pharyngeal closure for the entire duration of the functional scan. They were provided with white noise through MR-compatible headphones to mask out the switching sound produced at odor onset as well as to reduce the loud gradient switching sounds. An alarm bell was also provided to the subject in case he/she needed to come out of the scanner urgently during the scan. After each functional scan, the subjects were asked to rate the overall intensity and pleasantness of banana and cinnamon odors on a continuous scale of -2 to +2. This ratings scale was also used in the previously cited study conducted by O'Doherty[49] and colleagues.

2.2.5 Preprocessing of Functional MRI data

As a first step, using the retrospective image-based correction[18] (RETROICOR), physiological noise was minimized in the functional images. Next, the functional images for each individual subject were preprocessed with the FMRI Expert Analysis Tool (FEAT) from FMRIB's Software Library (FSL), version 5.98 (www.fmrib.ox.ac.uk/fsl). The functional images were then motion-corrected using McFLIRT.[86] Motion correction results for each subject were closely observed to look for any absolute or relative motion exceeding 1.5mm. However, motion was found to be minimal and hence no scans were discarded. After the motion correction, non-brain tissue was removed from both functional and high-resolution images using FSL's brain extraction tool[87] (BET). After that, the functional images were spatially smoothed with a Gaussian kernel having a full width at half maximum (FWHM) of 6 mm and were temporally smoothed using a high pass filter with a cutoff of 60s. Finally, the functional images were co-registered to subject-specific high-resolution images and spatially normalized into standard Talairach space[88] using the FSL normalization algorithm.[86]

2.2.6 Selection of Regions of interest (ROIs)

ROIs of primary and secondary olfactory areas were selected a priori and used to extract the time series information from the functional MRI data within them. Separate ROIs were selected instead of a combined mask of the olfactory areas since the temporal profiles of primary and secondary areas have been previously reported to be different.[56-58]
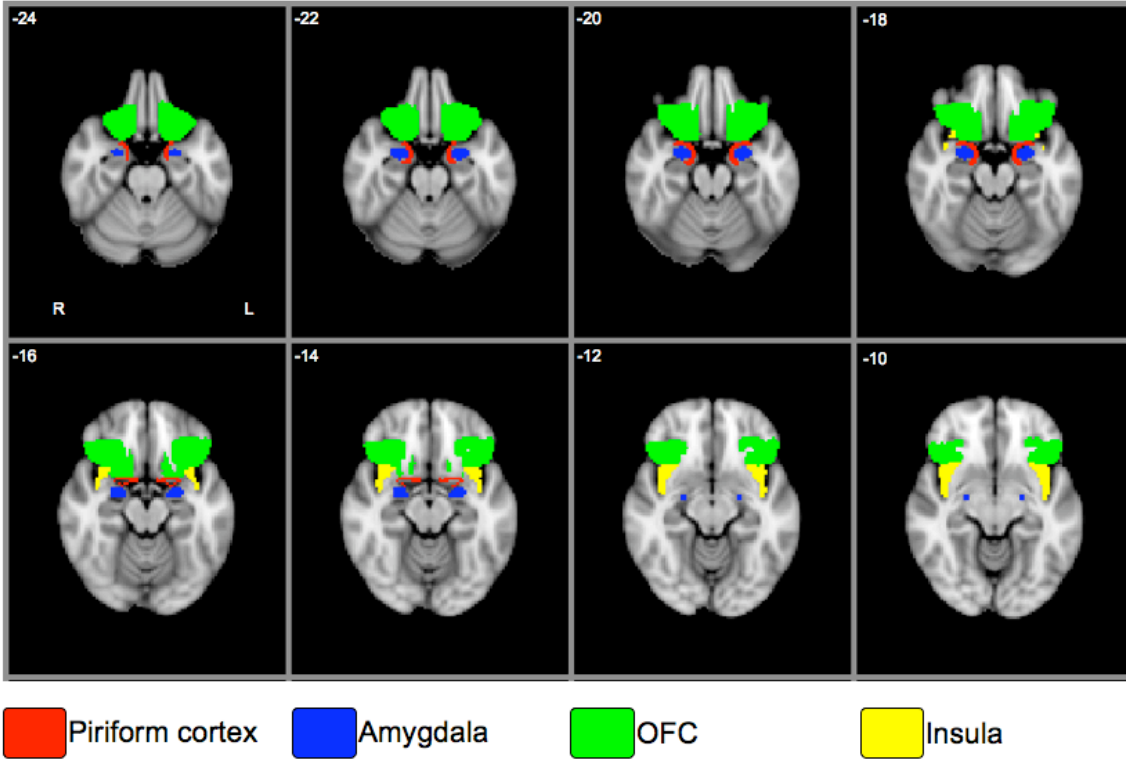
Figure 2-2: Regions of interest representing the primary and secondary olfactory cortical areas were selected a-priori for extracting timeseries data.

Two primary olfactory areas: Piriform cortex (PIR) and Amygdala (AMY) and two secondary olfactory areas: Orbitofrontal cortex (OFC) and Insular cortex (INS) were chosen for further data analysis (Fig.1.2). OFC and INS ROIs were created by thresholding (>50) the Harvard-Oxford Cortical probabilistic structural (HOC) atlases, which is part of FMRIB's Software Library. PIR and AMY ROIs were created from the Pickatlas software[89] and were based on the Automated Anatomical Labeled Atlas[90] because these regions were not available in the HOC atlas. The ROIs selected were transformed to each individual subject's functional MRI space using the transformation matrix created during the normalization process.

2.2.7 Data analysis

The following analysis was conducted separately for each paradigm, subject, session and ROI. For each voxel, the baseline was calculated by averaging the intensity value of three time points preceding the start of a stimulation block. The percent signal change at each time point within a 20s window (10 time points from stimulation onset) was then calculated by subtracting the baseline intensity from the intensity at that time point, dividing the result by the baseline intensity and multiplying this result by 100. In this manner, eight 20s epochs of percent signal change were obtained per voxel. Each of these eight epochs was averaged separately across all the voxels within a particular ROI. It is important to note that (a) the baseline used was a pre-stimulation block average as opposed to an average across all the time points within a run. Conceptually, the pre-stimulation block average method is the more accurate one, although the choice of either baseline calculation methods does not typically cause drastic changes in percent signal change calculation. (b) The percent signal change values were calculated for each voxel separately and then averaged across voxels as opposed to timeseries intensity averaging across voxels first. The latter method would have allowed voxels with low baseline intensity (caused by, for e.g. inhomogeneity) to affect the average timeseries of the ROI.

Various temporal parameters were then extracted from each 20s percent signal change epoch. Peak signal change (PSC) was chosen as the most positive peak within the 20s epoch. Time to peak (TTP) was computed by multiplying the number of frames occurring from the stimulus onset to the most positive peak, by 2s (TR). The integral of the area (AUC) subtended by the BOLD response was calculated within the 20s window. As mentioned in the introduction of this chapter, PSC will enable the comparison of the magnitude of the BOLD signal across paradigms,

TTP along with averaged peristimulus plots will indicate if the paradigms differ in their temporal dynamics and the sustainability of a paradigm will be evaluated by AUC.

Reproducibility of each paradigm was computed based on the intra-subject (session 1 and session 2) temporal parameters (PSC, TTP, AUC). First, for each subject, the fractional difference between the parameters of session 1 and session 2 were computed, defined as a percentage difference relative to the mean (Δ) (Eq. 1);

$$\Delta = \frac{100\ (x_1-x_2)}{x_{avg}} \qquad (1)$$

where x_1 and x_2 are the parameters acquired in session 1 and session 2 respectively, and x_{avg} is the mean of the two values. The mean of this difference (Δ_{mean}) provides information about any order effects that may exist across sessions for a particular parameter (e.g., PSC greater in session 1 than session 2) and the standard deviation (σ_Δ) of these Δ values provides information about the reproducibility of the measurement.[78] We computed intra-subjects variability (CV_{intra}) as:

$$CV_{intra} = \frac{100\sigma_\Delta}{\sqrt{2}} \qquad (2)$$

where the σ_Δ has been adjusted by dividing it by square root of 2 (Eq. 2).[75,78] A CV value of 33% can be used as the upper fiducial limit for acceptable variability in a normal distribution.[91]

2.2.8 Statistical Analyses

Subjective Ratings:

Separate paired t-tests were conducted to see if there were any significant differences in the perceived intensity and pleasantness ratings between the two odorants and between the two sessions for each odorant. A one-way analysis of variance with repeated measures was conducted for each session separately to see if there were any significant differences in the ratings between the five paradigms.

Parameters from preprocessed timeseries data:

All statistical analysis mentioned in this section were performed on each ROI separately. A paired t-test was used to test if there were any significant difference between the Banana and Cinnamon PSC in any of the paradigms. One-way analysis of variance with repeated measures (Factor: Paradigm, Levels: 5) was applied separately to all computed parameters (PSC, TTP and AUC) using SPSS16 (SPSS Inc., Chicago, USA) to find significant differences between the five paradigms for each parameter. Wherever significant differences were found, the paradigms were tested for linear, quadratic or cubic trends and also pairwise multiple group comparisons were done.

In order to identify any significant order effects (the case where one session's mean is consistently higher than the other) paired t-tests were performed between the parameters from session 1 and session 2. Reproducibility of a measure was assessed with a repeated measures analysis of variance with five levels (A1 to A5) to determine if Δ differed significantly between the five paradigms.

Additional analysis

An additional parameter, Fall Time (FT), was extracted from each paradigm. It was defined as the first time point within the 20s epoch after the peak, when the response drops to below baseline level and stays below till the end of the epoch. Additionally, a timeseries regression analysis was performed by using a 16s square wave model convolved with a double-gamma HRF to model the timeseries of each paradigm in a voxelwise manner. The average regression coefficient (Beta) was extracted from each paradigm. Also, the number of active voxels were extracted after thresholding ($z=2.3$ and cluster p-threshold of 0.05) the statistical maps generated after regression.

2.3. Results

2.3.1 Subjective Ratings

Two-tailed paired t-tests revealed no significant differences in the intensity and pleasantness ratings between Banana and Cinnamon odors in either session of all paradigms.

(a)
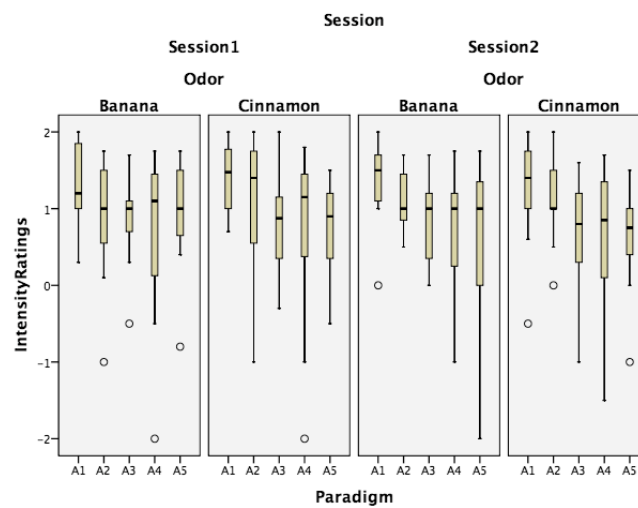
(b)
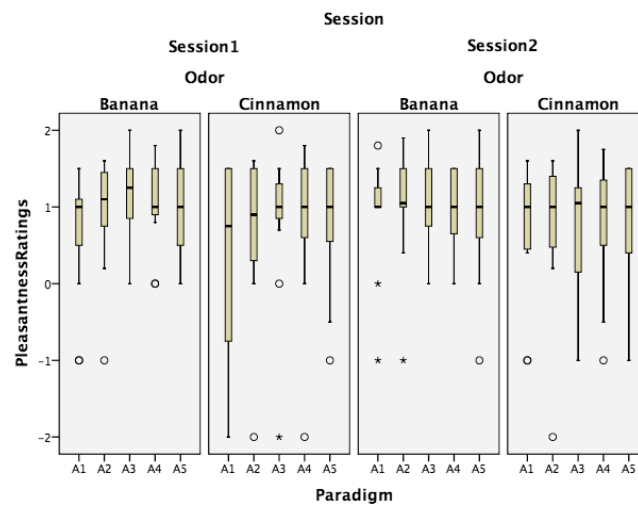
Figure 2-3: (a) Box plots showing intensity and (b) pleasantness ratings for Banana and Cinnamon odors after each Functional MRI session for paradigms A1 to A5 using a ratings scale for Intensity (+2 = very intense, 0 = moderate, -2 = very weak) and for Pleasantness (+2 = very pleasant, 0 = neutral, -2 = very unpleasant).

There were no significant differences in subjective ratings of the two odors between *session 1* and *session 2*. The subjective ratings are summarized in Fig. 2-3.

Intensity ratings comparison:

In *session 1*, a comparison of the intensity ratings using a one-way analysis of variance for repeated measures did not show a significant difference between the five paradigms for either banana or cinnamon. However, in *session 2* there was a significant difference between the five paradigms in banana ($F(1,4)=4.804, p=0.003$) and cinnamon intensity ratings ($F(1,4)=3.064$, $p=0.026$). The ratings of the five paradigms were found to have a significant linear trend (Banana: $F=13.94$, $p=0.003$; Cinnamon: $F(1,4)=3.064$, $p=0.026$). Group comparison contrasts revealed significant differences between individual paradigms for banana: A1>A3 ($p=0.014$); A1>A4 ($p=0.007$); A1>A5 ($p=0.006$) and cinnamon: A1>A5 ($p=0.021$).

Pleasantness ratings comparison:

A comparison of the pleasantness ratings using a one-way analysis of variance for repeated measures did not show any significant differences between the five paradigms in either odors or sessions.

2.3.2 ROI Analysis of timeseries data

Paired t-tests revealed no significant differences in PSC between banana and cinnamon odors in any ROI, session or paradigm. Therefore, all the parameters extracted from the timeseries data corresponding to these two odors were averaged within each session for further analyses.

The peristimulus plots of mean percent signal change (Fig. 2-4) in the primary olfactory areas

show desensitization in all paradigms in both sessions. It was observed that the mean percent signal change in primary olfactory areas peaks at ~7-8s after which it rapidly falls to baseline levels at ~11-12s. Similarly, in the secondary olfactory areas, the mean percent signal peaks at ~7-8s but the response appears to be more sustained than in primary olfactory areas. The mean percent signal change in all the paradigms was below 0.5% with A1 and A2 paradigms evoking the highest peak response.

(a)

(b)

(c)

(d)
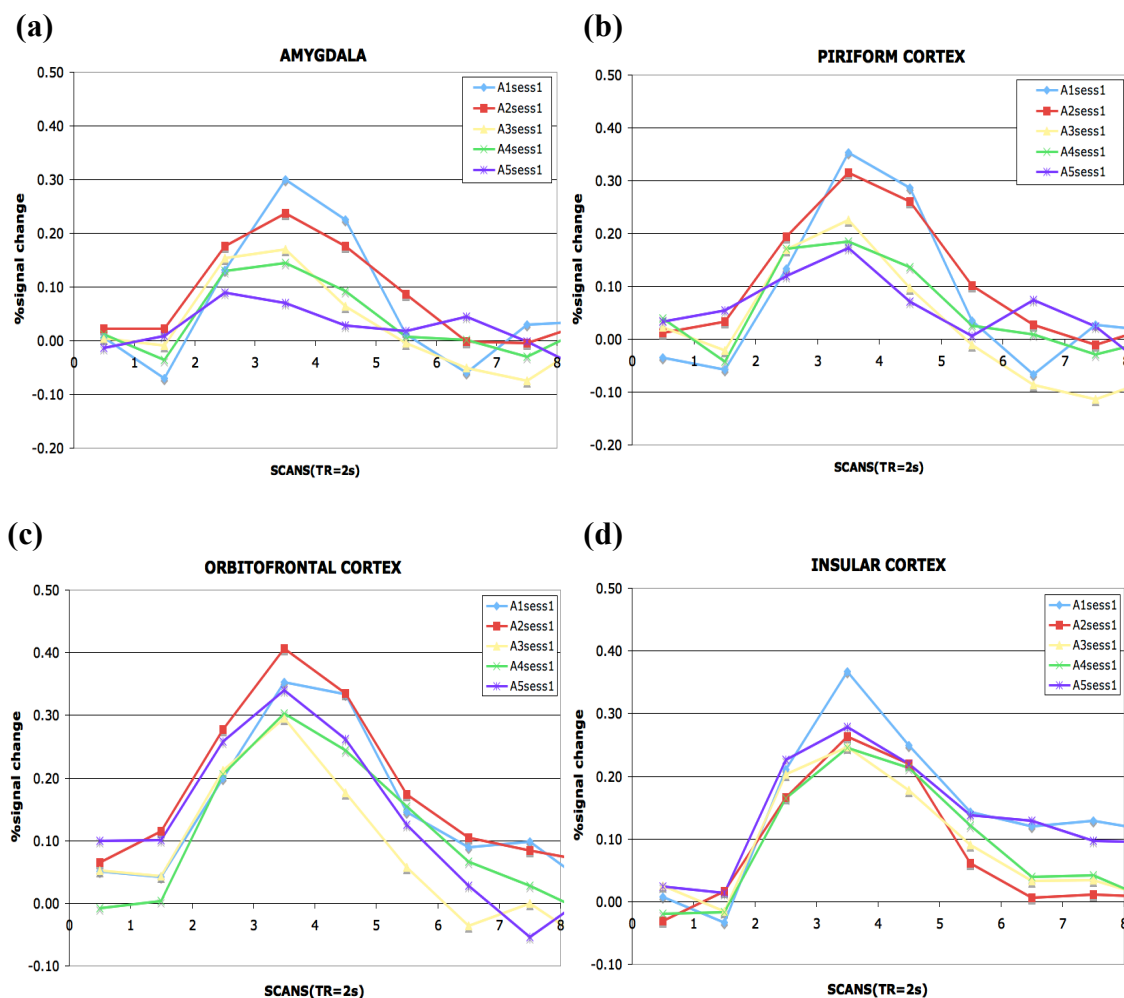
Figure 2-4: Peristimulus plots of mean percent signal change from **primary** (a, b) and **secondary** (c, d) olfactory brain areas. (Only session 1 results are shown).

The comparative results of PSC, AUC, TTP, Δ and CV_{intra} values between the five paradigms are presented below for individual regions of interest. A repeated measures analysis of variance using PSC, AUC, TTP and Δ as independent measures and paradigm as within-subjects factor with five levels was implemented separately on each region of interest to find differences between the five paradigms. Due to the large number of comparisons the results shown below are in the following format and order: *Plots of mean parameter, Table of Δ and CV_{intra} values, Result of the repeated measures analysis of variance, Result of the linear trend test and the Result of multiple comparisons test.*

1. AMYGDALA

(a)
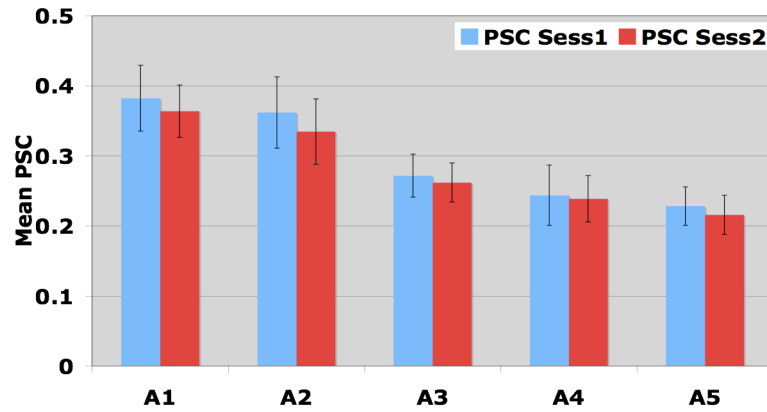
(b)
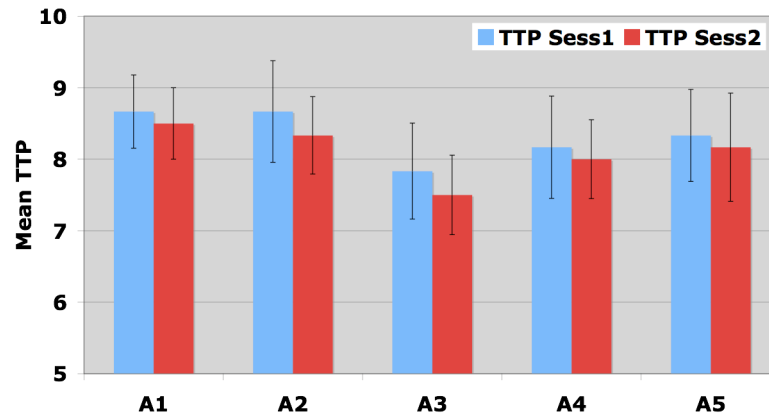
(c)

Figure 2-5: Plots of mean PSC (a), TTP (b) and AUC (c) values for session 1 (blue) and session 2 (red) of the five olfactory stimulation paradigms in **Amygdala** ROI. The PSC and AUC values were significantly different between the paradigms in both sessions. (PSC=Peak Signal Change; TTP=Time To Peak; AUC=Area Under the Curve)

	PSC			TTP			AUC		
	Δ_{mean} (%)	SD	CV_{intra}	Δ_{mean} (%)	SD	CV_{intra}	Δ_{mean} (%)	SD	CV_{intra}
A1	2.26	21.43	15	1.85	23.58	17	3.96	34.78	25
A2	10.03	23.20	16	2.54	29.57	21	12.23	35.47	25
A3	2.07	23.26	16	2.00	31.06	22	4.10	42.86	30
A4	-4.35	27.55	19	0.65	36.80	26	-3.87	45.14	32
A5	3.56	36.77	26	2.25	37.20	26	5.60	47.16	33

Table 2-1: The mean and standard deviation of Δ along with the coefficient of variation between sessions (CV_{intra}) for each paradigm is reported for PSC, TTP and AUC parameters in **Amygdala**. (PSC=Peak Signal Change; TTP=Time To Peak; AUC=Area Under the Curve)

Session 1

PSC: Significant differences found (F(1,4)=3.575, p=0.013); Significant linear trend found (F=9.827, p=0.009);

Multiple comparisons: A1>A5(p=0.012), A2>A5(p=0.051).

TTP: No significant differences found.

AUC: Significant differences found (F(1,4)=4.243, p=0.005); Significant linear trend found (F=12.905, p=0.004);

Multiple comparisons: A1>A3(p=0.015), A1>A4(p=0.046),A1>A5(p=0.002); A2>A3(p=0.034); A2>A5(p=0.015).

Session 2

PSC: Significant differences found (F(1,4)=3.725, p=0.011); Significant linear trend found (F=11.436, p=0.006);

Multiple comparisons: A1>A4(p=0.027), A1>A5(p=0.013), A2>A5(p=0.027)

TTP: No significant differences found.

AUC: Significant differences found (F(1,4)=3.437, p=0.016); Significant linear trend found (F=8.517, p=0.014);

Multiple comparisons: A1>A3(p=0.031), A1>A4(p=0.026),A1>A5(p=0.019); A2>A3(p=0.025).

2. PIRIFORM CORTEX

(a)
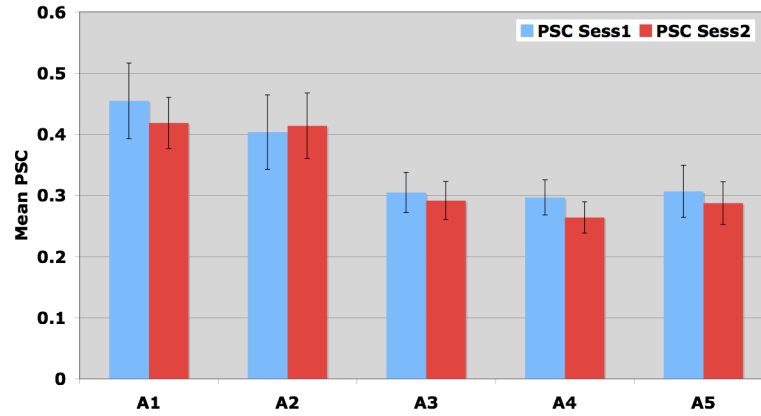
(b)
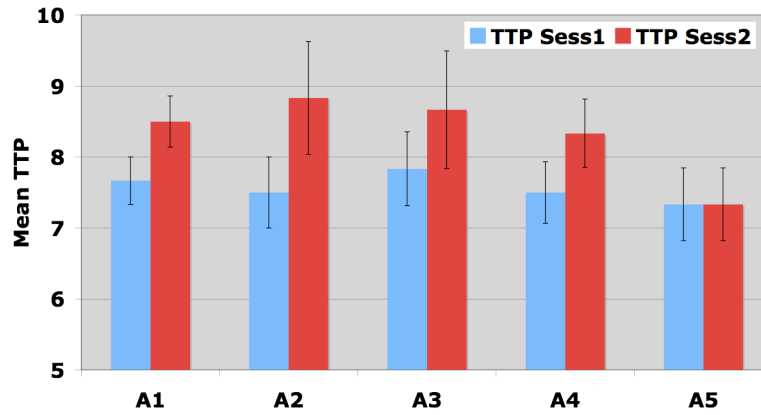
(c)

Figure 2-6: Plots of mean PSC (a), TTP (b) and AUC (c) values for session 1 (blue) and session 2 (red) of the five olfactory stimulation paradigms in **Piriform cortex** ROI. The PSC and AUC values were significantly different between the paradigms in both sessions. (PSC=Peak Signal Change; TTP=Time To Peak; AUC=Area Under the Curve)

	PSC			TTP			AUC		
	Δ_{mean} (%)	SD	CV_{intra}	Δ_{mean} (%)	SD	CV_{intra}	Δ_{mean} (%)	SD	CV_{intra}
A1	-0.95	36.09	26	-10.19	23.12	16	-11.57	36.00	25
A2	-6.79	21.72	15	-13.80	31.81	22	-20.21	32.48	23
A3	4.20	26.87	19	-8.66	28.88	20	-4.47	42.52	30
A4	11.27	15.50	11	-10.38	30.49	22	0.73	37.70	27
A5	3.92	34.20	24	-0.16	29.36	21	3.55	46.34	33

Table 2-2: The mean and standard deviation of Δ along with the coefficient of variation between sessions (CV_{intra}) for each paradigm is reported for PSC, TTP and AUC parameters in the **Piriform Cortex**. (PSC=Peak Signal Change; TTP=Time To Peak; AUC=Area Under the Curve)

Session1

PSC: Significant differences found ($F_{(1,4)}$=2.553, p=0.052); Significant linear trend found (F=5.854, p=0.034);

Multiple comparisons: A1>A3(p=0.043), A1>A4(p=0.04).

TTP: No significant differences found.

AUC: Significant differences found ($F_{(1,4)}$=2.521, p=0.055); Significant linear trend found (F=5.349, p=0.041);

Multiple comparisons: A1>A4(p=0.037).

Session2

PSC: Significant differences found ($F_{(1,4)}$=4.785, p=0.003); Significant linear trend found (F=10.743, p=0.007);

Multiple comparisons: A1>A3(p=0.016), A1>A4(p=0.009), A1>A5(p=0.038), A2>A3(p=0.012), A2>A4(p=0.034), A2>A5(p=0.03).

TTP: No significant differences found.

AUC: Significant differences found ($F_{(1,4)}$=5.26, p=0.001); Significant linear trend found (F=12.236, p=0.005);

Multiple comparisons: A1>A3(p=0.04), A1>A4(p=0.021), A1>A5(p=0.019), A2>A3(p=0.016), A2>A4(p=0.023), A2>A5(p=0.01).

3. ORBITOFRONTAL CORTEX
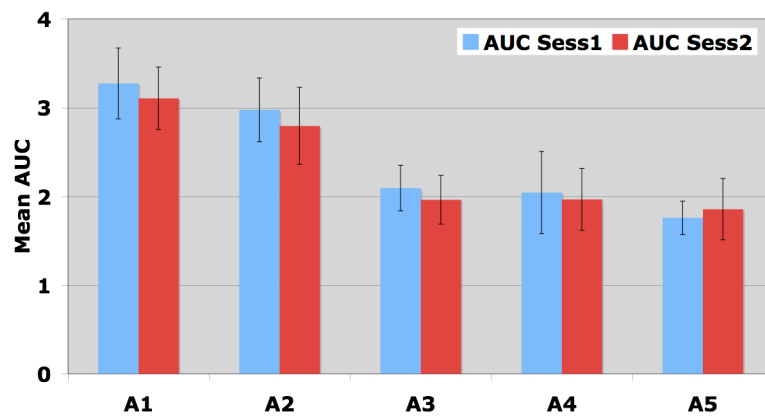
(a)
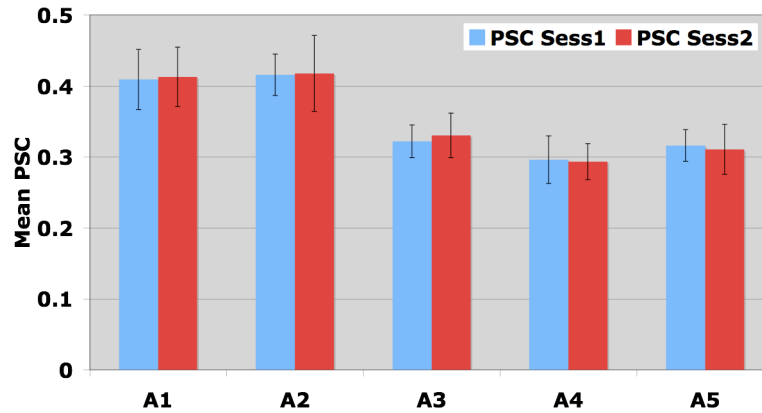
(b)
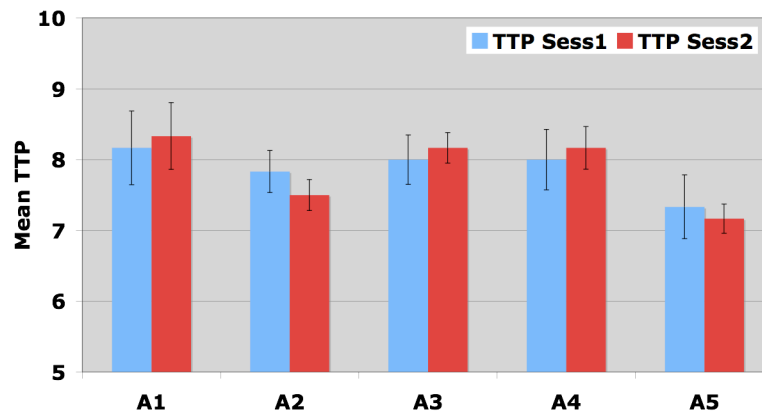
(c)
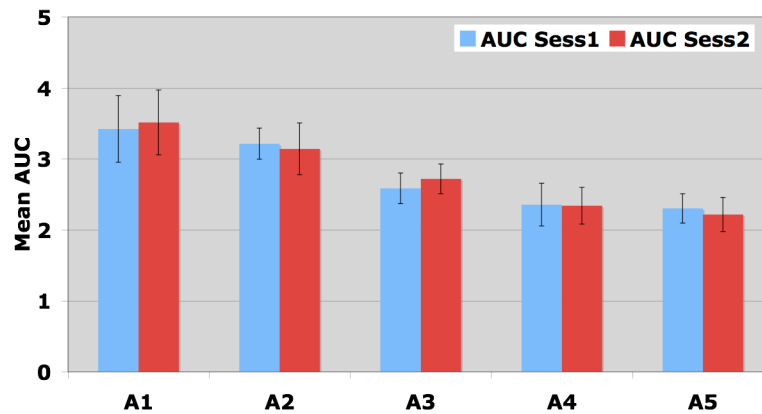
Figure 2-7: Plots of mean PSC (a), TTP (b) and AUC (c) values for session 1 (blue) and session 2 (red) of the five olfactory stimulation paradigms in **Orbitofrontal cortex** ROI. The PSC and AUC values were significantly different between the paradigms in both sessions. (PSC=Peak Signal Change; TTP=Time To Peak; AUC=Area Under the Curve)

	PSC			TTP			AUC		
	Δ_{mean} (%)	SD	CV_{intra}	Δ_{mean} (%)	SD	CV_{intra}	Δ_{mean} (%)	SD	CV_{intra}
A1	-2.79	28.42	20	-3.31	24.55	17	-6.01	31.67	22
A2	1.13	28.44	20	6.15	28.78	20	6.76	45.02	32
A3	-3.25	25.54	18	-2.38	17.50	12	-5.34	33.83	24
A4	-0.08	25.14	18	-2.38	19.90	14	-2.47	26.66	19
A5	2.95	24.28	17	2.22	30.51	22	5.23	30.26	21

Table 2-3: The mean and standard deviation of Δ along with the coefficient of variation between sessions (CV_{intra}) for each paradigm is reported for PSC, TTP and AUC parameters in the **Orbitofrontal Cortex**. (PSC=Peak Signal Change; TTP=Time To Peak; AUC=Area Under the Curve)

Session 1

PSC: Significant differences found ($F_{(1,4)}$=3.987, p=0.008); Significant linear trend found (F=7.788, p=0.018);

Multiple comparisons: A2>A3(p=0.018), A2>A4(p=0.01), A2>A5(p=0.005).

TTP: No significant differences found.

AUC: Significant differences found ($F_{(1,4)}$=3.41, p=0.016); Significant linear trend found (F=7.158, p=0.022);

Multiple comparisons: A1>A4(p=0.045), A2>A3(p=0.037), A2>A4(p=0.028), A2>A5(p=0.006).

Session 2

PSC: Significant differences found ($F_{(1,4)}$=3.927, p=0.008); Significant linear trend found (F=12.284, p=0.005);

Multiple comparisons: A1>A4(p=0.01), A1>A5(p=0.036), A2>A4(p=0.015), A2>A5(p=0.034).

TTP: No significant differences found.

AUC: Significant differences found ($F_{(1,4)}$=3.27, p=0.02); Significant linear trend found (F=10.522, p=0.008);

Multiple comparisons: A1>A4(p=0.006), A1>A5(p=0.03), A3>A5(p=0.045).

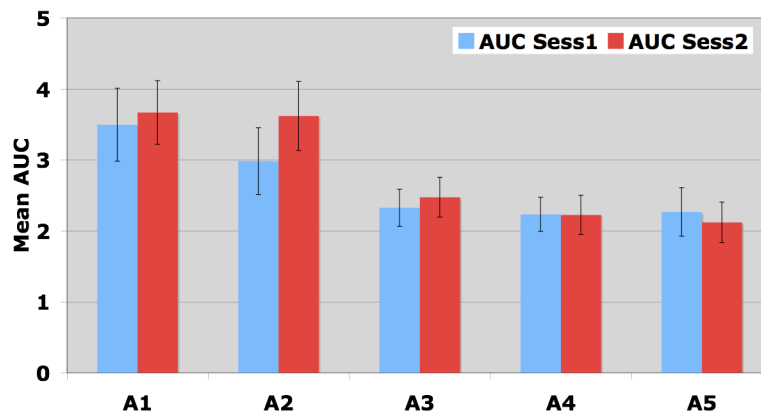# 4. Insular Cortex

(a)
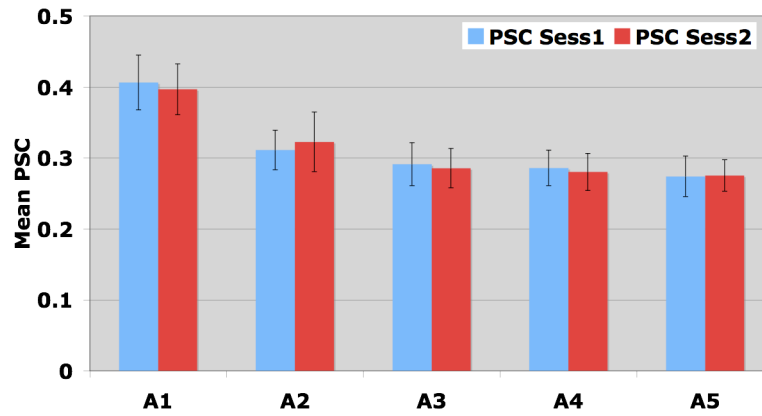
(b)
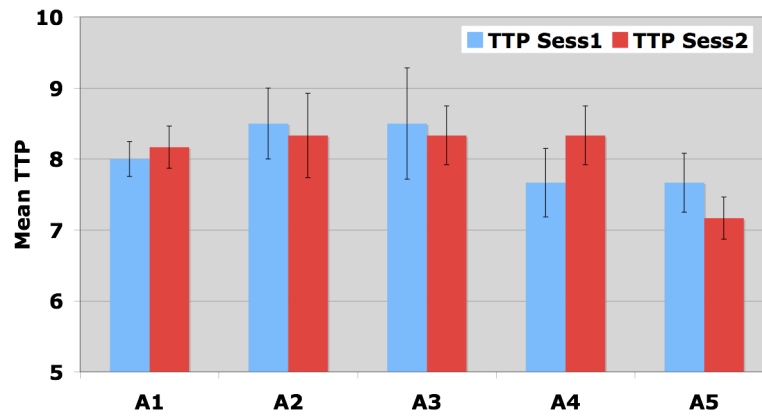
(c)
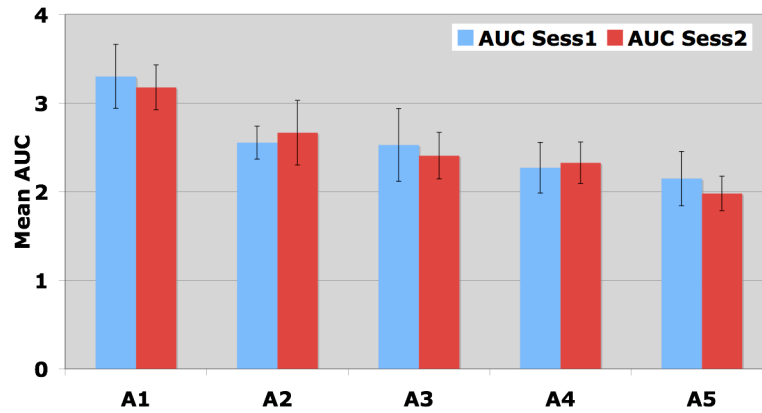
Figure 2-8: Plots of mean PSC (a), TTP (b) and AUC (c) values for session 1 (blue) and session 2 (red) of the five olfactory stimulation paradigms in **Insular cortex** ROI. The PSC and AUC values were significantly different between the paradigms in both sessions. (PSC=Peak Signal Change; TTP=Time To Peak; AUC=Area Under the Curve)

	PSC			TTP			AUC		
	Δ_{mean} (%)	SD	CV_{intra}	Δ_{mean} (%)	SD	CV_{intra}	Δ_{mean} (%)	SD	CV_{intra}
A1	1.46	21.68	15	-1.79	19.69	14	-0.37	25.27	18
A2	1.89	35.83	25	2.43	30.07	21	3.95	40.13	28
A3	1.36	31.32	22	-0.39	25.31	18	0.68	37.99	27
A4	2.52	35.69	25	-9.45	22.37	16	-5.64	46.02	33
A5	-2.81	41.29	29	6.08	23.85	17	2.81	46.61	33

Table 2-4: The mean and standard deviation of Δ along with the coefficient of variation between sessions (CV_{intra}) for each paradigm is reported for PSC, TTP and AUC parameters in the **Insular Cortex**. (PSC=Peak Signal Change; TTP=Time To Peak; AUC=Area Under the Curve)

Session1

PSC: Significant differences found ($F(1,4)=4.257$, $p=0.005$); Significant linear trend found ($F=7.314$, $p=0.02$);

Multiple comparisons: A1>A2($p=0.021$),A1>A3($p=0.002$), A1>A4($p=0.008$), A1>A5($p=0.015$).

TTP: No significant differences found.

AUC: Significant differences found ($F(1,4)=2.499$, $p=0.056$); Significant linear trend found ($F=5.74$, $p=0.035$);

Multiple comparisons: A1>A2($p=0.028$),A1>A3($p=0.03$), A1>A4($p=0.013$), A1>A5($p=0.036$).

Session2

PSC: Significant differences found ($F(1,4)=5.139$, $p=0.002$); Significant linear trend found ($F=14.46$, $p=0.003$);

A1>A2($p=0.044$),A1>A3($p=0.0002$), A1>A4($p=0.011$), A1>A5($p=0.0003$).

TTP: No significant differences found.

AUC: Significant differences found ($F(1,4)=4.248$, $p=0.005$); Significant linear trend found ($F=23.431$, $p=0.001$);

Multiple comparisons: A1>A3($p=0.003$), A1>A4($p=0.021$), A1>A5($p=0.00002$).

The intra-subject reproducibility of PSC, TTP and AUC values in Amygdala, Piriform Cortex, Orbitofrontal Cortex and Insular Cortex are summarized in Tables 2-1 – 2-4 respectively, in terms of the mean and standard deviation of the fractional difference between the two sessions ($\Delta_{mean}\pm SD$) and the coefficient of variation between sessions (CV_{intra}). Positive values of Δ_{mean} would indicate a larger parameter value in session 1 compared to session 2 and vice versa. However, the Δ_{mean} values were low for all the paradigms. Furthermore, two-tailed paired t-tests did not show significant differences between the two sessions in any paradigm. The repeated measures analysis of variance using Δ as an independent measure and the paradigm as within-subjects factor with three levels, confirmed that there was no significant difference in Δ between the paradigms in any of the ROIs. CV_{intra} values for all the paradigms were well below the fiducial level of 33% for all the parameters. This indicated that all paradigms showed low variability in measurements across sessions. Lastly, Fig. 2-5 – 2-8 also indicate only small differences between the parameters of session 1 and session 2.

Fall Time

In piriform cortex (Fig. 1-8a), a one-factor analysis of variance between paradigms revealed significant differences ($F(1,4)=5.48$, $p=0.0013$) in FT between paradigms and multiple comparisons showed that FT in A1 and A2 were significantly greater than A3, A4 and A5. In OFC (Fig.1.8b), a one-factor analysis of variance between paradigms revealed near significant differences ($F(1,4)=2.71$, $p=0.051$) in FT between paradigms and multiple comparisons showed that FT in A1 and A2 were significantly greater than A3, A4 and A5. These results were another indication that A1 and A2 were more sustainable than the remaining paradigms.

(a)
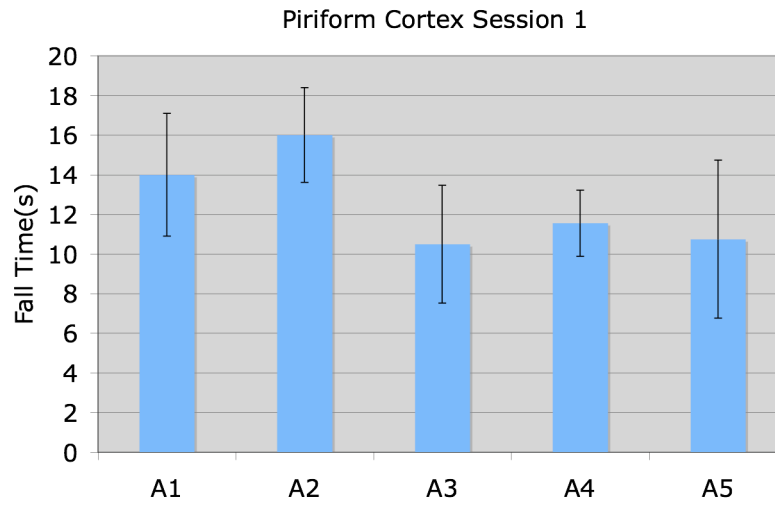
(b)
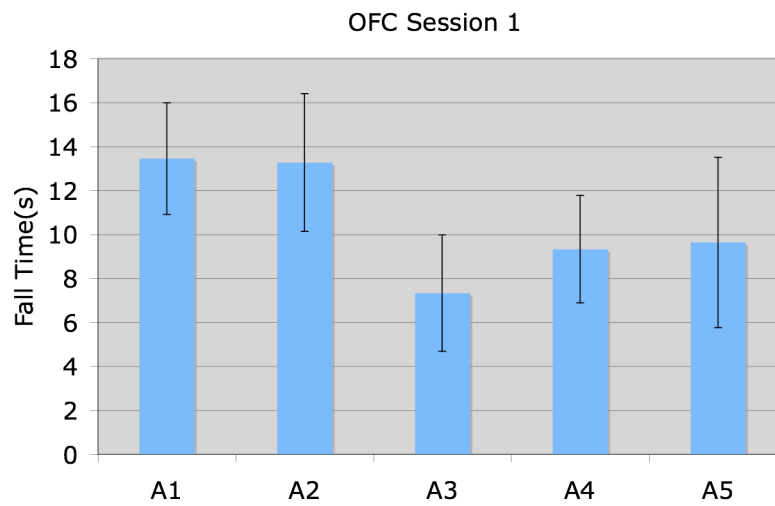
Figure 2-9: Fall Time(s) across paradigms shows that the BOLD response in A1, A2 stayed above baseline levels for a significantly longer duration than A3, A4 and A5 in **primary (a) and secondary (b)** olfactory brain areas.

Mean Beta

A timeseries regression analysis on each paradigm was performed using a 16s square wave model convolved with a double-gamma HRF. The model-fit parameter (Beta) was highest in A1 and A2 in both piriform cortex and OFC (Fig. 2-10). Keeping a nominal threshold of $z=2.3$ and cluster p-threshold of 0.05, it was found that in the Piriform Cortex, only A1 produced any active voxels (59 voxels). Again, only A1 produced active voxels in the OFC (397 voxels). Although the efficacy of the 16s-model was not tested, these results do suggest that the detectability of activation may be higher in A1 as compared to other paradigms.

(a)
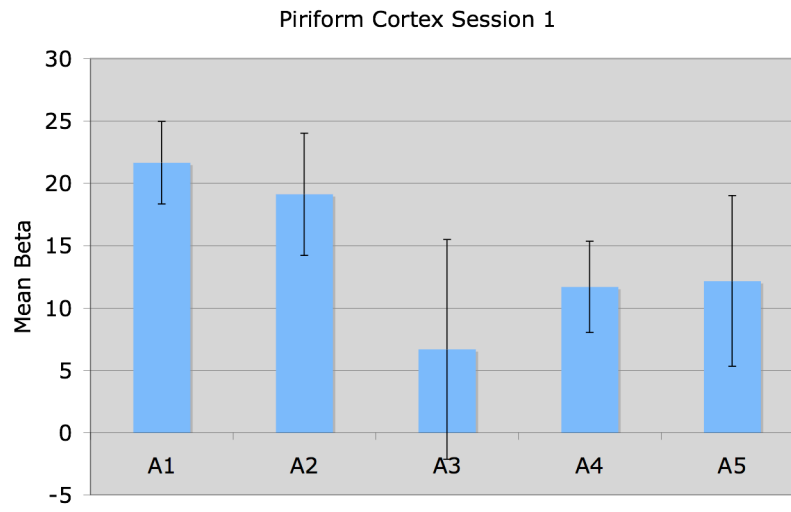
(b)
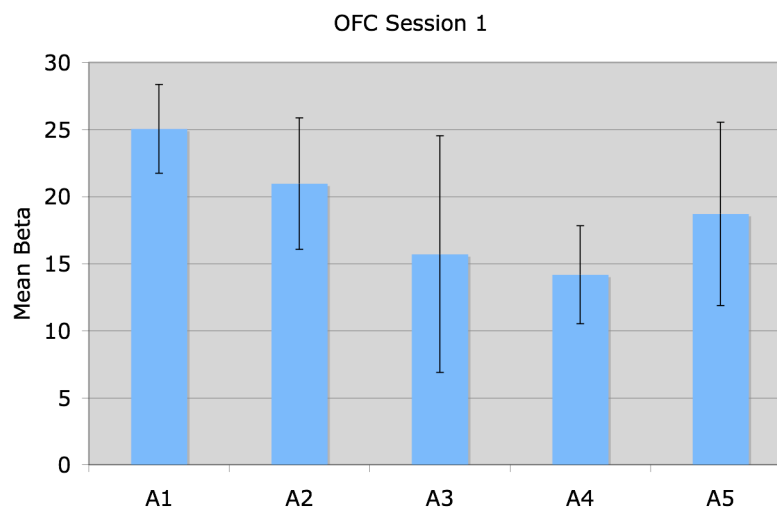
Figure 2-10: Higher Beta associated with A1 in **primary (a) and secondary (b)** olfactory brain areas after timeseries regression analysis with a 16s square wave convolved with double-gamma HRF. The number of voxels that passed thresholding was also the highest in A1 and A2 in this preliminary regression analysis. Note: Model used may not be the optimized model.

2.4. Discussion

The goal of the current study was to select a paradigm that evoked a BOLD response that was not only high in magnitude but was also sustainable and reproducible, so that this optimized paradigm could eventually be used in an interventional study (final goal of this dissertation). One paradigm with continuous odor blocks and four paradigms with pulsed odor blocks were used to test the hypothesis that BOLD response evoked by pulsed odor paradigms would be more sustainable and reproducible as compared to continuous odor paradigms possibly due to less desensitization caused by the former. Two primary olfactory ROIs (Amygdala, Piriform Cortex) and two secondary olfactory ROIs (Orbitofrontal Cortex, Insular Cortex) were chosen for ROI analysis. The choice was based on their functionality in olfactory processing demonstrated by electrophysiological[92-95] and neuroimaging studies.[49, 59, 62, 63, 96-103]

Averaged peristimulus plots from session 1 timeseries data (Fig. 2-4) illustrate that desensitization of BOLD response is not only seen in the continuous odor paradigm (A1) but in all the pulsed odor paradigms (A2 to A5) as well. Moreover, the amplitude of BOLD response decreased linearly from A1 to A5. The secondary olfactory ROIs showed a slightly more sustained response compared to the primary olfactory ROIs, which has also been observed in previous olfactory studies.[56-58] The averaged peristimulus plots from session 2 were similar to the session 1 results (not shown).

Since it was not possible to form conclusions based on averaged peristimulus plots alone, a detailed analysis was performed by extracting parameters PSC, TTP and AUC from the timeseries data of each ROI. Although, there were no significant differences in TTP values, there were however, significant differences in PSC and AUC between the paradigms. The

reproducibility of each paradigm was evaluated by computing the fractional difference (Δ) between the parameters of session 1 and session 2 (see Section 2.2.7). Firstly, we found no systematic bias between session 1 and session 2 parameters suggesting that there was **no cross-session desensitization** occurring in any paradigm. Moreover, the CV_{intra} values of all the parameters in all paradigms were either close to or well below the upper fiducial limit[91] of 33%. These results suggest that all the paradigms gave highly reproducible results when repeated within the time frame used in this study.

These results do not support our hypothesis that pulsed odor block paradigms used in this study will give a more sustainable and reproducible response than continuous odor block paradigm. In fact, according to the results, the continuous odor block paradigm A1 had higher AUC values than A3, A4, and A5. One of the explanations for these results may be that the AUC parameter used in this study to quantify sustainability may be dependent on the peak of the BOLD response more than the width of the BOLD response. Since the total amount of odorant in the on-block in A1 and A2 is higher than the other paradigms, their peak responses can be expected to be higher because of the linear summation property of the BOLD response.[104] If AUC is dependent more on the peak then this may explain why sustainability (as measured by AUC) in A1 and A2 is more than the others. Therefore, another parameter was extracted, Fall Time (FT). By definition (see Section 2.2.8), this parameter may be a more accurate representation of the degree of desensitization within a paradigm as compared to AUC as it does not depend on peak height. The results show that FT in A1 and A2 was significantly greater than A3, A4 and A5 in both primary and secondary olfactory brain areas. These results reaffirm what we observed with AUC analysis, that the BOLD response in A1 and A2 was more sustained than

A3, A4 and A5. Therefore it is unlikely that the results that we got were merely due to AUC being biased towards the peak of the response.

Another series of experiments using the same total amount of 'on-block odor' across paradigms by varying the block duration may better help differentiate between desensitization caused by continuous and pulsed odor paradigms.

Another explanation why the pulsed paradigms did not have a sustained response may be based on the physiological properties of the olfactory system. It was observed from the peristimulus plots that the BOLD response peaked at ~7-8s before it started to decay. The fact that all the paradigms used the same odorant concentration and irrespective of ISI and stimulus duration, decayed at nearly the same time during the stimulation, suggests that this was caused by some intrinsic property of the olfactory system itself. Desensitization to prolonged stimulation is a feature that may help differentiate novel odors from existing odor stimulus. Schafer[105] and colleagues postulated a hierarchical system for adaptation/desensitization, which necessitates that adaptation increases with each layer (olfactory receptors to the brain) and that the activity in a more central layer will not be able to recover until those layers that feed into it have also recovered. They further explained that such a hierarchical mechanism could continuously acquire static environmental information, while allowing only fresh stimuli to reach more central areas and influence behavior. Another study[57] suggested that OFC, Mediodorsal thalamus and caudate nucleus may play a role in early detection of a stimulus and become quiescent after initial exposure to odor and may influence the desensitization of piriform cortex via their feedback projections. The difference between these two studies is that the former proposes a peripheral to central influence while the latter proposes an influence from within the central layer itself. Under either system, it may be deciphered that the paradigms used in this study desensitized in

the same manner because the same odor was presented for a prolonged period within the block. It may therefore be possible to reduce desensitization by pulsing different odorants of the same perceptive quality within the block instead of a single odorant. However, this decision often depends on the experimental goals of the study and therefore is not always feasible.

Based on the results of this study, a paradigm had to be selected that would have the best possibility of detecting activation in the olfactory brain areas for the following experiments so that reliable results could be expected in the final interventional study. The results of this study show that A1 and A2 not only evoke the highest BOLD response among all the paradigms but the BOLD response from these paradigms was also reproducible. Therefore the choice of the paradigm to be used in the interventional study had to made between A1 and A2. The decision in this regard should be based on the arguments involving (a) linear decreasing trend in parameters between paradigms and (b) the detection of activation. The linear trend was not only observed in the averaged peristimulus plots but also in the PSC and AUC values between the paradigms. In fact, a similar trend was observed in the box plots (Fig. 2-3a) of intensity ratings for both banana and cinnamon odors. This trend is expected if one considers that with the concentration of the odorant solution kept constant across paradigms, the total time of odorant delivered during the 16s block by each paradigm varied across paradigms (A1=16s, A2=6.4s, A3=3.2s, A4=2s, A5=1s). The BOLD signal and ratings' dependence on the amount of odor has been shown in previous olfactory Functional MRI studies[36] as well as studies involving other modalities[71,106,107]. However, since the total time of odor delivered from A1 to A5 decreased almost exponentially, it is important to note that rather than a corresponding exponential decrease, only a linear decrease was observed in BOLD signal parameters and intensity ratings across paradigms. This may be because the peak response in some paradigms saturated more than

others due to the fast rate of odor presentation (saturated hemodynamic system) and/or desensitization[108] (saturated neuronal system). This is supported by the observation that the peak and area in A2 was not significantly different than that in A1 even though the amount of odor presented in A2 is less than half of that presented in A1. This only reaffirms the result that the response in A1 was inconsistent with the near-linear summation property observed in previous Functional MRI studies.[104, 109] This observation however may not be consequential from the standpoint of detecting activation in this study. A1 and A2 had the highest peak response and area among the paradigms used in this study as seen in Figs. 2-5 – 2-8. Therefore these paradigms should be most sensitive to activation compared to the other three paradigms used in this study. This was verified using a linear regression analysis on all the paradigms (see Section 2.2.8). The results of this analysis suggest that the 16s-model fit and detection of activation in olfactory brain areas was highest in A1. It is important to note that the assumption in this type of analysis is that BOLD response is sustained and therefore the 16s-model was used to fit the functional timeseries. As seen from the results of this study it seems unlikely that 16s-model may be provide the best fit to the data. Optimization of the model will be the subject of the next experiment in this thesis.

2.5. Conclusion

The underlying aim of this study in lieu of the final goal of this dissertation was to select a paradigm that gives a high BOLD response that is sustainable and reproducible. It is with the intention of improving sustainability (reduce within-block desensitization) and reproducibility (across-sessions desensitization) that the continuous odor block was split into four pulsed odor block paradigms. It was observed that all the paradigms desensitized in the same manner. It can therefore be concluded that the within-block desensitization of the BOLD signal cannot be decreased merely by pulsing the odorants instead of stimulating continuously. This may be due to an intrinsic feature of the olfactory system and future studies need to be done perhaps using more odorants within blocks, systematically vary odor concentrations, block durations and rest periods in order to test if one or a combination of these factors minimize desensitization. However, among the paradigms used in this study, A1 had the highest BOLD response. It also gave a reproducible BOLD response and was the only paradigm that produced activated voxels as seen from the results of a preliminary timeseries regression analysis. Therefore, we can conclude that among the paradigms used in this study, the continuous odor paradigm (A1) is the most likely to give reliable results in the olfactory interventional functional MRI study.

CHAPTER 3   COMPARISON OF METHODS FOR MODELING ODORANT-INDUCED SIGNAL CHANGES IN THE HUMAN OLFACTORY CORTEX.

In the first part of this thesis, the aim was to select an olfactory stimulation paradigm that gives a high and reproducible BOLD response. In the second part of this thesis, the aim was to optimize the detection of activation of the Functional MRI data acquired from the paradigm selected in the first experiment. The following paragraph provides a background of the measures that were taken to achieve this goal.

3.1. Introduction

Various model-based[20, 21] and model-free[23] methods have been used to process Functional MRI data. However, model-based methods involving general linear modeling (GLM) continue to be the mainstay in BOLD Functional MRI data analysis because of the ease in implementation and interpretation. Typically, a square-wave model corresponding to On/Off times of the stimulus is convolved with a hemodynamic response function (HRF) e.g. double gamma HRF[110, 111] to create a model that represents the timeseries data. However, the success of the model-based techniques is based on the assumption that the shape of the BOLD response is known. In this type of analysis, if there are prolonged periods of stimulation (e.g. Block designs), it is critical that the BOLD response is also sustained over the entire period of stimulation. However, this assumption is not always valid especially in the case of olfactory block stimulation paradigms.

Early olfactory neuroimaging studies[56, 59, 63, 102, 103] employing GLM based analysis, could not detect activation in the primary olfactory cortex, e.g., amygdala, piriform cortex, on a consistent basis. Electrophysiological recordings on rats[55] revealed that neurons in the primary olfactory cortex desensitized to prolonged olfactory stimulation (i.e. 50s). Functional MRI studies with human subjects[56-58] also showed a transient response to prolonged olfactory stimulation in the primary olfactory cortex. These studies demonstrated that the mismatch between the sustained response modeled and the brief transient response observed in the primary olfactory cortex was the cause of inconsistent activation seen in some studies. They further proposed new models that took desensitization into account thereafter detecting robust odorant-induced activity in the primary olfactory cortex. Sobel et al.[56] modeled the desensitization to a 40s continuous odor using an exponentially decaying reference waveform that decreased to baseline levels within 30 to 40s. Poellinger et al.[57] shortened the square wave on-duration to 9s for a 60s stimulation. Tabert et al.[58] validated the results of these studies and further improved activation by shortening the square-wave on-duration to 6s for a 12s stimulation. These studies relied on stimulation-based templates to model the timeseries data. Another method of improving activation results involved acquiring a perception-based template[40] from subjects outside the scanner and using this template to model the Functional MRI timeseries. It was found that the perception-based template better represented brain activity in response to their olfactory stimulation.[40] In this chapter, each of these methods is evaluated in their ability to improve activation results in response to the 16s continuous odor block stimulation paradigm used in the previous study. We chose not to use only one modeling strategy in particular since experimental conditions in each one of the previous studies were in many aspects different from ours e.g. Perception based

profiles were acquired in response to retronasal stimulation as opposed to orthonasal in other studies.

Ultimately, in this second part of the thesis, the model that provided the best fit to the Functional MRI timeseries was used in the third part of the thesis for the final interventional study.

3.2. Materials and Methods

For all the data analysis described in this chapter, the Functional MRI data acquired from the continuous odor block paradigm (A1) (see Section 2.2.3) was used i.e. in this part of the thesis only psychophysical data of odor perception was acquired while no new functional images acquired. The materials and methods were therefore similar to the previous study but are described below from the perspective of the current study only.

3.2.1 Subjects

Six healthy volunteers (4/6 males, Average age=30.5years[SD 7.68], 5 Asians and 1 Caucasians) had participated in the current Functional MRI study. Volunteers were nonsmokers and reported an absence of nasal or sinus complaints, allergies, and nasal deformities or obstruction. All volunteers had normal olfactory function (mean bilateral TDI score=38.83 [SD=3.33]) as assessed by Sniffin' Sticks odor threshold, discrimination and identification tests.[79-81] This study was approved by the Virginia Commonwealth University's Institutional Review Board and informed consent was obtained from all volunteers.

3.2.2 Stimulation-based models

Twelve square-wave models with different on-block durations (2s, 4s, 6s, 8s, 10s, 12s, 14s, 16s, 18s, 20s, 22s and 24s) were each convolved with a double-gamma HRF function. The model that assumed a sustained BOLD response was the 16s-model and this was used as a reference to compare with the other models.

3.2.3 Acquisition of perception profiles
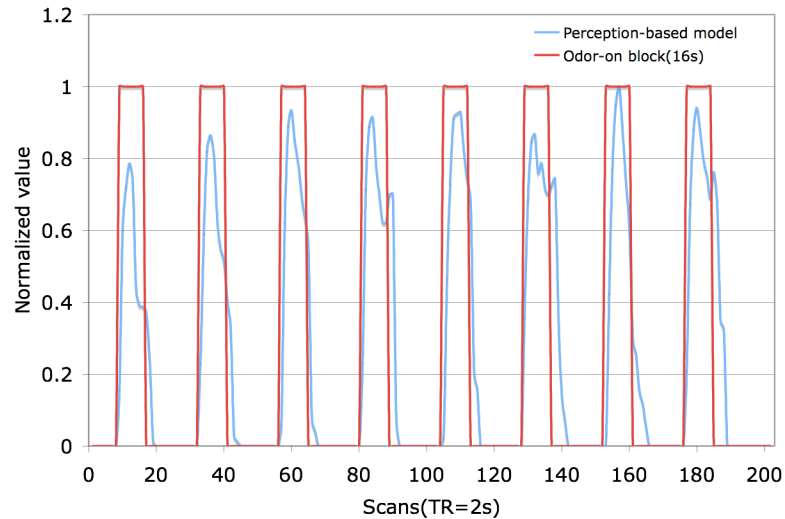
Figure 3-1: Six normalized perception-based profiles were averaged to create the perception-based model. This was used to model the timecourse of functional brain images.

All subjects participated in one session outside the scanner to acquire a perception profile under conditions simulating the ones during Functional MRI scanning in the previous study. They were presented with paradigm A1. Paradigm A1 consisted of four 16s blocks of banana odor and four 16s blocks of cinnamon odor alternating with 32s blocks of clean air. Both odorants were presented continuously throughout the 16s on-block. As in the Functional MRI

experiment in the first part of the thesis, the odorants were applied by a vapor-dilution olfactometer (Burghart OM4b, Hamburg, Wedel) and velo-pharyngeal closure was performed (for details see Section 2.2.2).

During the session, subjects were asked to continuously report the intensity of the perceived odor by using a mouse to move a sliding bar on a computer screen marked from 0 to 10. The data was acquired at rate of 1Hz using a custom-developed program (LabView 7.1, National Instruments Corp.). These perception profiles recorded the intensity rating per second during the stimulation with paradigm A1. However, the profiles were later resampled to match the rate at which the functional images were acquired (0.5Hz, TR=2s). Each perception profile was then normalized with respect to the peak of the perceived intensity in a single run. The six normalized profiles were then averaged to form the perception-based model (Fig. 3-1) and used in modeling the timecourse of odorant-induced signal changes.

3.2.4 Processing of Functional MRI data

Functional images acquired during the first session only were used in the analyses. As a first step, using the retrospective image-based correction (RETROICOR) (Glover et. al, 2000), physiological noise was minimized in the functional images. Next, the functional images for each individual subject were preprocessed with the FMRI Expert Analysis Tool (FEAT) from the FMRIB's (Oxford Center for Functional MRI of the Brain) Software Library (FSL), version 5.98 (www.fmrib.ox.ac.uk/fsl). The functional images were then motion-corrected using McFLIRT.[86] Motion correction results for each subject were closely observed to look for any absolute or relative motion exceeding 1.5mm. However, motion was found to be minimal and hence no scans were discarded. After the motion correction, non-brain tissue was removed from both

functional and high-resolution images using FSL's brain extraction tool[87] (BET). After that, the functional images were spatially smoothed with a Gaussian kernel having a full width at half maximum (FWHM) of 6 mm and were temporally smoothed using a high pass filter with a cutoff of 60s. Finally, the functional images were co-registered to subject specific high-resolution images and spatially normalized into standard Talairach space[88] using the FSL normalization algorithm.[86]

3.2.5 Extraction of Regression Coefficient (Beta)

After pre-processing the functional data, separate whole-brain timeseries statistical analyses were carried out voxel-wise for each subject using FMRIB's Improved Linear Model (FILM) with local autocorrelation correction[112] using the twelve stimulation-based models and the perception-based model. Using the same primary ROIs i.e. Piriform cortex (PIR), Amygdala (AMY) and secondary ROIs i.e. Orbitofrontal cortex (OFC), Insular cortex (INS) defined in the previous chapter (see Section 2.2.6), the mean regression coefficient (Beta) was extracted for each ROI, subject and model. In the context of this study, Beta is the same as the R^2 value obtained from the correlation analyses between a model and the timeseries data and indicates the amount of variance in the data accounted for by the model.

The first aim within the data analysis part of this thesis, was to verify that the 9s-model proposed by Poellinger et al.[57], the 6s-model proposed by Tabert et al.[58] and the perception-based model Cerf Ducastel and Claire Murphy[40] provide a better fit to the data in olfactory related brain areas as compared to the reference 16s-model. The 9s-model (tested in Poellinger and Tabert studies) could not be constructed in this study since the functional images were acquired at a repetition rate of 2s. Instead, 8s-model and 10s-model were specified for comparison with

the reference 16s-model. The next specific aim was to find out if there was any other stimulation-based model that further improved the model-fit. Separate paired t-tests using mean Beta as the dependent variable were used to compare any two models within each ROI.

3.2.6 Extraction of activation results

Group level analysis was conducted using FLAME (FMRIB's Local analysis of mixed-effects) stage 1[113-115] to quantify the specificity of each model in detecting odorant-induced activation in the olfactory related brain regions (for details regarding fixed-effects, mixed-effects and FLAME visit http://www.fmrib.ox.ac.uk/fsl/feat5/detail.html#higher). The resultant z-statistical images were thresholded using clusters determined by $z > 2.3$ and a corrected cluster significance threshold of $p < 0.05$ (Woolrich, 2001). Measures such as mean z-scores and number of active voxels within each ROI were extracted from the thresholded z-statistical images.

3.3. Results

3.3.1 Model comparisons based on mean Beta

The relationship between the stimulation-based model duration and the mean Beta was curvilinear and peaked at the 4s model duration (Fig. 3-2). The mean Beta values at the peak of the curve for PIR, AMY, OFC, and INS were 29.94, 28.2, 13.05 and 22.22 respectively. A 176% and 189% gain was observed in mean Beta for PIR and AMY respectively by using the 4s-model as opposed to the reference 16s-model while these gains were only 50% and 53% for OFC and INS respectively (Table 3-1). This was in part due to the observation that although the later phase (12s to 2s) of the mean Beta curves of the primary and secondary areas were relatively similar in shape, there was a pronounced difference in the shape of the curves between the two areas in the initial phase (24s to 12s). In the secondary areas, we observed a plateau in the initial phase (gain: OFC: 18%; INS: 2%) as opposed to a consistent linear increase (gain; PIR: 104%; AMY: 41%) observed in the primary areas. Irrespective of the differential gains in the primary and secondary olfactory areas, the mean Beta curves indicate that model simulating a sustained response (16s-model) did not explain the odorant-induced signal change better than the shorter duration models. The mean Beta values in all ROIs corresponding to the perception-based model (PIR: 15.51; AMY: 13.46; OFC: 10.16; INS: 15.11) were lower than those for the 4s-model and were in fact quite similar to those for the 10s-model (PIR: 16.68; AMY: 13.78; OFC: 9.41; INS: 15.64).

Separate paired t-tests were conducted in each ROI to verify the statistical significance of the above observations. Mean Beta for the 16s-model was significantly lower than that for (a) 8s-model (PIR: $p<0.001$; AMY: $p<0.01$) (b) 10s-model (PIR: $p<0.001$; AMY: $p<0.01$; INS: $p<0.01$) (c) 6s-model (PIR: $p<0.001$; AMY: $p<0.001$; INS: $p<0.05$) and (d) perception-based model (PIR:

p<0.05; AMY: p<0.05). We also found that the 6s-model had a significantly higher mean Beta than the 8s-model (PIR: p<0.001; AMY: p<0.001; OFC: p<0.01; INS: p<0.001) as well as the 10s-model (PIR: p<0.001; AMY: p<0.001; OFC: p<0.01; INS: p<0.001).

Based on the mean Beta curves, tests were done to verify the 4s-model as the optimized model in this study. In the primary olfactory areas, the mean Beta associated with the 4s-model was significantly higher than all stimulation-based models (p<0.01) as well as the perception-based model (p<0.001). We saw similar results in the secondary olfactory areas except that the difference between the 4s-model and the 2s-model was close to significance (p=0.06) and no significant difference was found between the 4s-model and the perception-based model in the OFC (p=0.1).

(a)

(b)

Figure 3-2: Mean Beta in (a) primary (AMY=Amygdala, PIR=Piriform cortex) and (b) secondary (INS=Insular cortex, OFC=Orbitofrontal cortex) olfactory areas obtained by regression analysis of the timeseries data from paradigm A1 using stimulation-based models. Square-wave or boxcar functions with a duration that was either shorter (14s to 2s) or longer (18s to 24s) than the actual stimulation period (16s) were convolved with the double-gamma HRF.

Table 3-1: Mean Beta and standard deviations (SD, shown in parentheses) in primary (AMY=Amygdala, PIR=Piriform cortex) and secondary (INS=Insular cortex, OFC=Orbitofrontal cortex) olfactory areas obtained by regression analysis of the timeseries data from paradigm A1 using stimulation-based models with duration varying from longer (18s to 24s) to shorter (14s to 2s) than the actual stimulation period (16s) and a perception-based model.

Model	Mean Beta (SD)			
	PIR	AMY	OFC	INS
24s	6.91 (6.15)	8.21 (5.91)	7.57 (5.83)	14.42 (4.69)
22s	8.26 (6.12)	8.91 (5.80)	7.66 (5.46)	14.39 (4.58)
20s	9.42 (6.15)	9.38 (5.76)	8.08 (5.19)	14.39 (4.55)
18s	10.10 (6.25)	9.51 (5.77)	8.51 (5.08)	14.52 (4.57)
16s	10.82 (6.25)	9.73 (5.68)	8.73 (5.04)	14.51 (4.62)
14s	12.28 (6.16)	10.48 (5.47)	8.76 (4.98)	14.47 (4.69)
12s	14.12 (6.00)	11.61 (5.27)	8.93 (5.06)	14.68 (4.82)
10s	16.68 (5.76)	13.78 (5.09)	9.41 (5.27)	15.64 (4.91)
8s	20.24 (5.57)	17.59 (4.92)	10.35 (5.30)	17.09 (4.85)
6s	26.32 (6.00)	23.81 (5.28)	12.26 (5.61)	20.03 (5.12)
4s	29.94 (6.50)	28.19 (5.83)	13.05 (5.60)	22.22 (5.36)
2s	25.73 (6.24)	25.14 (5.90)	10.66 (4.97)	19.09 (5.02)
Perception	15.51 (6.53)	13.46 (6.14)	10.16 (4.75)	15.11 (4.66)

3.3.2 Model comparisons based on activation

Group mean activation maps were generated for all stimulation-based models and the perception-based model. In order to see the effect of model duration on activation parameters, the number of active voxels and the mean z-scores were extracted from each ROI from the group mean activation maps (Fig. 3-3). Similar to the mean Beta curve, the 4s-model produced the highest number of active voxels within all the ROIs (PIR=247, AMY=307, OFC=1105, INS=1770). In comparison, the reference 16s-model produced far less number of active voxels (PIR=20, AMY=41, OFC=396, INS=1205). The perception-based model produced more number of active voxels (# Active voxels: PIR=122, AMY=111, OFC=950, INS=1223) than the reference model but not more than the 4s-model. Similar trends were observed in the mean z-scores. Fig. 3-4 shows large activations in primary and secondary areas when 4s-model was applied. These activations were greater than those produced by the 16s-model and the perception-based model. Table 3-2 provides details of the extent and magnitude of activation within each ROI as well as the location of the maximum z-score voxel.

(a)
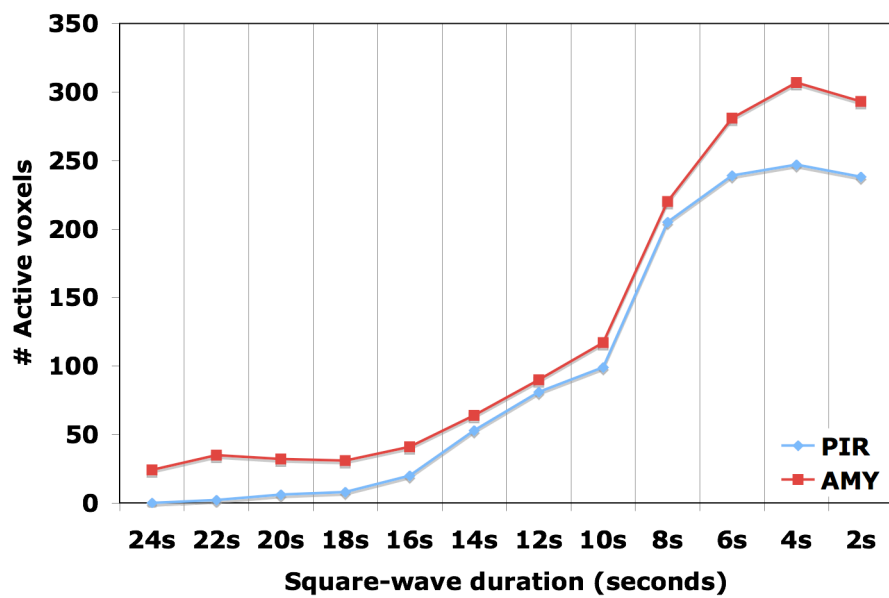
(b)
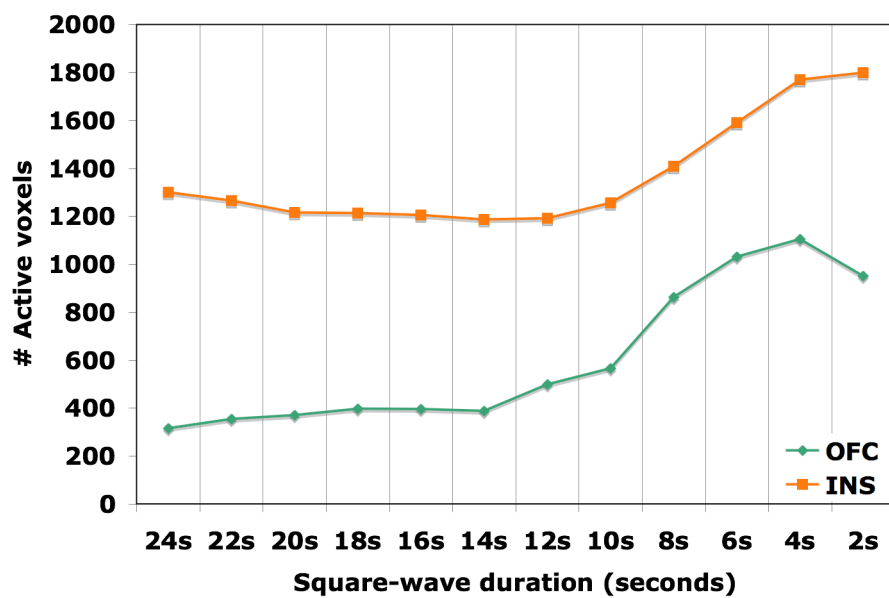
(c)
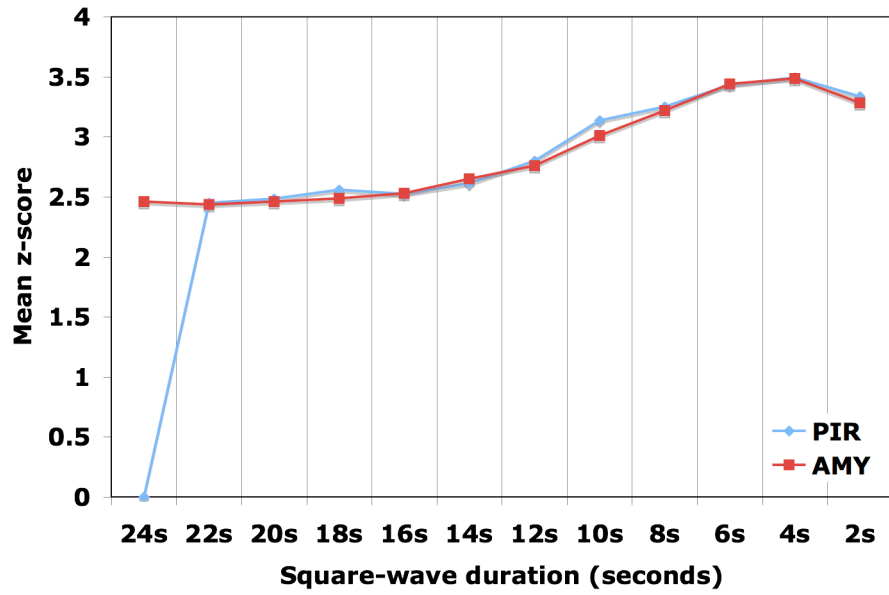
(d)

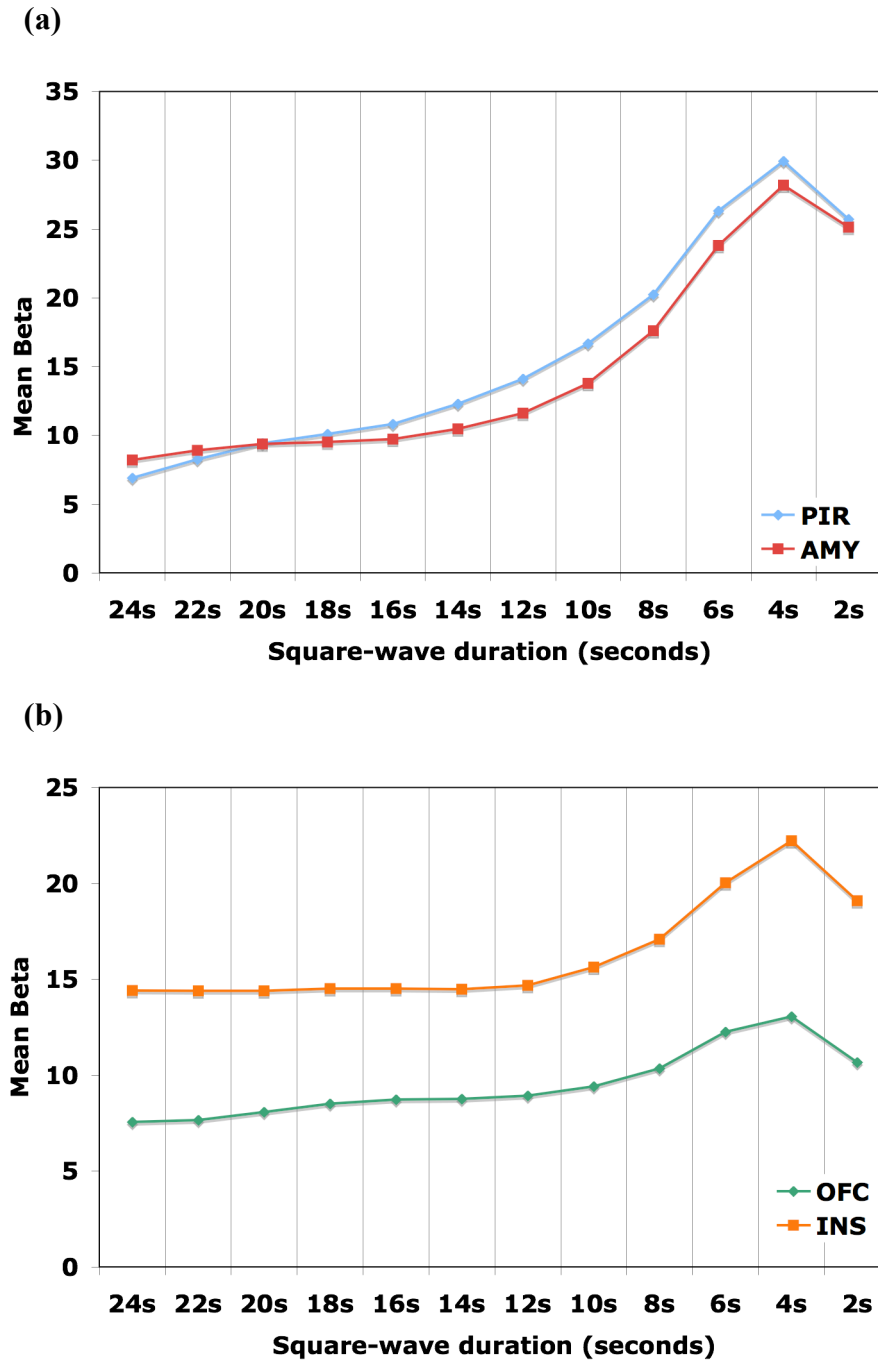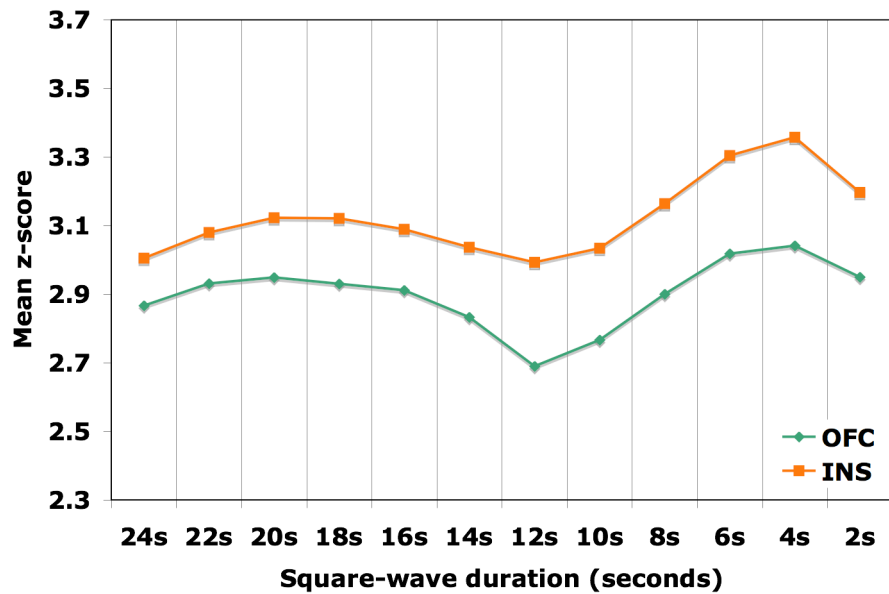**Figure 3-3:** Number of active voxels (a, b) and Mean z-scores (c, d) in primary (AMY=Amygdala, PIR=Piriform cortex) and secondary (INS=Insular cortex, OFC=Orbitofrontal cortex) olfactory areas extracted from statistical z-score images derived from GLM analyses (within FSL) using stimulation-based models. All images were thresholded using clusters determined by $z > 2.3$ and a corrected cluster significance threshold of $p < 0.05$.

(a)   16s-model
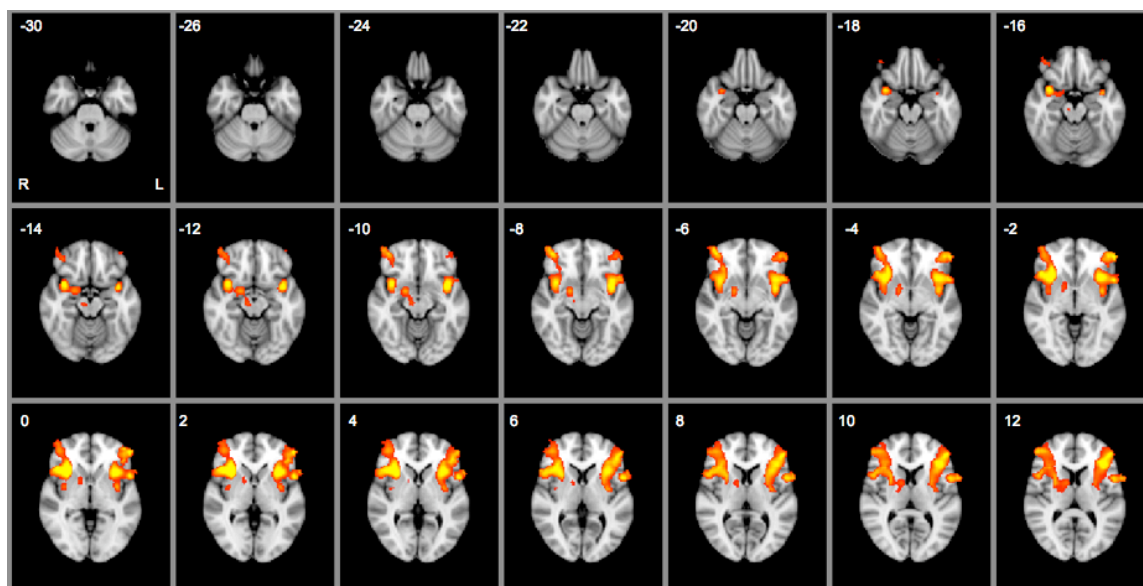
(b)   Perception-based model
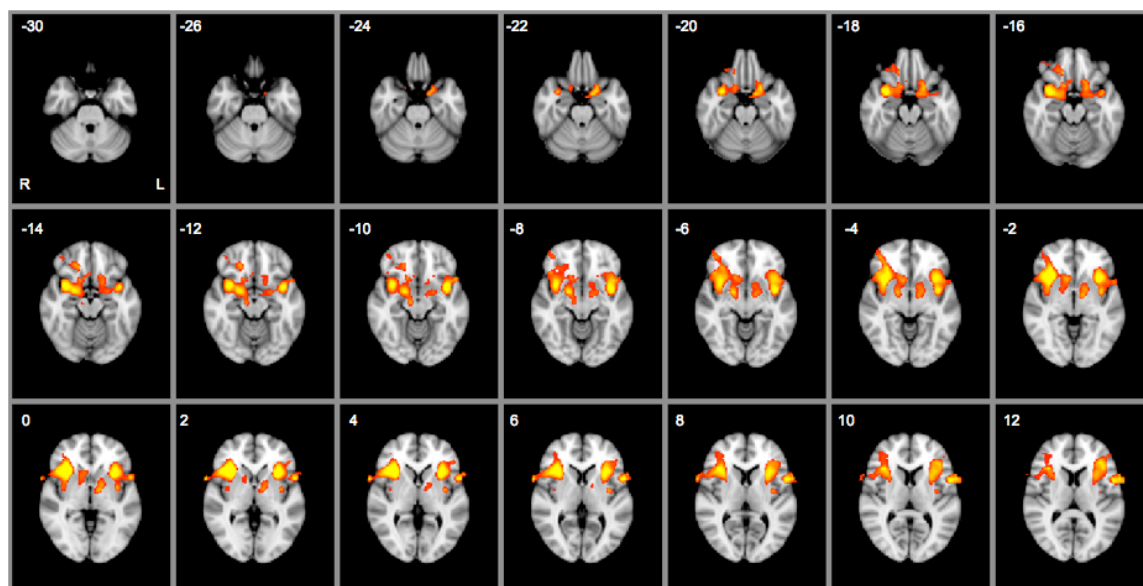
(c)   4s-model
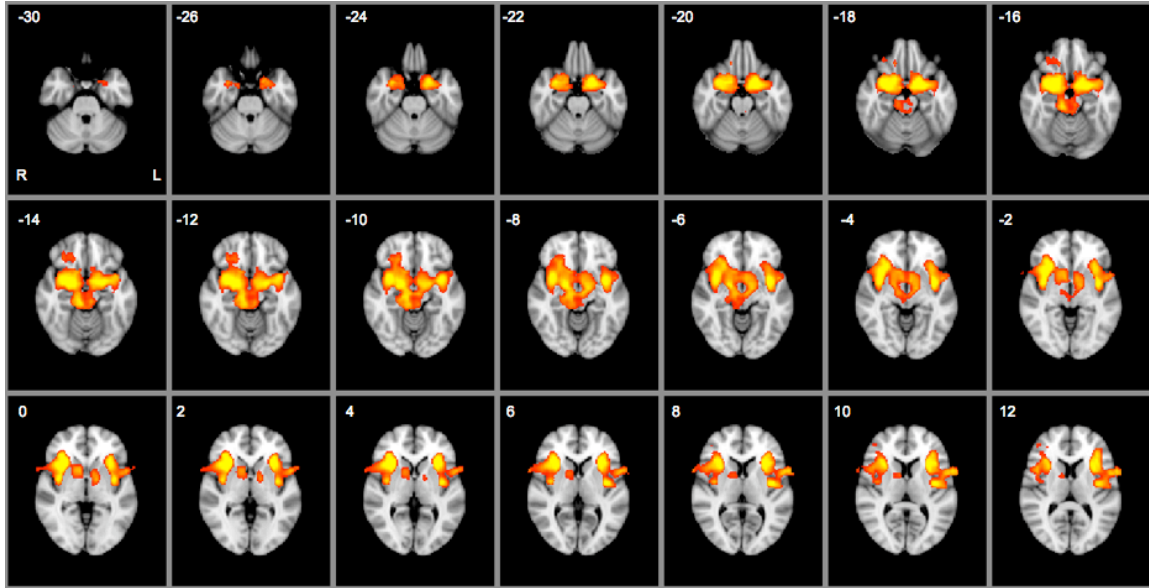
Figure 3-4: Activation maps generated by voxel-wise GLM analyses of functional data using (a) reference 16s-model (b) perception-based model and (c) 4s model. All images were thresholded using clusters determined by z > 2.3 and a corrected cluster significance threshold of p < 0.05. Twenty-one slices were selected in axial plane from z = -30mm to 12mm (MNI/Talairach space). The activation maps were overlaid onto a standard MNI brain. Color scale: Red=2.3; Yellow=4. Note that 4s-model yields large activations in primary and secondary olfactory areas.

Table 3-2: Clusters of activation found with voxel-wise GLM analyses in primary (AMY=Amygdala, PIR=Piriform cortex) and secondary (INS=Insular cortex, OFC=Orbitofrontal cortex) olfactory areas for all stimulation-based models and a perception-based model.

PIR			MNI coordinates (mm)		
Model	# Voxels	Max Z	Xmax	Ymax	Zmax
24s	0	0.00	-	-	-
22s	2	2.45	20	0	-16
20s	6	2.64	20	0	-16
18s	8	2.75	20	0	-14
16s	20	2.90	20	0	-14
14s	53	3.30	30	4	-18
12s	81	3.59	30	4	-20
10s	99	3.86	22	4	-18
08s	205	4.48	20	4	-18
06s	239	4.52	24	4	-20
04s	247	4.58	-16	2	-20
02s	238	4.49	-16	0	-20
Perception	122	3.80	30	4	-18

AMY			MNI coordinates (mm)		
Model	# Voxels	Max Z	Xmax	Ymax	Zmax
24s	24	2.65	22	-10	-10
22s	35	2.60	20	-2	-14
20s	32	2.72	20	-2	-14
18s	31	2.80	20	-2	-14
16s	41	2.94	20	-2	-14
14s	64	3.15	20	-2	-14
12s	90	3.38	22	-2	-16
10s	117	3.92	24	2	-18
08s	220	4.52	22	0	-18
06s	281	4.72	24	0	-18
04s	307	4.43	-20	0	-20
02s	293	4.41	-20	0	-18
Perception	111	3.41	20	-2	-14

OFC				MNI coordinates (mm)		
Model	# Voxels	Max Z	Xmax	Ymax	Zmax	
24s	316	3.43	34	26	-4	
22s	355	3.67	32	28	-4	
20s	370	3.85	32	28	-4	
18s	397	3.94	32	28	-4	
16s	396	3.91	32	28	-4	
14s	388	3.76	32	28	-4	
12s	499	3.61	32	28	-4	
10s	566	3.70	32	28	-4	
08s	863	3.99	18	8	-20	
06s	1031	4.19	32	28	-4	
04s	1105	4.32	-18	8	-22	
02s	951	4.13	-18	8	-22	
Perception	950	3.80	32	28	-4	

INS				MNI coordinates (mm)		
Model	# Voxels	Max Z	Xmax	Ymax	Zmax	
24s	1301	4.08	32	16	0	
22s	1265	4.26	32	16	0	
20s	1216	4.33	32	16	0	
18s	1214	4.32	-34	18	0	
16s	1205	4.31	32	20	-2	
14s	1187	4.29	32	20	-2	
12s	1192	4.24	32	20	-2	
10s	1256	4.40	30	22	-2	
08s	1409	4.66	30	22	-2	
06s	1590	4.87	32	20	-2	
04s	1770	4.85	30	24	-2	
02s	1800	4.34	30	24	0	
Perception	1223	4.42	32	20	-2	

3.4. Discussion

The goal of this part of the thesis was to find a model to be used in GLM analysis that best represented the odor-induced BOLD signal in the brain. This issue would be trivial if the olfactory brain areas produced a sustained response to a 16s prolonged odor stimulation as seen with other sensory stimuli.[15,104,116] However, desensitization to prolonged odor stimulation needs to be accounted for in the model if robust activation is expected in the olfactory brain areas especially in the piriform cortex. In this study, the methods used by Cerf Ducastel and C. Murphy[40], Poellinger et al.[57] and Tabert et al.[58] for modeling odorant-induced signal changes in response to prolonged stimulation were compared, validated and optimized. Twelve square-wave functions of 2s to 24s durations were created in increments of 2s and convolved with a double-gamma HRF to produce twelve stimulation-based models. Additionally, odor perception profiles in response to paradigm A1 were acquired in 6 subjects and were averaged across subjects to create a perception-based model. Using timeseries regression, the 'goodness of fit' of each model to the functional data from paradigm A1 was then compared.

ROI analyses confirmed that the 6s-model proposed by Tabert et al.[58], 8s- /10s-model similar to the 9s-model proposed by Poellinger et al.[57] and the perception-based model proposed by Cerf Ducastel and C. Murphy[40] provided a better fit to the data than the reference 16s-model which represented the standard approach of modeling a sustained response. Results also confirmed that the 6s-model proposed by Tabert et al.[58] was more sensitive to odorant-induced signal changes than both 8s- and 10s-models although further analysis found that the 6s-model did not yield the best fit to the data. A significant increase in the sensitivity was observed when the 4s-model was applied to the data as compared to the 6s-model. However, there was no improvement when the model duration was further reduced to 2s. A direct comparison between the 4s-model and the

perception-based model revealed that the former yielded a better model fit than the latter. The perception-based model provided a model fit that was similar to the 10s-model. Similar results were observed when number of active voxels and mean z-scores were compared between models.

Therefore, overall results suggest that the 4s-model is the best model for detection of activation for paradigm A1 in not only primary but secondary olfactory brain areas as well. This result makes sense taking into account the peristimulus plots for paradigm A1 seen in the previous chapter. The BOLD response peaks at ~7-8s and then quickly falls to baseline levels at ~11-12s post stimulus onset. This profile is best matched by a 4s-model (Fig. 3-5). Physiologically, this result further indicates the presence of desensitization in the olfactory brain areas in response to paradigm A1 and the effect it can have if the data in not modeled correctly. It is important to note that the effect of other parameters of the HRF such as initial dip, delay, lag etc on the Beta and z-scores were not tested and further studies are required in this regard.
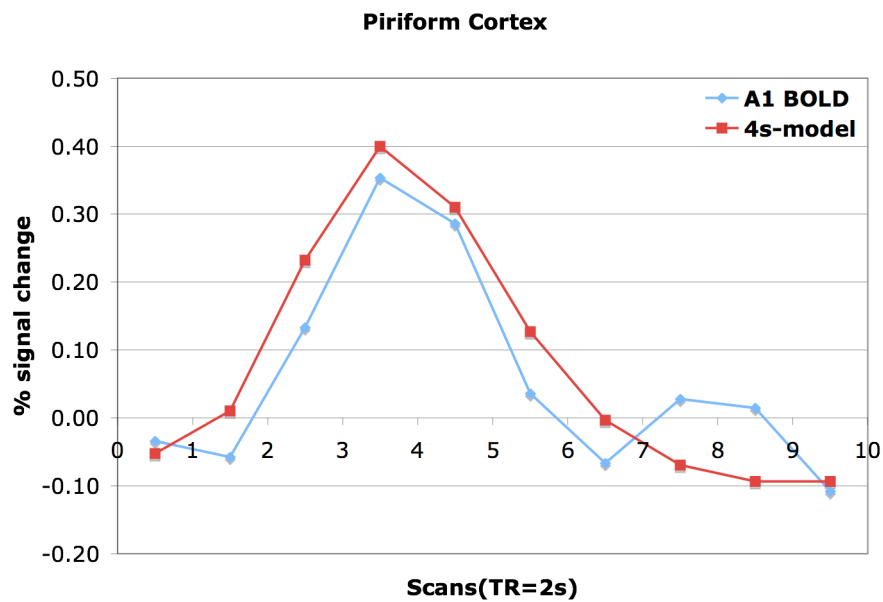

Figure 3-5: The 4s-model closely follows the BOLD profile in the piriform cortex for paradigm A1.

The main reason for the difference in result between this study and the studies by Tabert et al.[58] and Poellinger et al[57] is that they did not test the 'goodness of fit' for the 4s-model. One reason may be that the TR used in both studies was 3s. This study used a 2s TR and therefore the higher temporal resolution enabled detecting the efficacy of the 4s-model. Therefore, at higher temporal resolution (< 2s), other models (varying in shape and/or duration) may possibly detect greater activation although the differences are unlikely to be significant.

The results of this study revealed that the 16s reference model detected very less activation in the primary olfactory areas but in contrast detected significant activation in the secondary olfactory areas. Early olfactory imaging studies [56, 59, 63, 102, 103] found similarly dissociate patterns of activations between the primary and secondary olfactory areas. In fact many of these studies did not detect activation in the primary olfactory areas at all. It was also verified in this study that the perception-based model produced greater activation than the 16s-model in the primary and secondary olfactory areas. This corroborates the findings of Cerf Ducastel and C. Murphy[40] that the perception-based model represents the olfactory-based brain activity better than stimulation-based model. However, it was also found in this study that the stimulation-based 4s-model detected greater activation than the perception-based model in olfactory brain areas. Part of the explanation of this difference in results is that their study compared a perception-based template to a single stimulation-based template that modeled a sustained response. They did not use shorter duration stimulation-based models for comparison. The stimulation paradigm used in that study delivered odorants in a retronasal manner via small amount of liquids in discrete boluses, instead of a continuous flow of liquid throughout the stimulation on-block. They assumed that this would limit the desensitization within the stimulation block. However, based on the results of the first part of this thesis, it was observed that desensitization occurred not only with

continuous odor paradigms but also with pulsed-odor paradigms. Therefore, it is likely that they could have detected greater activation with the use of a shorter duration stimulation based model compared to using the perception-based model in their data analysis. Another explanation why the perception-based model was not found to provide the 'best-fit' to the functional data in this part of the thesis could stem from subject-induced error during data acquisition. It was observed that the perception-based profiles returned to the baseline level a few seconds later than the stimulation based models did, possibly due to the lag in subject response from the end of the odor perception and movement of the cursor down to zero.

Overall, the findings of this study validate the use of shorter duration models in GLM analyses in producing robust activation in primary and secondary olfactory areas.

3.5. Conclusion

We can conclude based on the results of this study that the stimulation-based 4s-model best represents the odorant-induced signal change evoked by the olfactory stimulation paradigm A1 in the primary and secondary olfactory brain areas and hence shall be used in the analysis of functional data acquired during the final interventional study.

CHAPTER 4   APPLICATION OF OPTIMIZED METHODS TO AN INTERVENTIONAL OLFACTORY FUNCTIONAL MRI STUDY.

In the final part of this thesis, the aim was to apply the paradigm and model chosen from the previous parts of this thesis, to an olfactory interventional Functional MRI study with the aim of demonstrating sensory specific satiety in normal human volunteers. The following section provides a brief background for the intervention taken in this study.

4.1. Introduction

When a food is eaten to satiety, its reward value decreases. Neuroimaging, electrophysiological and behavioral measures have shown that this decrease is usually greater for the food eaten to satiety than for other foods.[49,50,117-119] This phenomenon is called sensory specific satiety and is one of the mechanisms by which food intake may be controlled. The brain area in primates consistently implicated in coding for sensory specific satiety is the orbitofrontal cortex (OFC).

It has been shown in rats, monkeys and humans that the OFC contains secondary taste and olfactory cortical areas.[94,120] Additionally, OFC also receives inputs from visual cortex. Primate OFC contain neurons that respond to taste, odor or sight of food only when hunger is present.[117] Furthermore, studies have investigated the effect of feeding to satiety on the neuronal responses in OFC to the taste[119], sight, odor[117] and texture[121] of food. The results have shown that there is a gradual decrease in the neuronal response in the OFC while the food is being fed to satiety, while

the neuronal response to other foods not being fed to satiety remains the same. These studies also demonstrated that this relative responsiveness of the neurons reflected the preference of the monkeys for the foods. It is thus the relative reward value of the taste, olfactory, visual and texture stimuli that is represented in the OFC. Further evidence for this was obtained in a study that also showed that neuronal responses in the macaque OFC reflect relative reward preference.[122]

Only few studies have investigated the role of OFC in coding the relative reward value of different stimuli in humans. In a Functional MRI investigation in humans, O'Doherty and colleagues[49] showed that in a region of the OFC (which also encodes pleasantness of odors[52]) activation produced by the odor of food just eaten to satiety decreased, whereas there was no similar decrease for the odor of a food not eaten in that meal. Another study on humans using Functional MRI found a sensory-specific reduction in OFC activations that was also correlated with subjective pleasantness of the food.[50] Thus olfactory sensory specific satiety is a useful phenomenon by which the pleasantness of a food related stimulus (olfactory, visual, taste or texture) could be altered. Conversely, reward value of a high calorific food could potentially be decreased after prolonged stimulation with visual or olfactory stimulus of that food. With the prevalence of obesity in current times and its associated health issues (NIH Obesity Research Task Force[54]) it is important to understand the brain mechanisms that control food intake. Hence, more interventional olfactory Functional MRI studies need to be done to further investigate the role of sensory specific satiety in controlling food intake. However, prior to an interventional study, reproducibility of the activation produced by the olfactory stimulation paradigm has to be verified. The results of the first and second part in this thesis helped to create an improved experimental design by selecting from all the paradigms and models tested, an olfactory block

stimulation paradigm and a model that gave the best possibility of detecting reproducible activation in olfactory related brain areas. In this chapter, applying these 'optimized' methods i.e. paradigm A1 for odor stimulation and the 4s-model for data analysis provided a valid basis for interpreting the effect of an intervention (food) in normal volunteers.

4.2. Materials and Methods

4.2.1 Subjects

Sixteen healthy volunteers (13/16 males, Average age= 29.38 years [SD 4.94], 12 Asians and 4 Caucasians) participated in the olfactory interventional Functional MRI study. Volunteers were nonsmokers and reported an absence of nasal or sinus complaints, allergies, and nasal deformities or obstruction. All volunteers had normal olfactory function (mean bilateral TDI score=37.38 [SD=2.52]) as assessed by Sniffin' Sticks odor threshold, discrimination and identification tests.[79-81] Volunteers were requested to be hungry at scan time i.e. atleast 3 hrs fasting before the scan. This study was approved by the Virginia Commonwealth University's Institutional Review Board and informed consent was obtained from all volunteers.

4.2.2 Stimulus presentation

As previously described in Chapter 2, the selected paradigm A1 contained banana and cinnamon odors as stimulants. Paradigm A1 had four 16s blocks of banana odor and four 16s blocks of cinnamon odor alternating with 32s blocks of clean air. Banana and Cinnamon can both be considered as easily identifiable food like odors; both are rated as pleasant odors by most human subjects and can be used as pure chemicals without possible confounding influence of

mixtures. Both odorants used were matched in intensity and pleasantness in a pre-test. Odorants were applied in the same manner as described in Chapter 2 (see Section 2.2.2).

4.2.3 Data Acquisition

All imaging parameters were the same as in the experiment detailed in Chapter 2 although in the first experiment the subjects were not asked to fast and were not provided with any food after the first scanning session. In this experiment the subjects were first scanned when hungry. Then they were taken out of the scanner and asked to eat bananas till satiated. After that, subjects were placed back into the scanner and post-satiety functional images were acquired. All remaining protocols such as subject instructions, subject setup, acquisition of subjective ratings and physiological measures were the same as in experiment 1 (see Section 2.2.4). (The amount of bananas eaten was registered).

4.2.4 Processing of Functional MRI data

All image pre-processing was done exactly as in Chapter 2 (see Section 2.2.5). For further statistical analyses, the optimized model resulting from previous part (see Chapter 3) of this thesis i.e. 4s-model, was used in a whole-brain voxel-wise timeseries analyses using FILM with local autocorrelation correction.[112] Appropriate contrasts were specified to identify brain regions that were activated by each odor i.e. ban vs. air and cin vs. air. Session 1 contrasts were assigned with 'pre' prefix and session 2 contrasts were assigned with 'post' prefix.

Sensory specific satiety related effects were tested for in each subject using the contrast: [(preBan+preCin+postCin)/3 − postBan].[49,50] This contrast included only those voxels in the data analysis that were active in conditions preBan, preCin and postCin. Group level analysis was then conducted on this contrast using FLAME[113,115,123] (FMRIB's Local analysis of mixed-effects). The resultant z-statistical images were thresholded using clusters determined by z > 2.3 and a corrected cluster significance threshold[112] of p < 0.05. Additionally, we also tested for any interventional effect by using paired pre vs. post comparisons for each odor at the group level.

4.3. Results

4.3.1 Brain areas activated by odors

Group activation maps for banana and cinnamon in both sessions are illustrated in Fig. 4-1. Both odors evoked significant bilateral activation in primary olfactory areas such as piriform cortex (PIR) and amygdala (AMY) as well as secondary olfactory areas such as insular cortex (INS) and orbitofrontal cortex (OFC) in session 1. Similar patterns of activations were observed in session 2 with the exception of cinnamon for which no significant OFC activation was detected (see Table 4-1). Tertiary areas such as pallidum, paracingulate gyrus, anterior cingulate gyrus, inferior frontal gyrus and central opercular cortex were also found to be activated (not shown in figure). These active areas are consistent with the results of previous neuroimaging studies[36, 49, 96, 98, 124] investigating cortical responses to odors.

(a)   Banana (session 1)
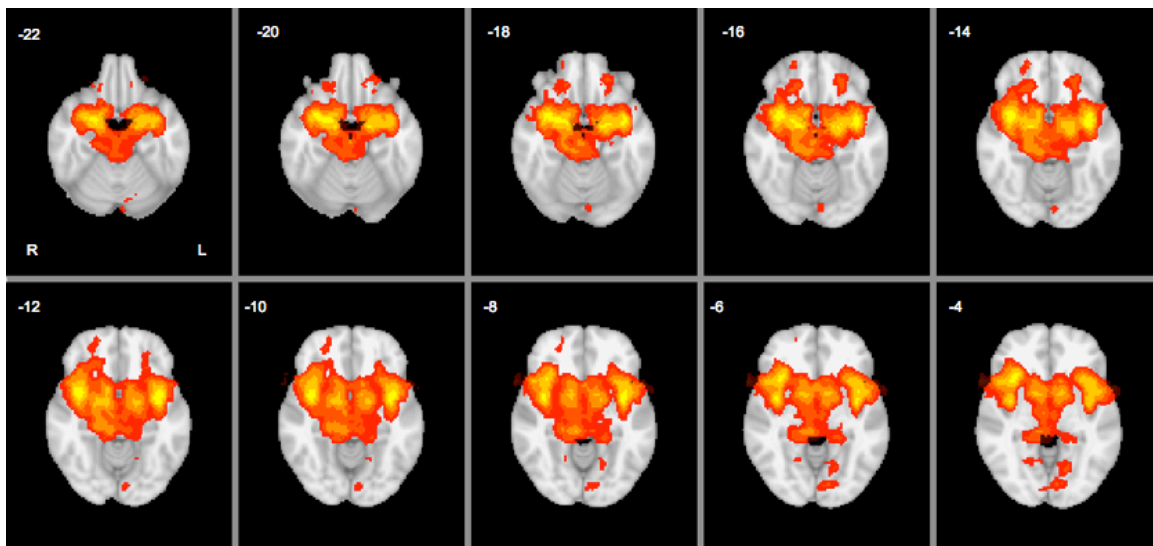
(b)   Banana (session 2)
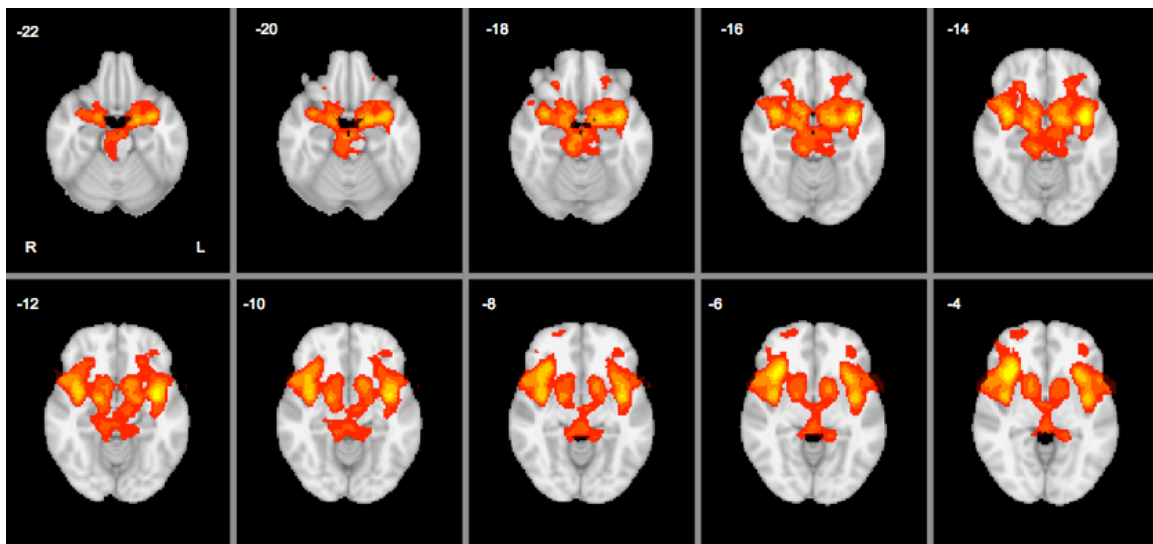
(c)   Cinnamon (session 1)
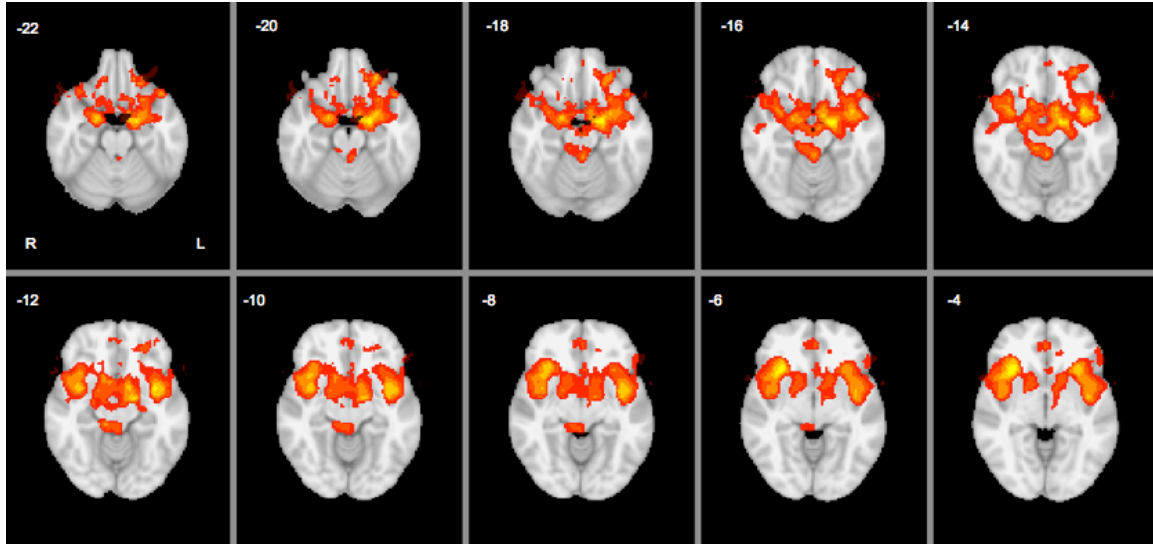
(d)   Cinnamon (session 2)
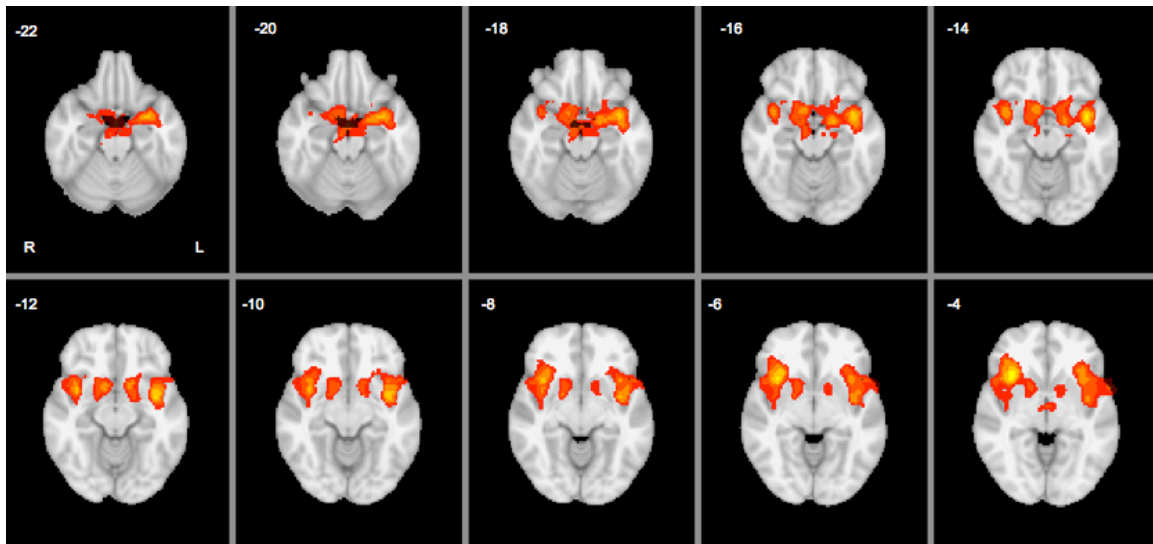
Figure 4-1: Activation of human primary and secondary olfactory brain areas in response to banana odor in session 1 (a) and session 2 (b), and cinnamon odor in session 1 (c) and session 2 (d). All images were thresholded using clusters determined by z > 2.3 and a corrected cluster significance threshold of p < 0.05. Ten slices were selected in axial plane from z = -22mm to -4mm (MNI/Talairach space). The activation maps were overlaid onto a standard MNI brain. Color scale: Red=2.3; Yellow=4.

Table 4-1. Activation detected for banana and cinnamon odors in both sessions. (Group analysis, n=16, Cluster thresholding z>2.3 and p<0.05)

Brain region	No. of active voxels	Peak Z	MNI coordinates (mm)		
			x	y	z
(a). Banana odor (session 1)					
Piriform cortex	273	5.15	22	4	-22
Amygdala	319	5.14	18	-4	-14
Insular cortex	2064	5.30	-38	2	-14
OFC	704	2.75	18	20	-20
(a). Banana odor (session 2)					
Piriform cortex	238	4.27	-18	2	-18
Amygdala	273	4.32	-20	0	-18
Insular cortex	1945	5.25	34	22	-2
OFC	342	2.66	26	32	-14
(a). Cinnamon odor (session 1)					
Piriform cortex	258	3.97	-16	-4	-18
Amygdala	305	4.18	-18	-6	-16
Insular cortex	1747	4.10	34	24	-6
OFC	325	2.99	-24	36	-18
(a). Cinnamon odor (session 2)					
Piriform cortex	158	3.2	-18	0	-16
Amygdala	143	3.3	-28	0	-20
Insular cortex	1659	4.5	34	22	0
OFC	-	-	-	-	-

4.3.2 Subjective Ratings

The pleasantness and intensity ratings for banana and cinnamon odors for both sessions are summarized in Fig. 4-2. No significant difference was found in the mean pleasantness or mean intensity ratings for banana odor from pre- to post-satiety although there was a slight decreasing trend in the mean pleasantness ratings for both odors across sessions. The mean pleasantness rating for cinnamon was found to be less than banana although this difference was not statistically significant. Overall, a large variability was observed among subjects in rating the pleasantness of cinnamon. The subjective ratings in this study did not indicate the presence of olfactory sensory specific satiety to banana. After the first scanning session, the subjects were asked to eat bananas till satiated. The average amount of banana eaten was 464gms ± 152.

(a)

Pleasantness

(b)
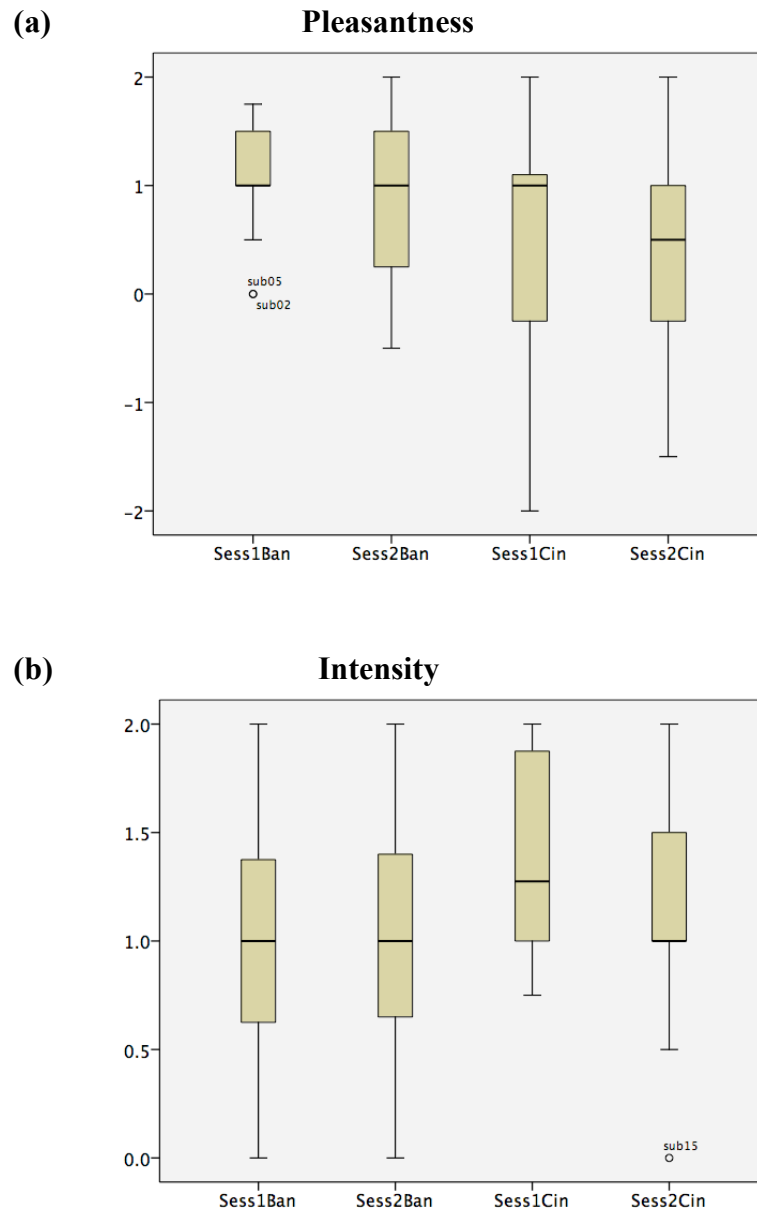
Intensity

Figure 4-2: Box-plots indicating pleasantness (a) and intensity (b) ratings of banana and cinnamon odors for both sessions. Session 1 was followed by the subject eating bananas to satiety. For Intensity (+2 = very intense, -2 = very weak); For Pleasantness (+2 = very pleasant, 0 = neutral, -2 = very unpleasant).

4.3.3 Brain areas showing olfactory sensory specific satiety

Group mean analysis on the sensory specific contrast did not reveal any brain areas related to sensory specific satiety. Furthermore, no brain areas showed significant differences between pre-satiety and post-satiety condition for banana at the group level.

An additional contrast (preBan - postBan) - (preCin - postCin) was also tested as another method to find brain areas showing sensory specific satiety. Activation clusters found would have then been masked to include only those voxels that had $z > 0$ in preBan, postBan, preCin and postCin. However, we did not find any activated clusters using this contrast. An unpaired t-test was then performed to investigate brain areas that demonstrated significant differences between the (pre - post) contrast in the interventional study and (session 1 – session 2) contrast in the non-interventional study (Chapter 2). Again, no brain activations were found with these contrasts for either banana or cinnamon odor.

4.4 Discussion and Conclusion

The results of this study do not support the findings from previous studies[50,125] that demonstrated a certain area within the OFC that is responsible for sensory specific satiety related changes in activation. According to Rolls[118], these changes are most likely implemented by habituation of the synaptic afferents to the orbitofrontal neurons with a time course of the order of the length of a course of a meal. These signals along with visceral and other satiety related signals reach orbitofrontal cortex (via thalamic areas) and there modulate the representation of food, resulting in an output that reflects the reward (or appetitive) value of each food. According to the results of the first part of this thesis, paradigm A1 did not prevent desensitization (or habituation) to the odors (see Fig. 1.4 in Chapter 2). Therefore in this study, the synaptic afferents to the OFC may already have been habituated due to banana and cinnamon odors and may explain why no sensory specific satiety effects were observed in the brain. It is unlikely that the use of any other paradigm tested in the first part of the thesis may have been better suited to demonstrate sensory specific satiety effect in the brain since all the paradigms caused desensitization to the odors. However, there may have been other methodological factors influencing the lack of sensory specific satiety related activation and are discussed below.

In the previous parts of this thesis, the results revealed that the 4s-model represented the functional timeseries better than the 16s-model in the primary olfactory areas as well as the secondary olfactory areas. However, in that experiment the two odors were treated as a single regressor in the GLM analysis. This was done to increase the number of trials and thus improve statistics. It was valid to do so because no significant difference was found between the PSC of the two odors in the first part of the thesis (see Section 2.3.2 in chapter 2). However, in the context of the current study, it was important to verify if 4s-model was better than the 16s-model

for each odor, in primary as well secondary olfactory brain areas using the functional data from paradigm A1 (acquired in experiment 1). The consequence of this analysis is that if for e.g. BOLD response for banana habituated less than that for cinnamon then the appropriate models for each odor would be different and may provide a physiological as well as methodological explanation regarding the lack of sensory specific satiety related activation in the brain. The results (Fig. 4-2) reaffirmed that the 4s-model is significantly better than 16s-model for both odors in primary as well as secondary olfactory areas. Similar results were observed when the two models were used to analyze the functional data from paradigm A1 acquired in this experiment (only session 1 functional data were analyzed in both cases).

(a)
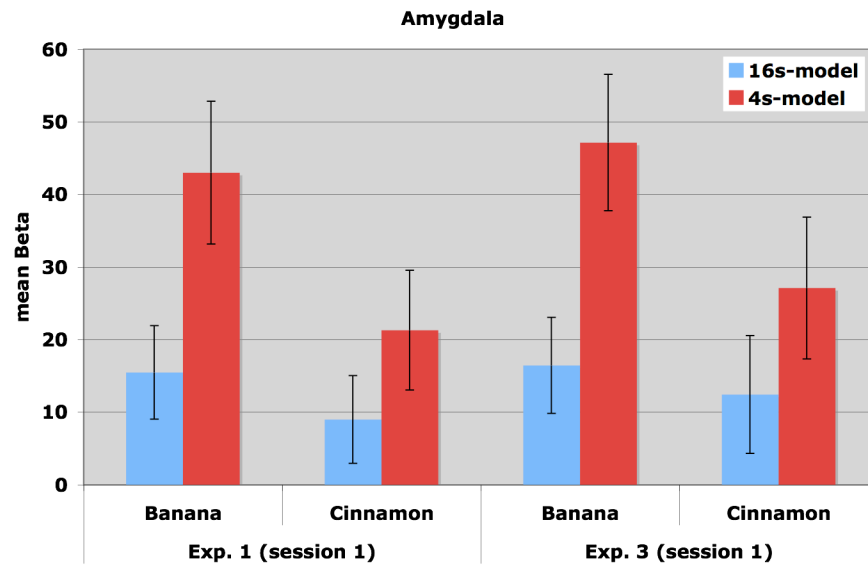
(b)
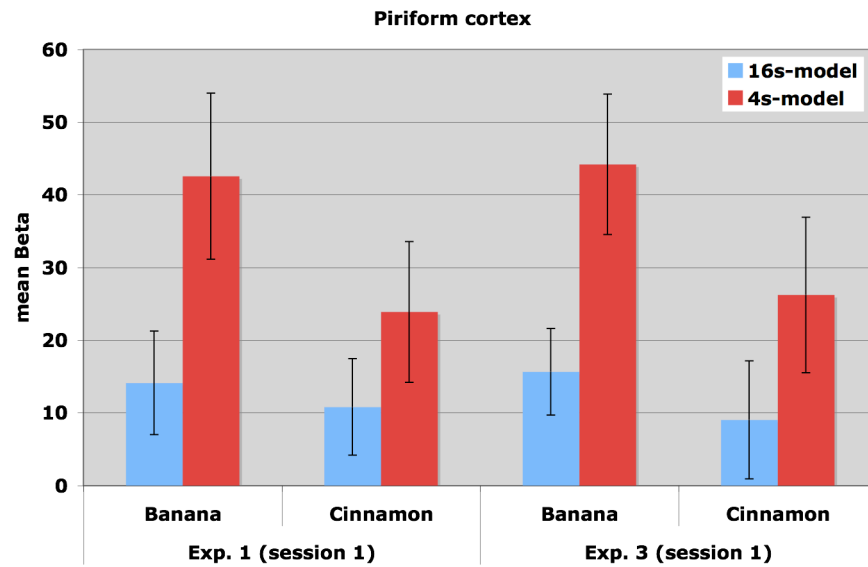
(c)

(d)

Figure 4-3: Mean Beta estimates (±SD across subjects) for banana and cinnamon odors in primary (a, b) and secondary (c, d) olfactory brain areas after timeseries regression with 4s-model (red) and 16s-model (blue).
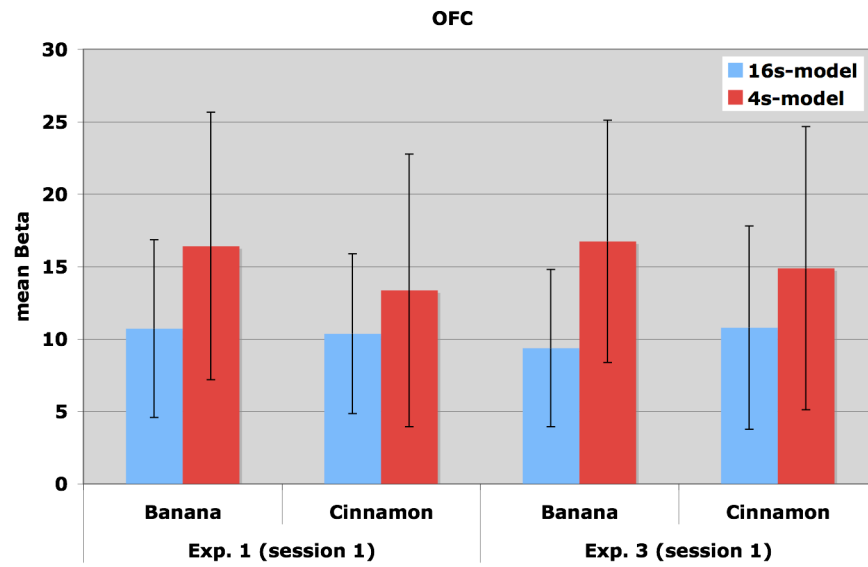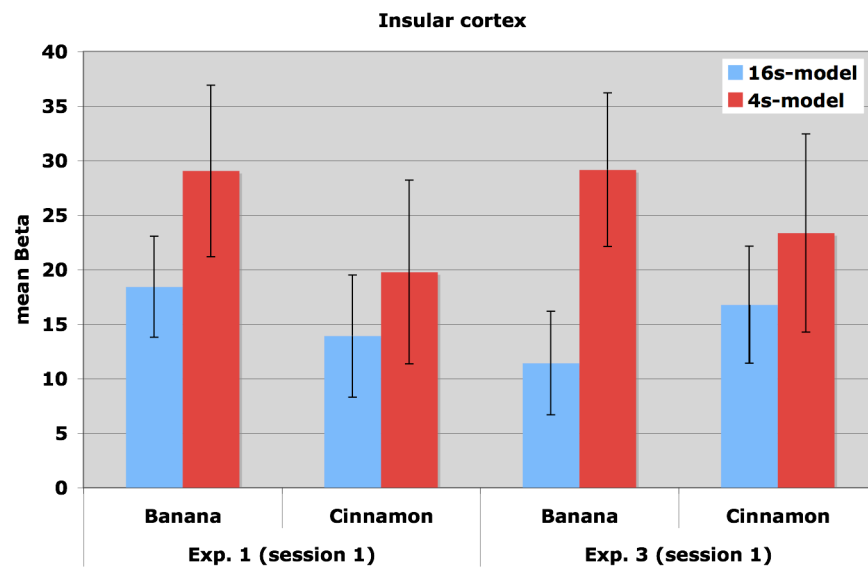
Additionally, it was also tested whether there were any tertiary areas that did not desensitize to odor (higher Beta for 16s-model than 4s-model) and at the same time were involved in olfactory sensory-specific satiety related changes. For this purpose, both sessions of the functional data acquired in this study were analyzed using the 16s-model and were tested with the same sensory specific satiety contrasts that were used in the analysis with the 4s-model. However, similar to the results for the 4s-model, no activation was found related to any contrast for the 16s-model either. So it seems unlikely that the lack of detection of olfactory sensory specific satiety areas was influenced by the choice of model.

Another methodological cause for not detecting sensory specific satiety areas may have been related to the contrast used in post GLM analysis. The sensory specific satiety contrast[49] used was [(preBan+preCin+postCin)/3 – postBan]. This contrast would detect voxels where activation in response to only post-satiety banana odor decreased compared to the other three conditions. However, this contrast assumes that pre-satiety banana and cinnamon odors produce similar levels of activation. It also assumes that pre- and post-satiety cinnamon odors produce similar levels of activation. In the results, no brain areas were found with significant differences between banana and cinnamon odors or between pre- and post-satiety conditions at the threshold level used in this study. However, although not significant, it was observed that banana odor produced greater overall activation than cinnamon odor in both sessions and that there was a decrease in activation in session 2 for both odors (Fig. 4-1). At first glance this could be the reason why no olfactory sensory specific satiety related brain areas were detected in this study. Therefore, another contrast (preBan - postBan) - (preCin - postCin) was tested in an attempt to detect these areas/area. Such a contrast should be able to detect brain areas where (pre – post) satiety differences for banana odor are significantly greater than (pre – post) satiety differences for

cinnamon odor. However, no brain areas were activated by this contrast. Therefore, although it is understandable that the former contrast did not detect any olfactory sensory specific satiety areas, the fact that the latter contrast did not detect these areas either, suggests that this methodological factor may not be the primary cause. It also contributes to the initial discussion that the lack of sensory specific satiety related activation was based on already habituated synaptic afferents.

If indeed there are no satiety effects occurring in this study then activation produced by the odors in this study should not be significantly different from the non-interventional study. Higher level GLM analysis with an unpaired t-test model was used to compare the activation produced by banana and cinnamon odors in the interventional study (functional data acquired in this experiment) with that evoked in the non-interventional study (functional data acquired in experiment 1) in each session. Comparisons were also drawn using GLM analysis between the (pre – post) contrasts of the interventional data and the (session1 – session2) contrasts of the non-interventional data. Additionally, comparisons were drawn between the sensory specific satiety contrasts of the interventional data and the sensory specific satiety contrasts of the non-interventional data. For each of the above contrasts tested no brain areas were found with significant differences between the interventional study and the non-interventional study thus further supporting the alternative hypothesis that there are no sensory specific satiety effects occurring in this study. This can be visualized from the mean Beta plot in Fig. 4-4. The mean Beta estimates in experiment 1 are not significantly different from those in experiment 2 in the piriform cortex.

In sensory specific satiety it is expected that response to an odor decreases in an area within the OFC after the food related to that odor is eaten to satiety while the response to the other food odor not related to the food eaten to satiety remains the same or increases.[49] The behavioral data

108

in this study (Fig. 4-2) shows that the mean cinnamon pleasantness rating was less than banana. Also, there was large variability across subjects in rating the pleasantness of cinnamon odor. While there was variability in the pleasantness ratings of banana as well, only one subject rated banana pleasantness below zero whereas five subjects rated cinnamon pleasantness below zero. This variability between subjects in associating the cinnamon stimulus as pleasant (high reward value) or unpleasant (low reward value) may have resulted in the group statistics not reaching significance in OFC areas since it has been shown that pleasant and unpleasant odors activate different parts of the OFC.[52]

(a)
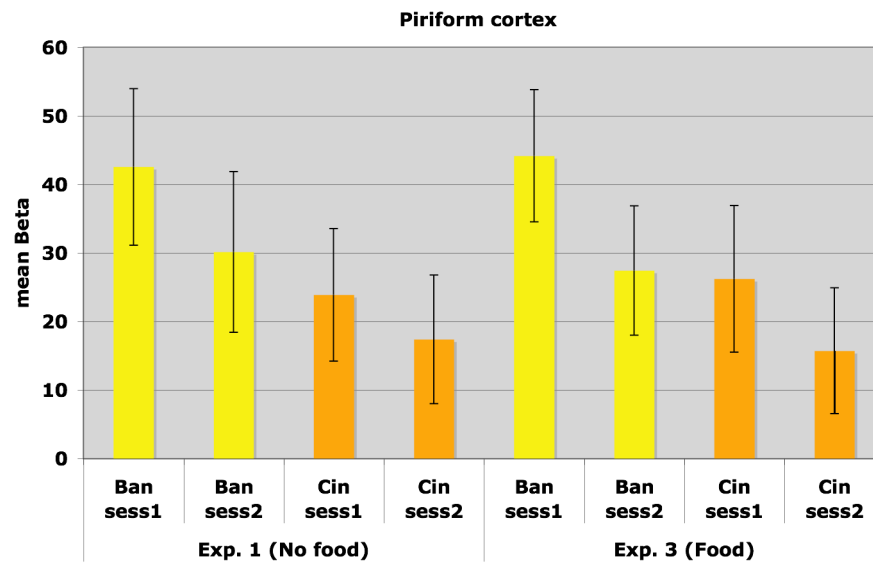
(b)

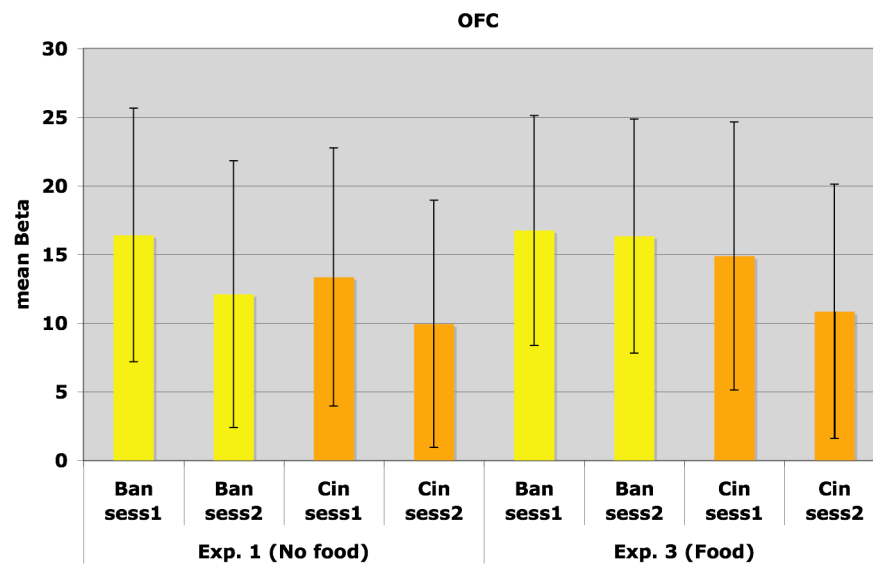**Figure 4-4:** Mean Beta estimates (±SD across subjects) for banana (yellow) and cinnamon (orange) odors from each session in piriform cortex (a) and OFC (b). First four bars are from experiment 1 data (no banana fed between sessions) and last four bars are from experiment 3 (banana fed to satiety between sessions). Beta estimates are from timeseries regression with the 4s-model.

It was also noted from subject interactions that cinnamon odor was not as consistently associated with food as compared to banana. If a subject does not associate cinnamon closely with food then based on the principle of sensory specific satiety it may be possible that the reward value of cinnamon would not be increased even after eating bananas to satiety. This could also potentially influence the affective value of post-satiety banana odor in that it could remain at the same level as pre-satiety banana instead of decreasing even after eating bananas to satiety. Some evidence to support this can be seen in Fig. 4-3(b) as the difference in the mean Beta for banana odor between session 1 and session 2 in the non-interventional study is larger than that in the interventional study, although these differences were not statistically significant. Future studies are needed to clarify how sensory specific satiety effect may depend at least in part on the familiarity of the odor with food.

One of the limitations of this study was that subject fasting period was not controlled diligently prior to scanning. The subjects were simply requested not to eat 2-3 hrs before scanning. In comparison, the subjects in another sensory specific satiety study[50] fasted for at least 6 hrs prior to scanning. Thus it was very difficult to guarantee uniformity in the motivational state for the food provided between sessions. The subjects' attentional state (e.g. button press) was also not controlled during the odor stimulation because of the confound that would have been potentially introduced in the brain activation by the correlated motor and odor responses. The subject demographics could also have been influential in the lack of sensory specific satiety effects. Twelve subjects out of sixteen were Asians. It may be possible that satiety effects could be dependant on ethnicity or race because of the differences in food preferences and consequently affective value of a particular food. Also influential could be the manner in which the odors were sampled (velo-pharyngeal closure or VPC). A recent PET study[60] did not find significant OFC

activation in response to odors sampled via VPC as compared to sniffing. The results of that study suggest that the manner in which odors are sampled may be important to higher order olfactory analysis and less naturalistic odorant sampling (VPC) may not evoke associative olfactory areas as easily. However we chose to use VPC instead of sniffing as the sampling technique in order to make the odor delivery independent of the breathing cycle and to avoid motor artifact introduced while sniffing. This method was also successfully used in another sensory specific satiety study.[49] Besides, sniffing has been shown to activate the olfactory cortices[126] even in the absence of odor and may thus confound the baseline data unless the subject respiration is controlled. The PET study[60] also suggests that VPC may divert attentional resources away from the frontal lobe, resulting in less OFC activity. Thus performing VPC itself could have affected sensory specific satiety effects. All or any of the above factors may have influenced the sensory specific satiety effects in this study and further studies are needed to determine the dependency of these effects on the factors mentioned above.

A theoretical consequence of sensory specific satiety is that availability of a large variety of foods should lead to enhanced eating. This may have been advantageous in evolution for intake of variety of necessary nutrients. However, in this age, when a variety of food is readily available for consumption, it may be a factor that can lead to overeating and obesity. In fact, it has been shown that variety of foods available led to obesity in rats.[127] Sensory specific satiety is a particularly useful phenomenon for studying affective representation of food in the brain, as it provides a means of altering the affective value of a stimulus, without modifying its physical attributes.[50,128] This phenomenon was used for e.g. in a study by De Araujo and Rolls.[129] They demonstrated that the perception and hedonics of food-related odor stimuli are also influenced by cognitive factors such as a word. In that study subjects rated the affective value of a test odor as

significantly more unpleasant when labeled "body odor" than when labeled "cheddar cheese". It has thus been shown that one of the ways food intake can be influenced is by a combination of various sensory inputs as well as cognitive factors. Hence, exploring such effects further is an important research avenue in preventing obesity. It may be interesting to investigate how habituation to a food related sensory input (odor in our case) might influence the affective value of the food related to that odor, the time scale of this effect and consequently influence on the consumption of that food. In this study, we were not able to demonstrate sensory specific satiety at the cortical level in humans, possibly due to the number of limitations mentioned earlier or merely due to the demographics of the study population.

CHAPTER 5   SUMMARY AND FUTURE WORK

The overall goal of this thesis was to ensure that in an olfactory Functional MRI interventional study, the effect of the intervention could be validly interpreted i.e. any or no change seen in post-intervention activation in the brain was a valid interventional effect rather than an effect due to confounds such as odor desensitization. In order to ensure interpretable results, (a) the olfactory paradigm used should produce robust activation in the olfactory related brain areas and (b) the activation produced should be reproducible in the absence of an intervention. Two important factors that improve the detection of activation in the brain via GLM analysis are (a) a large BOLD response and (b) a model that closely matches the BOLD response.[20]

BOLD response in olfactory Functional MRI can be severely affected by desensitization caused by the prolonged odor stimulation especially when block stimulation paradigms are used. The primary goal of the first part of this thesis was to select a block stimulation paradigm that would produce a large and reproducible BOLD response. It was hypothesized that a BOLD response of this nature could be produced if within-block and across-session desensitization could be minimized and that desensitization could be minimized by reducing the amount of odor by pulsing the odor stimulus within a block instead of providing a continuous odor throughout block duration. Several studies[44, 59-64, 102, 103] have used this approach with the assumption that it reduces desensitization. However, no study has systematically shown the efficacy of using pulse odor block paradigms. The results of the first part of this thesis showed that there was desensitization occurring in the primary and secondary olfactory brain areas with continuous as well as all four pulsed-odor paradigms used in the study. Although, the continuous odor block paradigm caused desensitization in the olfactory brain areas, this paradigm (A1) also produced

114

the highest BOLD response among all the paradigms tested and this response was also reproducible. Therefore, while the study failed in the attempt to find a paradigm that reduced desensitization, it did succeed in finding one that was still likely to yield high and reproducible activation in olfactory brain areas. Further studies are required that (a) test the possibility of reducing desensitization by pulsing different odorants of the same perceptive quality within the block instead of a single odorant and (b) compare paradigms with different within-block stimulus duration and ISI (similar to the first study in this thesis) while keeping the total amount of odor the same in all paradigms by, for e.g. extending the block duration.

The aim of the next part of the thesis was to find a model that best represented the functional timeseries acquired from paradigm A1 (the paradigm selected from the previous study) so that GLM analysis conducted on the functional data using this model would yield high amounts of activation in olfactory brain areas. Twelve stimulation models and one perception-based model were used in separate GLM analyses on the same functional data. It was concluded from the results from the second part of the thesis that the 4s-model best fit the functional timeseries from A1 and consequently produced the largest activation among all the models. It was expected that a model with duration smaller than the stimulation period would yield better results since the desensitized BOLD response in A1 was already observed from previous results. It was also observed from the results of this study that the perception-based profiles returned to the baseline level a few seconds later than the stimulation based models did, possibly due to the lag in subject response from the end of the odor perception and movement of the cursor down to zero. This raises questions about the efficacy of the perception-based profile being directly used as a model in GLM analysis as it may incorporate confounds like subject-error. It may instead be helpful to extract various timings from the perception profiles such as onset of odor perception and time to

peak perception, and use these measures to optimize the timing of a stimulation-based model. Another possibility is to construct an accurate model for GLM analysis from the output of model-free methods such as probabilistic independent component analysis.[130] Further studies are required to explore the above possibilities to improve model specification for analysis of olfactory Functional MRI data.

The hypothesis of the third part of this thesis was that applying the best paradigm and model selected from previous results would help demonstrate sensory specific satiety in the brain as an interpretable result in an olfactory interventional Functional MRI study. However, the study failed to demonstrate the olfactory sensory specific satiety effect in the brain possibly due to manner in which this effect manifests itself (hypothetically via habituation of synaptic afferents to the OFC[118]) and the fact the paradigm used in the study caused desensitization even without intervention. However, dependence of sensory specific satiety effects on other experimental factors such as subject attentional and motivational state, subject demographics, associability of cinnamon odor to food and control of the subject's hunger and satiety state, could not be ruled out and should be carefully accounted for in future studies investigating olfactory sensory specific satiety effects in humans. Finally, if indeed eating a food to satiety causes habituation of synaptic afferents to the OFC then it may be of consequence to obesity research to investigate if the converse were true i.e. if habituation to a food related sensory input (for e.g. odor or picture) influences the affective value of the food related to that odor, the time scale of this effect and consequently influence on the consumption of that food.

REFERENCES

1. Clarke E, Dewhurst K. *An Illustrated History of Brain Function* Oxford: Sandford Publications; 1972.

2. Penfield W, Rasmussen T. *The Cerebral Cortex of Man; a Clinical Study of Localization of Function.* New York: Macmillan; 1950.

3. Pauling L, Coryell CD. The magnetic properties and structure of hemoglobin, oxyhemoglobin and carbonmonoxyhemoglobin. *Proc Natl Acad Sci U S A*. 1936;22:210-216.

4. Thulborn KR, Waterton JC, Matthews PM, Radda GK. Oxygenation dependence of the transverse relaxation time of water protons in whole blood at high field. *Biochim Biophys Acta*. 1982;714:265-270.

5. Ogawa S, Lee TM, Kay AR, Tank DW. Brain magnetic resonance imaging with contrast dependent on blood oxygenation. *Proc Natl Acad Sci U S A*. 1990;87:9868-9872.

6. Ogawa S, Lee TM. Magnetic resonance imaging of blood vessels at high fields: In vivo and in vitro measurements and image simulation. *Magn Reson Med*. 1990;16:9-18.

7. Fox PT, Raichle ME, Mintun MA, Dence C. Nonoxidative glucose consumption during focal physiologic neural activity. *Science*. 1988;241:462-464.

8. Malonek D, Grinvald A. Interactions between electrical activity and cortical microcirculation revealed by imaging spectroscopy: Implications for functional brain mapping. *Science*. 1996;272:551-554.

9. Ernst T, Hennig J. Observation of a fast response in functional MR. *Magn Reson Med*. 1994;32:146-149.

10. Hu X, Le TH, Ugurbil K. Evaluation of the early response in fMRI in individual subjects using short stimulus duration. *Magn Reson Med*. 1997;37:877-884.

11. Menon RS, Ogawa S, Hu X, Strupp JP, Anderson P, Ugurbil K. BOLD based functional MRI at 4 tesla includes a capillary bed contribution: Echo-planar imaging correlates with previous optical imaging using intrinsic signals. *Magn Reson Med*. 1995;33:453-459.

12. Thompson JK, Peterson MR, Freeman RD. High-resolution neurometabolic coupling revealed by focal activation of visual neurons. *Nat Neurosci*. 2004;7:919-920.

13. Bandettini PA, Wong EC, Hinks RS, Tikofsky RS, Hyde JS. Time course EPI of human brain function during task activation. *Magn Reson Med*. 1992;25:390-397.

14. Buxton RB, Uludag K, Dubowitz DJ, Liu TT. Modeling the hemodynamic response to brain activation. *Neuroimage*. 2004;23 Suppl 1:S220-33.

15. Kwong KK, Belliveau JW, Chesler DA, et al. Dynamic magnetic resonance imaging of human brain activity during primary sensory stimulation. *Proc Natl Acad Sci U S A*. 1992;89:5675-5679.

16. Turner R, Jezzard P, Wen H, et al. Functional mapping of the human visual cortex at 4 and 1.5 tesla using deoxygenation contrast EPI. *Magn Reson Med*. 1993;29:277-279.

17. Le TH, Hu X. Retrospective estimation and correction of physiological artifacts in fMRI by direct extraction of physiological activity from MR data. *Magn Reson Med*. 1996;35:290-298.

18. Glover GH, Li TQ, Ress D. Image-based method for retrospective correction of physiological motion effects in fMRI: RETROICOR. *Magn Reson Med*. 2000;44:162-167.

19. Bandettini PA, Jesmanowicz A, Wong EC, Hyde JS. Processing strategies for time-course data sets in functional MRI of the human brain. *Magn Reson Med*. 1993;30:161-173.

20. Friston KJ, Holmes AP, Poline JB, et al. Analysis of fMRI time-series revisited. *Neuroimage*. 1995;2:45-53.

21. Worsley KJ, Friston KJ. Analysis of fMRI time-series revisited--again. *Neuroimage*. 1995;2:173-181.

22. Aguirre GK, Zarahn E, D'Esposito M. A critique of the use of the kolmogorov-smirnov (KS) statistic for the analysis of BOLD fMRI data. *Magn Reson Med*. 1998;39:500-505.

23. McKeown MJ, Makeig S, Brown GG, et al. Analysis of fMRI data by blind separation into independent spatial components. *Hum Brain Mapp*. 1998;6:160-188.

24. Genovese CR, Lazar NA, Nichols T. Thresholding of statistical maps in functional neuroimaging using the false discovery rate. *Neuroimage*. 2002;15:870-878.

25. Friston KJ, Josephs O, Rees G, Turner R. Nonlinear event-related responses in fMRI. *Magn Reson Med*. 1998;39:41-52.

26. PRICE J. The human nervous system; olfaction . 2004:1197 <last_page> 1211.

27. Zelano C, Sobel N. Humans as an animal model for systems-level organization of olfaction. *Neuron*. 2005;48:431-454.

28. Sherman SM, Guillery RW. *Exploring the Thalamus*. San Diego: Academic Press; 2001.

29. Gottfried JA. Smell: Central nervous processing. *Adv Otorhinolaryngol*. 2006;63:44-69.

30. Ojemann JG, Akbudak E, Snyder AZ, McKinstry RC, Raichle ME, Conturo TE. Anatomic localization and quantitative analysis of gradient refocused echo-planar fMRI susceptibility artifacts. *Neuroimage*. 1997;6:156-167.

31. Constable RT, Spencer DD. Composite image formation in z-shimmed functional MR imaging. *Magn Reson Med*. 1999;42:110-117.

32. Wilson JL, Jenkinson M, Jezzard P. Optimization of static field homogeneity in human brain using diamagnetic passive shims. *Magn Reson Med*. 2002;48:906-914.

33. Deichmann R, Josephs O, Hutton C, Corfield DR, Turner R. Compensation of susceptibility-induced BOLD sensitivity losses in echo-planar fMRI imaging. *Neuroimage*. 2002;15:120-135.

34. Glover GH, Law CS. Spiral-in/out BOLD fMRI for increased SNR and reduced susceptibility artifacts. *Magn Reson Med*. 2001;46:515-522.

35. Preston AR, Thomason ME, Ochsner KN, Cooper JC, Glover GH. Comparison of spiral-in/out and spiral-out BOLD fMRI at 1.5 and 3 T. *Neuroimage*. 2004;21:291-301.

36. Anderson AK, Christoff K, Stappen I, et al. Dissociated neural representations of intensity and valence in human olfaction. *Nat Neurosci*. 2003;6:196-202.

37. Gottfried JA, Deichmann R, Winston JS, Dolan RJ. Functional heterogeneity in human olfactory cortex: An event-related functional magnetic resonance imaging study. *J Neurosci*. 2002;22:10819-10828.

38. Zelano C, Bensafi M, Porter J, et al. Attentional modulation in human primary olfactory cortex. *Nat Neurosci*. 2005;8:114-120.

39. Huettel SA, Song AW, McCarthy G. *Functional Magnetic Resonance Imaging*. 2nd ed. Sunderland, Mass.: Sinauer Associates; 2009.

40. Cerf-Ducastel B, Murphy C. Improvement of fMRI data processing of olfactory responses with a perception-based template. *Neuroimage*. 2004;22:603-610.

41. Ferdon S, Murphy C. The cerebellum and olfaction in the aging brain: A functional magnetic resonance imaging study. *Neuroimage*. 2003;20:12-21.

42. Plailly J, Bensafi M, Pachot-Clouard M, et al. Involvement of right piriform cortex in olfactory familiarity judgments. *Neuroimage*. 2005;24:1032-1041.

43. Sabri M, Radnovich AJ, Li TQ, Kareken DA. Neural correlates of olfactory change detection. *Neuroimage*. 2005;25:969-974.

44. Suzuki Y, Critchley HD, Suckling J, et al. Functional magnetic resonance imaging of odor identification: The effect of aging. *J Gerontol A Biol Sci Med Sci*. 2001;56:M756-M760.

45. Birn RM, Cox RW, Bandettini PA. Detection versus estimation in event-related fMRI: Choosing the optimal stimulus timing. *Neuroimage*. 2002;15:252-264.

46. Brewer JB, Zhao Z, Desmond JE, Glover GH, Gabrieli JD. Making memories: Brain activity that predicts how well visual experience will be remembered. *Science*. 1998;281:1185-1187.

47. Huettel SA, Misiurek J, Jurkowski AJ, McCarthy G. Dynamic and strategic aspects of executive processing. *Brain Res*. 2004;1000:78-84.

48. Hopfinger JB, Buchel C, Holmes AP, Friston KJ. A study of analysis parameters that influence the sensitivity of event-related fMRI analyses. *Neuroimage*. 2000;11:326-333.

49. O'Doherty J, Rolls ET, Francis S, et al. Sensory-specific satiety-related olfactory activation of the human orbitofrontal cortex. *Neuroreport*. 2000;11:893-897.

50. Kringelbach ML, O'Doherty J, Rolls ET, Andrews C. Activation of the human orbitofrontal cortex to a liquid food stimulus is correlated with its subjective pleasantness. *Cereb Cortex*. 2003;13:1064-1071.

51. Rolls ET. Sensory processing in the brain related to the control of food intake. *Proc Nutr Soc*. 2007;66:96-112.

52. Rolls ET, Kringelbach ML, de Araujo IE. Different representations of pleasant and unpleasant odours in the human brain. *Eur J Neurosci*. 2003;18:695-703.

53. Gautier JF, Chen K, Salbe AD, et al. Differential brain responses to satiation in obese and lean men. *Diabetes*. 2000;49:838-846.

54. Strategic Plan for NIH Obesity Research Available at: http://www.obesityresearch.nih.gov/about/strategic-plan.htm. Accessed 10/28/2009, 2009.

55. Wilson DA. Habituation of odor responses in the rat anterior piriform cortex. *J Neurophysiol*. 1998;79:1425-1440.

56. Sobel N, Prabhakaran V, Zhao Z, et al. Time course of odorant-induced activation in the human primary olfactory cortex. *J Neurophysiol*. 2000;83:537-551.

57. Poellinger A, Thomas R, Lio P, et al. Activation and habituation in olfaction--an fMRI study. *Neuroimage*. 2001;13:547-560.

58. Tabert MH, Steffener J, Albers MW, et al. Validation and optimization of statistical approaches for modeling odorant-induced fMRI signal changes in olfactory-related brain areas. *Neuroimage*. 2007;34:1375-1390.

59. Dade LA, Jones-Gotman M, Zatorre RJ, Evans AC. Human brain function during odor encoding and recognition. A PET activation study. *Ann N Y Acad Sci*. 1998;855:572-574.

60. Kareken DA, Sabri M, Radnovich AJ, et al. Olfactory system activation from sniffing: Effects in piriform and orbitofrontal cortex. *Neuroimage*. 2004;22:456-465.

61. Qureshy A, Kawashima R, Imran MB, et al. Functional mapping of human brain in olfactory processing: A PET study. *J Neurophysiol*. 2000;84:1656-1666.

62. Savic I, Gulyas B. PET shows that odors are processed both ipsilaterally and contralaterally to the stimulated nostril. *Neuroreport*. 2000;11:2861-2866.

63. Zatorre RJ, Jones-Gotman M, Evans AC, Meyer E. Functional localization and lateralization of human olfactory cortex. *Nature*. 1992;360:339-340.

64. Wang J, Eslinger PJ, Smith MB, Yang QX. Functional magnetic resonance imaging study of human olfaction and normal aging. *J Gerontol A Biol Sci Med Sci*. 2005;60:510-514.

65. Hummel T, Kobal G. Differences in human evoked potentials related to olfactory or trigeminal chemosensory activation. *Electroencephalogr Clin Neurophysiol*. 1992;84:84-89.

66. Kobal G, Hummel T. Olfactory (chemosensory) event-related potentials. *Toxicol Ind Health*. 1994;10:587-596.

67. Kobal G, Hummel C. Cerebral chemosensory evoked potentials elicited by chemical stimulation of the human olfactory and respiratory nasal mucosa. *Electroencephalogr Clin Neurophysiol*. 1988;71:241-250.

68. Kobal G, Hummel T. Olfactory and intranasal trigeminal event-related potentials in anosmic patients. *Laryngoscope*. 1998;108:1033-1035.

69. Kettenmann B, Mueller C, Wille C, Kobal G. Odor and taste interaction on brain responses in humans. *Chem Senses*. 2005;30 Suppl 1:i234-i235.

70. Hummel T, Knecht M, Kobal G. Peripherally obtained electrophysiological responses to olfactory stimulation in man: Electro-olfactograms exhibit a smaller degree of desensitization compared with subjective intensity estimates. *Brain Res*. 1996;717:160-164.

71. Kobal G. Elektrophysiologische untersuchungen des menschlichen geruchssinnes. , georg thieme verlag, stuttgart. . 1981.

72. Rombouts SA, Barkhof F, Hoogenraad FG, Sprenger M, Scheltens P. Within-subject reproducibility of visual activation patterns with functional magnetic resonance imaging using multislice echo planar imaging. *Magn Reson Imaging*. 1998;16:105-113.

73. Neumann J, Lohmann G, Zysset S, von Cramon DY. Within-subject variability of BOLD response dynamics. *Neuroimage*. 2003;19:784-796.

74. Fernandez G, Specht K, Weis S, et al. Intrasubject reproducibility of presurgical language lateralization and mapping using fMRI. *Neurology*. 2003;60:969-975.

75. Magon S, Basso G, Farace P, Ricciardi GK, Beltramello A, Sbarbati A. Reproducibility of BOLD signal change induced by breath holding. *Neuroimage*. 2009;45:702-712.

76. Marshall I, Simonotto E, Deary IJ, et al. Repeatability of motor and working-memory tasks in healthy older volunteers: Assessment at functional MR imaging. *Radiology*. 2004;233:868-877.

77. Tjandra T, Brooks JC, Figueiredo P, Wise R, Matthews PM, Tracey I. Quantitative assessment of the reproducibility of functional activation measured with BOLD and MR perfusion imaging: Implications for clinical trial design. *Neuroimage*. 2005;27:393-401.

78. Leontiev O, Buxton RB. Reproducibility of BOLD, perfusion, and CMRO2 measurements with calibrated-BOLD fMRI. *Neuroimage*. 2007;35:175-184.

79. Kobal G, Hummel T, Sekinger B, Barz S, Roscher S, Wolf S. "Sniffin' sticks": Screening of olfactory performance. *Rhinology*. 1996;34:222-226.

80. Hummel T, Sekinger B, Wolf SR, Pauli E, Kobal G. 'Sniffin' sticks': Olfactory performance assessed by the combined testing of odor identification, odor discrimination and olfactory threshold. *Chem Senses*. 1997;22:39-52.

81. Hummel T, Kobal G, Gudziol H, Mackay-Sim A. Normative data for the "sniffin' sticks" including tests of odor identification, odor discrimination, and olfactory thresholds: An upgrade based on a group of more than 3,000 subjects. *Eur Arch Otorhinolaryngol*. 2007;264:237-243.

82. Albrecht J, Kopietz R, Linn J, et al. Activation of olfactory and trigeminal cortical areas following stimulation of the nasal mucosa with low concentrations of S(-)-nicotine vapor--an fMRI study on chemosensory perception. *Hum Brain Mapp*. 2009;30:699-710.

83. Wiesmann M, Kopietz R, Albrecht J, et al. Eye closure in darkness animates olfactory and gustatory cortical areas. *Neuroimage*. 2006;32:293-300.

84. Albrecht J, Wiesmann M. The human olfactory system. anatomy and physiology. *Nervenarzt*. 2006;77:931-939.

85. Deichmann R, Gottfried JA, Hutton C, Turner R. Optimized EPI for fMRI studies of the orbitofrontal cortex. *Neuroimage*. 2003;19:430-441.

86. Jenkinson M, Bannister P, Brady M, Smith S. Improved optimization for the robust and accurate linear registration and motion correction of brain images. *Neuroimage*. 2002;17:825-841.

87. Smith SM. Fast robust automated brain extraction. *Hum Brain Mapp*. 2002;17:143-155.

88. Talairach J, Tournoux P. *Co-Planar Stereotaxic Atlas of the Human Brain: 3-Dimensional Proportional System: An Approach to Cerebral Imaging*. Stuttgart ; G. Thieme ; 1988.; 1988.

89. Maldjian JA, Laurienti PJ, Kraft RA, Burdette JH. An automated method for neuroanatomic and cytoarchitectonic atlas-based interrogation of fMRI data sets. *Neuroimage*. 2003;19:1233-1239.

90. Tzourio-Mazoyer N, Landeau B, Papathanassiou D, et al. Automated anatomical labeling of activations in SPM using a macroscopic anatomical parcellation of the MNI MRI single-subject brain. *Neuroimage*. 2002;15:273-289.

91. JOHNSON NL, WELCH BL. APPLICATIONS OF THE NON-CENTRAL t-DISTRIBUTION *Biometrika*. 1940;31:362 <last_page> 389.

92. Carmichael ST, Clugnet MC, Price JL. Central olfactory connections in the macaque monkey. *J Comp Neurol*. 1994;346:403-434.

93. Critchley HD, Rolls ET. Olfactory neuronal responses in the primate orbitofrontal cortex: Analysis in an olfactory discrimination task. *J Neurophysiol*. 1996;75:1659-1672.

94. Rolls ET, Critchley HD, Treves A. Representation of olfactory information in the primate orbitofrontal cortex. *J Neurophysiol*. 1996;75:1982-1996.

95. Luskin MB, Price JL. The topographic organization of associational fibers of the olfactory system in the rat, including centrifugal fibers to the olfactory bulb. *J Comp Neurol*. 1983;216:264-291.

96. Cerf-Ducastel B, Murphy C. fMRI activation in response to odorants orally delivered in aqueous solutions. *Chem Senses*. 2001;26:625-637.

97. Fulbright RK, Skudlarski P, Lacadie CM, et al. Functional MR imaging of regional brain responses to pleasant and unpleasant odors. *AJNR Am J Neuroradiol*. 1998;19:1721-1726.

98. Kobal G, Kettenmann B. Cerebral representation of odor perception. *Adv Neurol*. 1999;81:221-229.

99. Levy LM, Henkin RI, Hutter A, Lin CS, Martins D, Schellinger D. Functional MRI of human olfaction. *J Comput Assist Tomogr*. 1997;21:849-856.

100. Royet JP, Koenig O, Gregoire MC, et al. Functional anatomy of perceptual and semantic processing for odors. *J Cogn Neurosci*. 1999;11:94-109.

101. Plailly J, Radnovich AJ, Sabri M, Royet JP, Kareken DA. Involvement of the left anterior insula and frontopolar gyrus in odor discrimination. *Hum Brain Mapp*. 2007;28:363-372.

102. Yousem DM, Oguz KK, Li C. Imaging of the olfactory system. *Semin Ultrasound CT MR*. 2001;22:456-472.

103. Zald DH, Pardo JV. Emotion, olfaction, and the human amygdala: Amygdala activation during aversive olfactory stimulation. *Proc Natl Acad Sci U S A*. 1997;94:4119-4124.

104. Boynton GM, Engel SA, Glover GH, Heeger DJ. Linear systems analysis of functional magnetic resonance imaging in human V1. *J Neurosci*. 1996;16:4207-4221.

105. Schafer JR, Kida I, Rothman DL, Hyder F, Xu F. Adaptation in the rodent olfactory bulb measured by fMRI. *Magn Reson Med*. 2005;54:443-448.

106. Frasnelli J, Wohlgemuth C, Hummel T. The influence of stimulus duration on odor perception. *Int J Psychophysiol*. 2006;62:24-29.

107. Wang L, Walker VE, Sardi H, Fraser C, Jacob TJ. The correlation between physiological and psychological responses to odour stimulation in human subjects. *Clin Neurophysiol*. 2002;113:542-551.

108. Miezin FM, Maccotta L, Ollinger JM, Petersen SE, Buckner RL. Characterizing the hemodynamic response: Effects of presentation rate, sampling procedure, and the possibility of ordering brain activity based on relative timing. *Neuroimage*. 2000;11:735-759.

109. Dale AM, Buckner RL. Selective averaging of rapidly presented individual trials using fMRI. *Hum Brain Mapp*. 1997;5:329-340.

110. Friston KJ, Frith CD, Turner R, Frackowiak RS. Characterizing evoked hemodynamics with fMRI. *Neuroimage*. 1995;2:157-165.

111. Glover GH. Deconvolution of impulse response in event-related BOLD fMRI. *Neuroimage*. 1999;9:416-429.

112. Woolrich MW, Ripley BD, Brady M, Smith SM. Temporal autocorrelation in univariate linear modeling of FMRI data. *Neuroimage*. 2001;14:1370-1386.

113. Beckmann CF, Jenkinson M, Smith SM. General multilevel linear modeling for group analysis in FMRI. *Neuroimage*. 2003;20:1052-1063.

114. Woolrich MW, Jenkinson M, Brady JM, Smith SM. Fully bayesian spatio-temporal modeling of FMRI data. *IEEE Trans Med Imaging*. 2004;23:213-231.

115. Woolrich MW, Jbabdi S, Patenaude B, et al. Bayesian analysis of neuroimaging data in FSL. *Neuroimage*. 2009;45:S173-86.

116. Tootell RB, Hadjikhani NK, Vanduffel W, et al. Functional analysis of primary visual cortex (V1) in humans. *Proc Natl Acad Sci U S A*. 1998;95:811-817.

117. Critchley HD, Rolls ET. Hunger and satiety modify the responses of olfactory and visual neurons in the primate orbitofrontal cortex. *J Neurophysiol*. 1996;75:1673-1686.

118. Rolls ET. Sensory processing in the brain related to the control of food intake. *Proc Nutr Soc*. 2007;66:96-112.

119. Rolls ET, Sienkiewicz ZJ, Yaxley S. Hunger modulates the responses to gustatory stimuli of single neurons in the caudolateral orbitofrontal cortex of the macaque monkey. *Eur J Neurosci*. 1989;1:53-60.

120. Ongur D, Price JL. The organization of networks within the orbital and medial prefrontal cortex of rats, monkeys and humans. *Cereb Cortex*. 2000;10:206-219.

121. Rolls ET, Critchley HD, Browning AS, Hernadi I, Lenard L. Responses to the sensory properties of fat of neurons in the primate orbitofrontal cortex. *J Neurosci*. 1999;19:1532-1540.

122. Tremblay L, Schultz W. Relative reward preference in primate orbitofrontal cortex. *Nature*. 1999;398:704-708.

123. Woolrich MW, Behrens TE, Beckmann CF, Jenkinson M, Smith SM. Multilevel linear modelling for FMRI group analysis using bayesian inference. *Neuroimage*. 2004;21:1732-1747.

124. Gottfried JA, O'Doherty J, Dolan RJ. Appetitive and aversive olfactory learning in humans studied using event-related functional magnetic resonance imaging. *J Neurosci*. 2002;22:10829-10837.

125. O'Doherty J, Kringelbach ML, Rolls ET, Hornak J, Andrews C. Abstract reward and punishment representations in the human orbitofrontal cortex. *Nat Neurosci*. 2001;4:95-102.

126. Sobel N, Prabhakaran V, Desmond JE, et al. Sniffing and smelling: Separate subsystems in the human olfactory cortex. *Nature*. 1998;392:282-286.

127. Rolls BJ, Van Duijvenvoorde PM, Rowe EA. Variety in the diet enhances intake in a meal and contributes to the development of obesity in the rat. *Physiol Behav*. 1983;31:21-27.

128. Rolls BJ, Laster LJ, Summerfelt A. Hunger and food intake following consumption of low-calorie foods. *Appetite*. 1989;13:115-127.

129. de Araujo IE, Rolls ET, Velazco MI, Margot C, Cayeux I. Cognitive modulation of olfactory processing. *Neuron*. 2005;46:671-679.

130. Beckmann CF, Smith SM. Probabilistic independent component analysis for functional magnetic resonance imaging. *IEEE Trans Med Imaging*. 2004;23:137-152.

VITA

Vishwadeep Ahluwalia was born on August 26th, 1980 in Mumbai, India. He received his Bachelor of Engineering in 2001 from University of Mumbai and Master of Science in 2003 in Biomedical Engineering from Virginia Commonwealth University. He joined the Medical Physics Ph.D. program at Virginia Commonwealth University in Fall-2004 and completed his doctorate degree in 2009.